

## **High-Efficiency Membrane Chromatography Devices**

High-Efficiency Membrane Chromatography Devices for Downstream Purification  
of Biopharmaceuticals: Design, Development, and Applications

By Pedram Madadkar, B. Sc.

A Thesis Submitted to the School of Graduate Studies in Partial Fulfilment of the  
Requirements for the Degree Ph.D. of Chemical Engineering

McMaster University © Copyright by Pedram Madadkar, December 2016

McMaster University Ph.D. of Engineering (2017) Hamilton, Ontario (Chemical  
Engineering)

TITLE: High-Efficiency Membrane Chromatography Devices for Downstream Purification of Biopharmaceuticals: Design, Development, and Applications

AUTHOR: Pedram Madadkar, B.Sc. (University of Tehran)

SUPERVISOR: Professor Raja Ghosh

NUMBER OF PAGES: xxxi, 181

**Abstract**

The biopharmaceutical industry has experienced remarkable progress in the upstream production capacity of life-saving proteins. This is while the downstream processing has failed to keep pace, including unit operations which are working close to their physical limit with no economy of scale. Column chromatography which is an integral unit in different stages of downstream purification is considered as the major bottleneck in this section. The packed-bed resin media is costly and the processes are labor-intensive and extremely time consuming. Membrane chromatography which uses a stack of adsorptive membranes as the chromatographic media is one of the most promising alternatives for conventional chromatography techniques. The performance of membrane adsorbers is consistent over a wide range of flow rates which is owing to the dominance of convective solute transport as opposed to the diffusion-based nature of mass transfer within the pores of the resin beads. This translates to much higher productivity and considerably lower buffer consumption (even as high as 95%), leading to much lower overall processing costs. The other advantages are significantly lower footprints and decreased pressure drops, both contributing to diminished capital costs. Membrane adsorbers are greatly scalable and used in a single-use manner. The latter eliminates the cleaning and validation steps and brings about much shorter processing times and higher flexibility in process development.

Due to the performance advantages of membrane chromatography, this technique is now widely used in purification of high volumes of samples in late-stage polishing. Currently available membrane adsorbers have radial-flow spiral-wound configuration with high frontal surface area to bed height ratio according to which dilute impurities are removed in a flow-through format at very high flow rates and low pressure drops. Nevertheless, they fail to give high-resolution for bind-and-elute separations which makes them unsuitable for many unit operations, highly restricting their application. Severe design deficiencies such as large dead

volumes and varying membrane area over the bed height result in broad and poorly resolved peaks.

Herein, a novel device design was successfully developed which addresses the abovementioned shortcomings. The laterally-fed membrane chromatography (LFMC) devices house a stack of rectangular membrane sheets with two rectangular lateral channels on both sides of the stack as the feed and permeate channels. The design offers balanced pressure over the sides of the stack as well as even solute flow path lengths due to which the solute residence time is very uniform. Also, the small dead volumes minimize the dispersion effects. These features make the LFMC technology highly suitable for bind-and-elute applications, the improvement which is brought about by a simple design. The devices are easy to fabricate and highly scalable.

The LFMC devices containing cation-exchange (CEX) membranes with 7 mL bed volume were examined for bind-and-elute separation where they outperformed the equivalent commercially available radial-flow devices. The design was further modified to give even lower dead volumes and more cost-effective fabrication. The latest embodiment of the device gave resolutions which were comparable with the ones obtained with the commercially packed resin columns in 1 mL and 5 mL scale with consistency over wide range of flow rates. The results were all acquired using a three component model protein system. Upon the approval of suitability of the device for bind-and-elute separation, the CEX-LFMC was used for purification of monoclonal antibodies (mAbs), the largest class of biopharmaceuticals. The device showed great performance in separation of mAb charge variants when extensively shallow gradients (60 membrane bed volumes) were required. The devices offered very stable conductivity gradients at high flow rates. LFMC devices in three different preparative scales gave great performance in separation of mAb aggregates which was approved for different mAb samples. The other application studied with the CEX-LFMC devices was the single-step preparative purification of mono-PEGylated proteins which is as well very challenging due to the

physicochemical similarities between the target molecules and the impurities. Collectively, the LFMC devices combine the high-resolution with high-productivity which is highly desirable in downstream purification of biological molecules with great potential to expand the application of membrane chromatography.

Finally, the LFMC devices were modified to adapt the analytical scale where they were integrated with a stack of hydrophilized PVDF membranes. The device successfully delivered ultra-fast separation of mAb aggregates in less than 1.5 minutes based on hydrophobic interaction membrane chromatography (HIMC). The assay times achieved with the HI-LFMC technique outclassed the currently available ultra-high performance chromatography (UPLC) methods at the same time with being extremely cost-effective. The application of the LFMC technology in analytical scale has great potential to offer cheap and rapid analysis in process development and quality control section of biopharmaceutical manufacturing.

## **Acknowledgements**

I'd like to start off by thanking my supervisor, Professor Raja Ghosh, for providing me with the much needed guidance and support throughout my PhD studies. It was an honor to work under the supervision of such a leading character in the field of bioseparations, and specifically membrane chromatography. Thank you for giving me the confidence to take the leap from my master's to the next big step. You've taught me the ways to babysit a project, from critical thinking at the early stages all the way to communicating the findings, on paper and at the conferences that I was fortunate to attend. Working with you, I've learned so much more than just science; commitment, hard work, and ambition, all to equip me for the scientific career ahead of me.

I should acknowledge my committee members for all their insights. Thank you Dr. Selvaganapathy for adopting me in your lab, helping me diversify my scientific skills and scope. I have not forgotten about those publications, I promise! I would also like to thank Dr. Latulippe for his constructive advice on my projects and TAsip.

During my time in the lab, I've been very lucky to work closely with a number of fantastic people. Special mention goes to Dr. Seung Mi, Rahul, and Si. It's been five and a half years guys! Also my summer students Sergio and Umathy and to the rest of the team including but not limited to Dr. Annabel, Dr. Aubrey, Evan, and Steve. You guys have helped me with questions and experiments big time. I would like to thank all the staff in the department of Chemical Engineering, specifically Paul Gatt whose great ideas in device fabrication always contributed to the success of this project.

Of course, this would not have been possible without the support from my family. Mom and Dad, thank you for sending me endless love from home. Also my sister Tara, you're my favourite person, best friend, and confidante. Special thanks goes to my family in Canada, my aunts Azar and Roya and my uncles Hooshang and

Javad for providing me with a home away from home. My cousins, Saba, Mana, Sam, Bita, Babak and Sepehr for making Toronto a fun place for me every time we got the chance to hang out. Lastly, I'd like to thank my friends here for knowing exactly how to cheer me up at rough times. Kaveh, kia, Shayan, Lili, Myrto and Ivan. You've been next level!

## Table of Contents

<b>Chapter 1</b> .....	<b>1</b>
<b>Introduction and Literature Review</b> .....	<b>1</b>
1.1. Downstream Purification: Chromatographic Separation .....	2
1.2. Membrane Chromatography.....	6
1.3. Membrane Chromatography Devices .....	8
1.4. Application of membrane chromatography .....	11
1.4.1. Protein capture and intermediate purification.....	11
1.4.2. Late-stage polishing.....	12
1.4.3. Monoclonal antibody purification.....	12
1.4.4. Purification of large biomolecules .....	14
1.5. Laterally-Fed Membrane Chromatography .....	15
1.6. Structure of the Thesis .....	16
1.7. References .....	18
<b>Chapter 2</b> .....	<b>29</b>
<b>A Laterally-Fed Membrane Chromatography Module</b> .....	<b>29</b>
2.1. Abstract .....	30
2.2. Introduction.....	31
2.3. Materials and Methods .....	33
2.4. Results and Discussion .....	37
2.5. Conclusions.....	47
2.6. Acknowledgment .....	47
2.7. References .....	47

<b>Chapter 3.....</b>	<b>51</b>
<b>High-Resolution Protein Separation Using a Laterally-Fed Membrane Chromatography Device .....</b>	<b>51</b>
3.1 Abstract .....	52
3.2 Introduction.....	53
3.3. Materials and Methods .....	57
3.4. Results and Discussion .....	61
3.5. Conclusions.....	73
3.6. Acknowledgements.....	74
3.7. References .....	74
<b>Chapter 4.....</b>	<b>78</b>
<b>Performance Comparison of Laterally-fed Membrane Chromatography (LFMC) Devices with Commercial Packed Resin Columns: Application Case Study for Preparative Separation of IgG1 Charge Variants .....</b>	<b>78</b>
4.1. Abstract .....	79
4.2. Introduction.....	80
4.3. Materials and Methods .....	83
4.3.1. Materials .....	83
4.3.2. LFMC device design and fabrication.....	83
4.3.3. Model protein separation .....	84
4.3.4. Lysozyme oxidation and CEX separation .....	84
4.3.5. Separation of mAb charge variants.....	85
4.4. Results and Discussion .....	85
4.5. Conclusions.....	94

4.6. Acknowledgements .....	95
4.7. References .....	96
<b>Chapter 5 .....</b>	<b>102</b>
<b>High-resolution, preparative purification of PEGylated protein using a laterally-fed membrane chromatography device .....</b>	<b>102</b>
5.1. Abstract .....	103
5.2. Introduction.....	104
5.3. Materials and Methods .....	107
5.3.1. Materials .....	107
5.3.2. LFMC device design and fabrication.....	108
5.3.3. Lysozyme PEGylation.....	110
5.3.4. Cation exchange LFMC .....	110
5.4. Results and Discussion.....	111
5.5. Conclusions.....	119
5.6. Acknowledgements .....	119
5.7. References .....	120
<b>Chapter 6 .....</b>	<b>124</b>
<b>Preparative Separation of Monoclonal Antibody Aggregates by Cation-Exchange Laterally-Fed Membrane Chromatography.....</b>	<b>124</b>
6.1. Abstract .....	125
6.2. Introduction.....	126
6.3. Materials and Methods .....	129
6.2.1. Materials .....	129
6.2.2. Device fabrication .....	129

6.2.3.	EG2-hFc Preparation .....	130
6.2.4.	Cation-exchange laterally-fed membrane chromatography (LFMC) 131	
6.2.5.	Hydrophobic interaction membrane chromatography (HIMC) .....	131
6.2.6.	Native polyacrylamide gel electrophoresis .....	132
6.2.7.	Size-exclusion high-performance liquid chromatography (SE-HPLC) 132	
6.2.8.	Theoretical plate number determination .....	133
6.3.	Results and Discussion .....	134
6.4.	Conclusions .....	145
6.5.	Acknowledgements .....	146
6.6	References .....	146
<b>Chapter 7</b>	<b>.....</b>	<b>152</b>
<b>Ultra-Fast Separation of Monoclonal Antibody Aggregates Using Analytical Laterally-Fed Membrane Chromatography (LFMC)</b>	<b>.....</b>	<b>152</b>
7.1.	Abstract .....	153
7.2.	Introduction .....	154
7.2.	Experimental .....	157
7.2.1.	Materials .....	157
7.2.2.	Size exclusion chromatography (SEC) .....	157
7.2.3.	Native polyacrylamide gel electrophoresis .....	158
7.2.4.	Device fabrication .....	158
7.2.5.	HETP determination .....	159
7.2.6.	Hydrophobic interaction LFMC .....	160

7.3. Results and Discussion .....	160
7.3.1. Feed analysis.....	160
7.3.2. Analytical HI-LFMC separation .....	161
7.3.3. Further improvement at lower dead volume.....	164
7.3.4. Validation.....	165
7.4. Conclusions.....	166
7.5. Acknowledgements .....	167
7.6. References .....	167
<b>Chapter 8.....</b>	<b>171</b>
<b>Contributions and Recommendations.....</b>	<b>171</b>
8.1. Contributions .....	172
8.2. Recommendations for Future Work.....	174
8.3. References .....	176
<b>Appendices .....</b>	<b>178</b>
<b>Copyrights.....</b>	<b>178</b>

## List of Figures

### Chapter 1

Fig 1.1. Solute transport in packed-bed column chromatography (A) and membrane chromatography (B) (adapted from (Orr et al., 2013))

Fig 1.2 Membrane chromatography devices: stacked-disk (A) radial-flow (B) hollow-fiber (C) (adapted from (Orr et al., 2013))

### Chapter 2

Fig 2.1. Flow distribution in conventional, centrally-fed circular membrane adsorber

Fig 2.2. Flow distribution in novel, laterally-fed, rectangular membrane adsorber

Fig 2.3. Blowout diagram of conventional, centrally-fed circular membrane module (from right to left: transparent acrylic top plate, woven wire mesh support/distributor, membrane spacer, membrane disk, membrane spacer, woven wire mesh support/distributor, bottom plate).

Fig 2.4. Blowout diagram of novel, laterally-fed rectangular membrane module (from right to left: transparent acrylic top plate, woven wire mesh support/distributor, membrane spacer, membrane disk, membrane spacer, woven wire mesh support/distributor, bottom plate).

Fig 2.5. Snapshots of the feed and permeate sides of the conventional and novel membrane modules obtained during dye tracer experiments at 0, 3, 6, 9, and 12 s (membrane: hydrophilized PVDF; pore size: 0.22  $\mu\text{m}$ ; feed: 10 times diluted McCormick red food dye in water; volume injected: 250 mL; flow rate: 10 mL/min)

Fig 2.6. Representation of gray scale intensity data obtained from snapshots shown in Fig. 2.5 using Image J (membrane: hydrophilized PVDF; pore size: 0.22

$\mu\text{m}$ ; feed sample: 10 times diluted McCormick red food dye; volume injected: 250 mL; flow rate: 10 mL/min)

Fig 2.7. Flow through lysozyme peaks obtained at non-binding condition with conventional (thin line) and novel (thick line) membrane modules (membrane: Sartobind Q; membrane area:  $12.57 \text{ cm}^2$ ; buffer: 20 mM sodium phosphate; pH=7.0; flow rate: 10 mL/min; A: 250 mL, 2 mg/mL; B: 5mL, 2 mg/ml, C: 10 mL, 1 mg/mL)

Fig 2.8. Breakthrough curves for adsorption of BSA on the anion-exchange membrane obtained using A: conventional (thin line) and B: novel (thick line) membrane modules (membrane: Sartobind Q; membrane area:  $12.57 \text{ cm}^2$ ; feed concentration: 2 mg/mL; volume injected: 30 mL; binding buffer: 20 mM phosphate; pH=7.0; flow rate: 10 mL/min)

Fig 2.9. BSA elution peaks and conductivity profiles obtained using conventional (thin line and thin dashed line respectively) and novel (thick line and thick dashed line respectively) modules (membrane: Sartobind Q; membrane area:  $12.57 \text{ cm}^2$ ; feed concentration: 2 mg/mL; volume injected: 30 mL; binding buffer: 20 mM sodium phosphate, pH 7.0; eluting buffer: binding buffer+0.5 M sodium chloride; flow rate: 10 mL/min)

Fig 2.10. BSA elution peaks and conductivity profiles obtained from pulse binding experiments carried out using conventional (thin line and thin dashed line respectively) and novel (thick line and thick dashed line respectively) modules (membrane: Sartobind Q membrane area:  $12.57 \text{ cm}^2$ ; feed concentration: 1 mg/mL; volume injected: 100 mL; binding buffer: 20 mM sodium phosphate, pH 7.0; eluting buffer: binding buffer+0.5 M sodium chloride; flow rate: 10 mL/min)

### Chapter 3

Fig 3.1. Radial-flow membrane chromatography device

Fig 3.2. Laterally-fed membrane chromatography device

Fig 3.3. Diagram of the prototype laterally-fed membrane chromatography device used in the current study (1: acrylic top plate; 2: delrin frame; 3: acrylic bottom plate)

Fig 3.4. Figure showing the top- and side-views of the plates (A) and the frame (B) used to assemble the laterally-fed membrane chromatography device used in this study. All dimensions are in mm

Fig 3.5. Salt tracer peaks obtained with the radial-flow (thin line) and the laterally-fed (thick line) membrane chromatography devices (membrane: Sartobind S; membrane bed volume: 7mL; feed: 0.5 M NaCl; running buffer: 20 mM sodium phosphate, pH=7.0; flow rate: 10 mL/min; volume injected: 2 mL (A) and 5mL (B))

Fig 3.6. Salt breakthrough curves obtained with the radial-flow (thin line) and laterally-fed (thick line) membrane chromatography devices (membrane: Sartobind; membrane bed volume: 7 mL; feed: 0.5 M NaCl; volume injected: 150 mL; running buffer: 20 mM sodium phosphate, pH=7.0; flow rate: 10 mL/min)

Fig 3.7. Lysozyme elution peaks obtained with the radial-flow (thin lines) and the laterally-fed (thick lines) membrane chromatography devices (membrane: Sartobind S; membrane bed volume: 7 mL; feed concentration: 8 mg/mL; volume injected: 2 mL; binding buffer: 20 mM sodium phosphate, pH=7.0; eluting buffer: binding buffer+0.5 M NaCl; flow rate: 10 mL/min; UV absorbance: solid lines; conductivity: dashed lines; pressure: dotted lines)

Fig 3.8. Lysozyme elution peaks obtained with the radial-flow (thin lines) and the laterally-fed (thick lines) membrane chromatography devices (membrane: Sartobind S; membrane bed volume: 7 mL; feed concentration: 8 mg/mL; volume injected: 5 mL; binding buffer: 20 mM sodium phosphate, pH=7.0; eluting buffer: binding buffer+0.5 M NaCl; flow rate: 10 mL/min; UV absorbance: solid lines; conductivity: dashed lines; pressure: dotted lines)

Fig 3.9. Single-protein peaks obtained with ovalbumin (thin line), conalbumin (medium line), and lysozyme (thick line) using the radial-flow device (membrane: Sartobind S; membrane bed volume: 7 mL; ovalbumin concentration: 0.25 mg/mL; conalbumin concentration: 0.5 mg/mL; lysozyme concentration: 0.25 mg/mL; loop size: 2 mL; binding buffer: 20 mM citrate, pH=5.5; eluting buffer: binding buffer+0.5 M NaCl; linear gradient length: 40 mL; flow rate: 10 mL/min; solid line: UV absorbance; dashed line: conductivity)

Fig 3.10. Ovalbumin flow-through and eluted conalbumin peaks obtained from multi-component separation experiments carried out with the radial-flow device to determine the effect of gradient elution start volume on resolution of bound and eluted proteins (thick lines: 20 mL start; thin lines: 10 mL start; solid line: UV absorbance; dashed line: % eluting buffer; membrane: Sartobind S; membrane bed volume: 7 mL; ovalbumin concentration: 0.25 mg/mL; conalbumin concentration: 0.5 mg/mL; loop size: 2 mL; binding buffer: 20 mM citrate, pH=5.5; eluting buffer: binding buffer+0.5 M NaCl; gradient volume: 40 mL; flow rate: 10 mL/min)

Fig 3.11. Multi-component separation peaks obtained with the radial-flow device using 40 mL (A), 60 mL (B) and 80 mL (C) linear gradients (membrane: Sartobind S; membrane bed volume: 7 mL; ovalbumin concentration: 0.25 mg/mL, conalbumin concentration: 0.5 mg/mL; lysozyme concentration: 0.25 mg/mL; loop size: 2 mL; binding buffer: 20 mM citrate, pH=5.5; eluting buffer: binding buffer+0.5 M NaCl; flow rate: 10 mL/min; solid line: UV absorbance; dashed line: conductivity)

Fig 3.12. Multi-component separation peaks obtained with the laterally device using 20 mL (A), 30 mL (B) and 40 mL (C) linear gradients (membrane: Sartobind S; membrane bed volume: 7 mL; ovalbumin concentration: 0.25 mg/mL, conalbumin concentration: 0.5 mg/mL; lysozyme concentration: 0.25 mg/mL; loop size: 2 mL; binding buffer: 20 mM citrate, pH=5.5; eluting buffer: binding buffer+0.5 M NaCl; flow rate: 10 mL/min; solid line: UV absorbance; dashed line: conductivity)

Fig 3.13. SDS-PAGE analysis of samples obtained from the multi-component protein separation experiment carried out with the laterally-fed device using 40 mL linear gradient elution (1: protein molecular weight markers; 2: flow-through peak, i.e. ovalbumin; 3: first eluted peak, i.e. conalbumin; 4: second eluted peak, i.e. lysozyme)

## Chapter 4

Fig 4.1. Performance comparison of the CEX-LFMC (thick line) and HiTrap SP HP (thin line) for separation of model proteins in 5 mL bed volume scale (membrane: Sartorius S; membrane bed volume: 4.7 mL; feed: 0.1 mg/mL ovalbumin, 1.0 mg/mL conalbumin, 0.5 mg/mL lysozyme; sample volume: 500  $\mu$ L; binding buffer: 20 mM sodium citrate pH 5.5; eluting buffer: binding buffer + 0.5 M NaCl; linear gradient volume: 15 mL (dashed line))

Fig 4.2. Model protein separation using the CEX-LFMC at higher flow rates of 25 mL/min (thin line) and 30 mL/min (thick line) (membrane: Sartorius S; membrane bed volume: 4.7 mL; feed: 0.1 mg/mL ovalbumin, 1.0 mg/mL conalbumin, 0.5 mg/mL lysozyme; sample volume: 500  $\mu$ L; binding buffer: 20 mM sodium citrate pH 5.5; eluting buffer: binding buffer + 0.5 M NaCl; linear gradient volume: 15 mL (dashed line))

Fig 4.3. Elution behavior of oxidized lysozyme (thick line) and the control sample (thin line) using the CEX-LFMC (membrane: Sartorius S; membrane bed volume: 4.7 mL; feed: 0.5 mg/mL lysozyme; sample volume: 2 mL; binding buffer: 20 mM sodium phosphate pH 6.0; eluting buffer: binding buffer + 0.5 M NaCl; linear gradient volume: 20 mL; flow rate: 15 mL/min)

Fig 4.4. Performance comparison of the CEX-LFMC (thick line) and HiTrap SP HP (thin line) for separation of model proteins in 1 mL bed volume scale (membrane: Sartorius S; membrane bed volume: 1 mL; feed: 0.1 mg/mL ovalbumin, 1.0 mg/mL conalbumin, 0.5 mg/mL lysozyme; sample volume: 100  $\mu$ L;

binding buffer: 20 mM sodium citrate pH 5.5; eluting buffer: binding buffer + 0.5 M NaCl; linear gradient volume: 10 mL (dashed line))

Fig 4.5. Model protein separation of the CEX-LFMC at higher flow rates of 10 mL/min (thin line) and 20 mL/min (thick line) (membrane: Sartorius S; membrane bed volume: 1.0 mL; feed: 0.1 mg/mL ovalbumin, 1.0 mg/mL conalbumin, 0.5 mg/mL lysozyme; sample volume: 100  $\mu$ L; binding buffer: 20 mM sodium citrate pH 5.5; eluting buffer: binding buffer + 0.5 M NaCl; linear gradient volume: 10 mL (dashed line))

Fig 4.6. Charge variant separation of HIgG1-CD4 using the CEX-LFMC with 250 mL (thin line) and 300 mL (thick line) salt gradients (membrane: Sartorius S; membrane bed volume: 4.7 mL; feed: 0.5 mg/mL HIgG1-CD4; sample volume: 2 mL; binding buffer: 20 mM sodium phosphate pH 6.0; eluting buffer: binding buffer + 0.5 M NaCl; flow rate: 15 mL/min)

Fig 4.7. Charge variant separation of HIgG1-CD4 using the HiTrap SP HP column with 250 mL (thin line) and 300 mL (thick line) salt gradients (column volume: 5.0 mL; feed: 0.5 mg/mL HIgG1-CD4; sample volume: 2 mL; binding buffer: 20 mM sodium phosphate pH 6.0; eluting buffer: binding buffer + 0.5 M NaCl; flow rate: 15 mL/min)

## Chapter 5

Fig 5.1. Schematic diagram of laterally-fed membrane chromatography (or LFMC)

Fig 5.2. A. Different components of the LFMC device: Acrylic top and bottom plates (shaded dark grey), and PVC middle frame (shaded light grey). B. Fully assembled LFMC device used in the current study (membrane bed volume: 9.25 mL; membrane: strong cation exchange S)

Fig 5.3. Single-step purification of mono-PEGylated lysozyme using 200 mL linear gradient (membrane: Sartorius S; membrane bed volume: 9.25 mL;

lysozyme concentration in reaction mixture: 1 mg/mL; molar ratio: 4:1; reaction time: 4 h; protein concentration in feed: ~2 mg/mL; sample volume: 5 mL; binding buffer: 20 mM sodium acetate pH 5.0; eluting buffer: binding buffer +0.5 M NaCl; flow rate: 15 mL/min; thick line: UV absorbance; dotted line: gradient; dashed line: conductivity)

Fig 5.4. Single-step purification of mono-PEGylated lysozyme using 150 mL linear gradient to 50% eluting buffer followed by a step-change (membrane: Sartorius S; membrane bed volume: 9.25 mL; lysozyme concentration in reaction mixture: 1 mg/mL; molar ratio: 4:1; reaction time: 4 h; protein concentration in feed: ~2 mg/mL; sample volume: 5 mL; binding buffer: 20 mM sodium acetate pH 5.0; eluting buffer: binding buffer +0.5 M NaCl; flow rate: 15 mL/min; thick line: UV absorbance; dotted line: gradient; dashed line: conductivity)

Fig 5.5. Single-step purification of mono-PEGylated lysozyme using 90 mL linear gradient to 50% eluting buffer followed by a step-change (sample injection condition: 20% eluting buffer; membrane: Sartorius S; membrane bed volume: 9.25 mL; lysozyme concentration in reaction mixture: 1 mg/mL; molar ratio: 4:1; protein concentration in feed: ~2 mg/mL; sample volume: 5 mL; binding buffer: 20 mM sodium acetate pH 5.0; eluting buffer: binding buffer +0.5 M NaCl; flow rate: 15 mL/min; thick line: 10 h residence time; thin line: 4 h reaction time; dotted line: gradient; dashed line: conductivity)

Fig 5.6. SDS-PAGE analysis of samples obtained from the single-step purification of mono-PEGylated lysozyme carried out by experiment represented in Fig. 5.5 (A: 4 h reaction time; B: 10 h reaction time; lane 1: molecular weight marker; lane 2: pure lysozyme; lane 4: reaction mixture; lane 5: first peak with shoulder; lane 6: second peak; lane 7: third peak)

Fig 5.7. Comparison of different elution conditions for single-step purification of mono-PEGylated lysozyme (sample injection condition: 20% eluting buffer; A: 90 mL linear gradient to 50% eluting buffer followed by a step-change; B: 120 mL

linear gradient to 50% eluting buffer followed by a step-change; C: 80 mL linear gradient to 30% eluting buffer +60 mL linear gradient to 50% eluting buffer followed by a step-change; membrane: Sartorius S; membrane bed volume: 9.25 mL; lysozyme concentration in reaction mixture: 5 mg/mL; molar ratio: 4:1; reaction time: 10 h; protein concentration in feed: ~10 mg/mL; sample volume: 5 mL; binding buffer: 20 mM sodium acetate pH 5.0; eluting buffer: binding buffer +0.5 M NaCl; flow rate: 15 mL/min; thick line: UV absorbance; dotted line: gradient; dashed line: conductivity)

Fig 5.8. SDS-PAGE analysis of samples obtained from the single-step purification of mono-PEGylated lysozyme carried out by experiment represented in Fig. 5.7A (lane 1: pure lysozyme; lane 4: reaction mixture; lane 5: peak 1, lane 6: peak 2; lane 7: peak 3)

Fig 5.9. Single-step purification of mono-PEGylated lysozyme using 90 mL linear gradient to 50% eluting buffer followed by a step-change (sample injection condition: 20% eluting buffer; membrane: Sartorius S; membrane bed volume: 9.25 mL; lysozyme concentration in reaction mixture: 5 mg/mL; molar ratio: 5:2; reaction time: 10 h; protein concentration in feed: 10 mg/mL; sample volume: 5 mL; binding buffer: 20 mM sodium acetate pH 5.0; eluting buffer: binding buffer +0.5 M NaCl; flow rate: 15 mL/min; thick line: UV absorbance; dotted line: gradient; dashed line: conductivity)

## Chapter 6

Fig 6.S1. Salt tracer using NaCl for determination of number of theoretical plates (membrane: Sartorius S, membrane bed volume: 9.2 mL, feed concentration: 0.8 M, sample volume: 100  $\mu$ L, running buffer: 0.4 M NaCl, flow rate: 15 mL/min)

Fig 6.1. Optimization of gradient elution for separation of 293 derived IgG1 Trastuzumab aggregates (top to bottom: 100 mL, 200 mL, 250 mL, 300 mL

gradient, membrane: Sartorius S, membrane bed volume: 4.6 mL, feed concentration: 0.5 mg/mL, sample volume: 2 mL, binding buffer: 20 mM sodium phosphate pH 6.0, eluting buffer: binding buffer + 0.5 M NaCl, flow rate: 20 mL/min)

Fig 6.2. Preparative LFMC separation of Trastuzumab aggregates (membrane: Sartorius S, membrane bed volume: 4.6 mL, feed concentration: 2.5 mg/mL, sample volume: 5 mL, binding buffer: 20 mM sodium phosphate pH 6.0, eluting buffer: binding buffer + 0.5 M NaCl, linear gradient length: 300 mL, flow rate: 20 mL/min, solid line: UV absorbance, dashed line: percent eluting buffer)

Fig 6.3. Analytical HPMC chromatograms obtained using samples collected from the preparative Trastuzumab aggregates separation experiment shown in Figure 6.2 (membrane: hydrophilized PVDF (0.22  $\mu\text{m}$  pore size), membrane bed volume: 0.4 mL, feed concentration: 0.2 mg/mL, sample volume: 500  $\mu\text{L}$ , binding buffer: 1.5 M ammonium sulfate in 20 mM sodium phosphate pH 7.0, eluting buffer: 20 mM sodium phosphate pH 7.0, linear gradient length: 40 mL, flow rate: 4 mL/min)

Fig 6.4. Native PAGE analysis of the samples collected from the preparative Trastuzumab aggregates separation experiment shown in Figure 6.2.

Fig 6.5. Preparative cation-exchange LFMC for separation of Campath-1H samples (thick solid line: UV absorbance for monomer-rich sample, thin solid line: UV absorbance for aggregates-rich sample or “dimers”, membrane: Sartorius S, membrane bed volume: 1.0 mL, feed concentration: 0.75 mg/mL, sample volume: 500  $\mu\text{L}$ , binding buffer: 20 mM sodium phosphate pH 6.0, eluting buffer: binding buffer + 0.5 M NaCl, linear gradient length: 150 mL, flow rate: 10 mL/min, dashed line: percent eluting buffer)

Fig 6.6. Optimization of operating pH for separation of EG2-hFc aggregates (thick solid line: pH 5.0, medium solid line: pH 5.5, thin solid line: pH 6.0, membrane: Sartorius S, membrane bed volume: 4.6 mL, feed concentration: 0.05

mg/mL, sample volume: 5 mL, binding buffer: 20 mM sodium phosphate, eluting buffer: binding buffer + 0.5 M NaCl, linear gradient length: 30 mL, flow rate: 20 mL/min, dashed line: percent eluting buffer)

Fig 6.7. Optimization of gradient length for separation of EG2-hFc aggregates (thin line: 30mL linear gradient, thick line: 60 mL linear gradient, membrane: Sartorius S, membrane bed volume: 4.6 mL, feed concentration: 0.05 mg/mL, sample volume: 5 mL, binding buffer: 20 mM sodium phosphate pH 6.0, eluting buffer: binding buffer + 0.5 M NaCl, flow rate: 20 mL/min, dashed line: percent eluting buffer)

Fig 6.8. Preparative cation-exchange LFMC for separation of EG2-hFc aggregates (membrane: Sartorius S, membrane bed volume: 9.2 mL, feed concentration: 0.05 mg/mL, sample volume: 45 mL, binding buffer: 20 mM sodium phosphate pH 6.0, eluting buffer: binding buffer + 0.5 M NaCl, linear gradient length: 60 mL, flow rate: 20 mL/min, dashed line: percent eluting buffer)

Fig 6.9. Size exclusion chromatography (SEC) of the samples collected during preparative separation of EG2-hFc aggregates (thin line: monomer peak, thick line: aggregate peak, column: TSK-GEL G3000SWXL 7.8 mm× 300 mm, sample volumes: 10  $\mu$ L, running buffer: 20 mM sodium phosphate buffer + 250 mM NaCl, flow rate: 0.3 mL/min)

## Chapter 7

Fig 7.1. Blowout diagram of the analytical laterally-fed membrane chromatography device (LFMC), A: acrylic top plate; B: membrane stack (three layers of hydrophilized PVDF membranes; 0.22  $\mu$ m pore size; GVWP14250); C: plastic shim spacer; D: acrylic bottom plate.

Fig 7.2. Feed analysis of the CHO cell line derived Alemtuzumab (campath-1H), A: SE-HPLC (thick line: monomer-rich sample; thin line: dimer rich sample; column: TSK-Gel G3000SWXL 7.8 mm× 300 mm; feed concentration: 0.25

mg/mL; sample volume: 10  $\mu$ L; running buffer: 20 mM sodium phosphate pH 7.0 + 250 mM NaCl; flow rate: 0.3 mL/min); B: native PAGE, 7% (1: monomer-rich sample; 2: dimer-rich sample)

Fig 7.3. Analysis of CHO cell line derived Alemtuzumab (campath-1H) aggregates using HI-LFMC (A: dimer-rich sample; B: monomer-rich sample; membrane: hydrophilized PVDF, 0.22  $\mu$ m pore size, GVWP14250; membrane bed volume: 0.4 mL; feed concentration: 0.2 mg/mL; sample volume: 250  $\mu$ L; eluting buffer: 20 mM sodium phosphate buffer pH 7.0; binding buffer: eluting buffer + 1.5 M ammonium; linear gradient: 40 mL; flow rate: 16 mL/min; dashed line: % eluting buffer)

Fig 7.4. Analysis of dimer-rich CHO cell line derived Alemtuzumab (campath-1H) aggregates using HI-LFMC (A: 40 mL gradient; B: 80 mL gradient; C: 120 mL gradient; membrane: hydrophilized PVDF, 0.22  $\mu$ m pore size, GVWP14250; membrane bed volume: 0.4 mL; feed concentration: 0.2 mg/mL; sample volume: 250  $\mu$ L; eluting buffer: 20 mM sodium phosphate buffer pH 7.0; binding buffer: eluting buffer + 1.5 M ammonium; flow rate: 16 mL/min)

Fig 7.5. Analysis of monomer-rich CHO cell line derived Alemtuzumab (campath-1H) aggregates using HI-LFMC (A: 30 mL gradient, lower dead volume; B: 40 mL gradient, lower dead volume; C: 40 mL gradient, higher dead volume; membrane: hydrophilized PVDF, 0.22  $\mu$ m pore size, GVWP14250; membrane bed volume: 0.4 mL; feed concentration: 0.2 mg/mL; sample volume: 250  $\mu$ L; eluting buffer: 20 mM sodium phosphate buffer pH 7.0; binding buffer: eluting buffer + 1.5 M ammonium; flow rate: 16 mL/min)

Fig 7.6. Analysis of monoclonal antibody (mAb) aggregates using HI-LFMC (A: HIgG1-CD4; B: HEK cell line derived IgG1; membrane: hydrophilized PVDF, 0.22  $\mu$ m pore size, GVWP14250; membrane bed volume: 0.4 mL; feed concentration: 0.2 mg/mL; sample volume: 250  $\mu$ L; eluting buffer: 20 mM sodium

phosphate buffer pH 7.0; binding buffer: eluting buffer + 1.5 M ammonium; linear gradient: 40 mL; flow rate: 16 mL/min)

## List of Tables

### Chapter 2

Table 2.1 Characteristics of flow-through peaks obtained from experiments carried out using lysozyme in non-binding condition with conventional and novel modules as shown in Fig. 2.7 (membrane: Sartobind Q; membrane area: 12.57 cm<sup>2</sup>; buffer: 20 mM sodium phosphate; pH=7.0; flow rate: 10 mL/min; A: 250 mL, 2mg/mL; B: 5 mL, 2 mg/ml, C: 10 mL, 1 mg/mL)

Table 2.2 Bovine serum albumin (BSA) binding capacity of the Sartobind Q anion-exchange membrane at two different breakthrough points designation for conventional and novel modules (membrane: Sartobind Q; membrane area: 12.57 cm<sup>2</sup>; feed concentration: 2 mg/mL; volume injected: till saturation ~30 mL; binding buffer: 20 mM phosphate; pH=7.0; flow rate: 10 mL/min)

Table 2.3 Characteristics of the elution curves obtained from the breakthrough experiments using bovine serum albumin (BSA) for conventional and novel modules as shown in Fig. 9 (membrane: Sartobind Q; membrane area: 12.57 cm<sup>2</sup>; feed concentration: 2 mg/mL; volume injected: ~30 mL; binding buffer: 20 mM sodium phosphate, pH 7.0; eluting buffer: binding buffer+0.5 M sodium chloride; flow rate: 10 mL/min)

Table 2.4 Characteristics of the elution curves obtained from the breakthrough experiments using bovine serum albumin (BSA) for conventional and novel modules as shown in Fig. 9 (membrane: Sartobind Q; membrane area: 12.57 cm<sup>2</sup>; feed concentration: 2 mg/mL; volume injected: ~30 mL; binding buffer: 20 mM sodium phosphate, pH 7.0; eluting buffer: binding buffer+0.5 M sodium chloride; flow rate: 10 mL/min)

### Chapter 3

Table 3.1 Characteristics of pulse tracer peaks (shown in Fig. 3.5) obtained with sodium chloride using the radial-flow and the laterally-fed membrane

chromatography devices (membrane: Sartobind S; membrane bed volume: 7 mL; tracer: 0.5 M NaCl; running buffer: 20 mM sodium phosphate, pH=7.0; flow rate: 10 mL/min)

Table 3.2 Characteristics of lysozyme elution peaks (shown in Figs. 3.7 and 3.8) obtained in the bind-and-elute mode with the radial-flow and the laterally-fed devices (membrane: Sartobind S; membrane bed volume: 7 mL; lysozyme concentration: 8 mg/mL; binding buffer: 20 mM sodium phosphate, pH=7.0; eluting buffer: binding buffer+0.5 M NaCl; flow rate: 10 mL/min)

#### **Chapter 4**

Table 4.1 Design details of the LFMC devices

Table 4.2 Pressure drops

#### **Chapter 6**

Table 6.1 Design details of the LFMC devices

**List of Abbreviations**

AEX	anion exchange
CEX	cation exchange
AFFF	asymmetric flow field fractionation
BSA	bovine serum albumin
C	carboxyl
CE	capillary electrophoresis
CE-LFMC	cation exchange laterally-fed membrane chromatography
CFD	computational fluid dynamics
CHO	Chinese hamster ovary
DEAE	diethylaminoethyl
DF	diafiltration
FDA	food and drug administration
HCP	host cell protein
HEK	human embryonic kidney
HETP	height equivalent to theoretical plates
HIC	hydrophobic interaction chromatography
HI-LFMC	hydrophobic interaction membrane chromatography
HIMC	hydrophobic interaction membrane chromatography
HP	high performance
HPLC	high performance liquid chromatography

HTPD	high throughput process development
IEX	ion exchange chromatography
IgG	immunoglobulin G
LFMC	laterally-fed membrane chromatography
LRV	log volume reduction
LS	light scattering
mAb	monoclonal antibody
MBV	membrane bed volume
NSERC	natural sciences and engineering research council of Canada
ORF-RE	Ontario research fund research excellence
pI	isoelectric point
PC	polycarbonate
PES	polyethersulfone
PVDF	polyvinylidene fluoride
Q	quaternary ammonium
RC	regenerated cellulose
S	sulphonated
SDS-PAGE	sodium dodecyl sulfate polyacrylamide gel electrophoresis
SEC	size exclusion chromatography
SE-HPLC	size exclusion high performance liquid chromatography
UF	ultrafiltration

UPLC        ultra-high performance (pressure) liquid chromatography

ZRM        zonal rate model

## Preface

This Ph.D. dissertation is organized in a sandwich style based on the published, submitted, and prepared for submission articles described below respectively:

1. Madadkar. P., Qijiayu. Wu., Ghosh. R. Laterally-fed membrane chromatography module. *J. Membr. Sci.* 487 (2015) 173-179. (Chapter 2)
2. Madadkar. P., Ghosh. R. High-Resolution Protein Separation Using a Laterally-Fed Membrane Chromatography Device. *J. Membr. Sci.* 499 (2016) 126-133. (Chapter 3)
3. Madadkar. P., Nino. S. L., Ghosh. R. High-resolution, preparative purification of PEGylated protein using a laterally-fed membrane chromatography device. *J. Chromatogr. B.* 1035 (2016) 1-7. (Chapter 5).
4. Madadkar. P., Sadavarte. R., Butler. M., Durocher. Y., Ghosh. R. Preparative separation of monoclonal antibody aggregates by cation-exchange laterally-fed membrane chromatography. Submitted to *Journal of Chromatography B.* (Chapter 6)
5. Madadkar. P., Sadavarte. R., Ghosh. R. Performance comparison of laterally-fed membrane chromatography (LFMC) devices with commercial packed resin columns: application case study in preparative separation of IgG1 charge variants. Pending submission to *Journal of Chromatography A.* (Chapter 4)
6. Madadkar. P., Umatheva. U., Hale. G., Ghosh. R. Ultra-fast separation of monoclonal antibody aggregates using analytical laterally-fed membrane chromatography (LFMC). Submitted to *Analytical Chemistry Journal.* (Chapter 7)

All the articles were prepared by Pedram Madadkar with direct supervision and guidance from Dr. Raja Ghosh who also contributed in all the manuscript preparations. For the project described in chapter 2, Dr. Qijiayu Wu conducted a portion of the experiments. All the experiments described in chapter 3 were run by Pedram Madadkar. Mr. Rahul Sadavarte contributed in conducting experiments for

the projects described in chapters 4 and 6. Mr. Sergio Luna Nino and Ms. Umatheny Umatheva helped with conducting experiments included in chapters 5 and 7 respectively as project students during summers 2015 and 2016 correspondingly in the Bioseparation Engineering research group under direct supervision of Pedram Madadkar. Dr. Michael Butler, Dr. Yves Durocher, and Dr. Geoff Hale kindly donated some of the samples used to conduct experiments described in chapters 6 and 7 and helped with manuscript preparation. The work reported in this dissertation was carried out from May 2013 to December 2016.

## **Chapter 1**

### **Introduction and Literature Review**

### **1.1. Downstream Purification: Chromatographic Separation**

Production of therapeutic proteins also referred to as Biopharmaceuticals in the upstream cell culture is accompanied by a wide range of contaminants including the product-related impurities which have very similar properties with the target biological molecules. Accordingly, the purification process development is very challenging, requiring an intricate combination of different bioseparation tools [1].

Downstream processing of biological molecules includes clarification [2], primary product capture, intermediate purification of impurities, and polishing which are followed by the concentration and formulation of the final product. While the clarification steps are heavily reliant on both filtration and non-filtration techniques, chromatographic separation is the workhorse in all the other stages [3,4].

The definition of chromatographic separation is the isolation of the target molecule from a mixture which is carried out by means of diverse chemical interactions with the stationary phase. The type of stationary phase, properties of the binding and elution buffers, and feed concentration are the main parameters which highly affect the performance of chromatography. The most widely used techniques are based on affinity [5], ion exchange [6], hydrophobic interaction [7], and reversed phase chromatography. Mixed-mode chromatography which uses a combination of these techniques has been also investigated in the recent years [8,9].

Commonly, the clarified bioreactor harvest firstly goes through primary protein capture which is usually carried out using bind-and-elute affinity chromatography or cation-exchange chromatography (CEX). The result is the major volume reduction and removal of contaminants. Capture chromatography is commonly followed by differential chromatography stages in which the impurities are separated based on their binding strength differences with the target molecule via gradient elution. Subsequently, low concentration of impurities are removed in the flow-through late-stage polishing operations [10,11].

Chromatographic separation is dominated by packed-bed resin columns which provide the bioseparation operations with high resolutions. However, there are major shortcomings associated with using porous beads and gels as the stationary phase. The solute transport to the binding sites within the pores is dominated by diffusion, the direct impact of which is the poor mass transfer rates and the dependency of the resolution on the operating flow rate. Therefore, the column chromatography processes are very slow, resulting in elongated processing times which cause degradation and denaturation of the molecules. The nature of mass transport in columns requires high liquid volumes which highly increases the sterile buffer consumption, acting as a major source of processing cost.

The pressure drops within packed bed columns are considerably high which demands for costly equipment such as high-pressure pumps and sealing. The problem which is exacerbated with bed consolidation. The looser packing density at the edges compared to the center region causes hysteresis i.e. difference in flow rates along the column cross section which causes the cheese-cake effect, namely, the cracking and collapsing of the packing material [12]. The formation of gaps often leads to channeling within the column and results in short-circuiting which is highly unwanted [13].

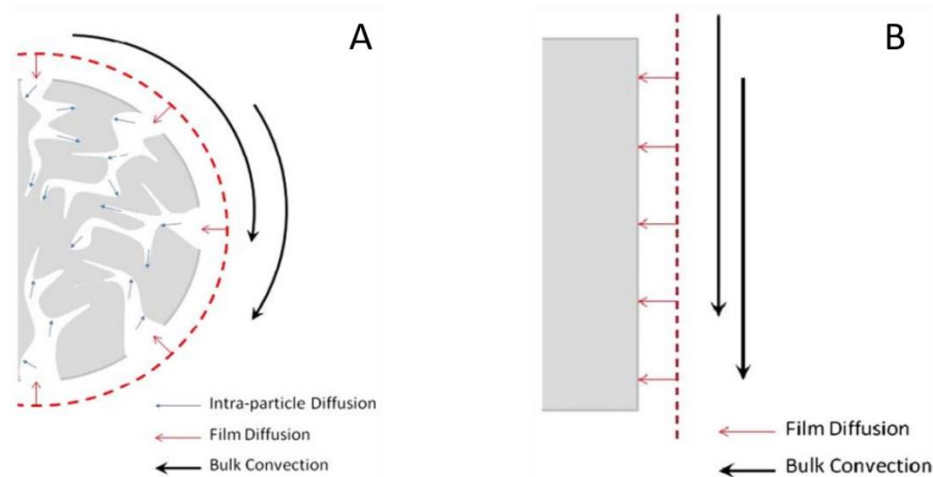


**Fig. 1.1:** Solute transport in packed-bed column chromatography (A) and membrane chromatography (B) (adapted from [14])

The scale up of columns are very complex [15] to the point that economy of scale does not exist beyond a certain point [16]. Scale-down studies are mostly carried out by milligrams of material using columns with 1 mL bed volume (2.5 cm bed height), based on which the standard laboratories (40 mL bed volume, 20 cm bed height) are carried out. The scale-up is then through keeping the same bed height and velocity [16]. Also, parameters such as residence time and column configuration should be maintained proportional. This is very hard to achieve in resin-based columns [17]. In practice, larger columns demand higher cost of resins and buffer as well as facility layouts and infrastructure. For instance, in order to capture 30 kg of protein, the column should have diameter as big as 2 m (with the typical bed height of 20 cm) assuming typical binding capacity of ~50 g/L [12].

Despite all the above-mentioned limitations column chromatography has remained the linchpin in separations where there is similarities between the physicochemical properties of the target molecule and the other cellular component impurities. This is because of the molecular-level complementarity of the technique and the resulting high resolutions [10].

Owing to the high capital cost and low-throughputs at the same time with being the inseparable technique in biopharmaceutical industry, column chromatography has remained as the bottleneck in biomanufacturing. This is while in the past couple of decades, there has been remarkable advancement in the upstream manufacturing which has kept up with the rapid increase in the demand for biopharmaceutical products. Recombinant proteins are now being manufactured with titers as high as 10 g/L with bioreactors available in several thousands of liters [12]. Orders of magnitude higher batch volumes and titers has removed the production costs from the cell culture while the downstream has failed to keep up. Currently, 50-60% of the overall cost for cell-derived products is leveraged on the downstream purification [18]. In addition, cell-culture manufacturing has experienced the development of single-use bioreactors which expedites process validation and enhances the flexibility of process development [19].

As packed-bed columns have been unsuccessful to meet the technical requirements towards the high-throughput, single-use, and continuous operations, the application of other stationary phases has been widely considered over the past few decades which include adsorptive membranes, monoliths, and mixed-matrix membranes. The rest of this chapter is focused around membrane chromatography and therefore, the other two chromatographic media have been only briefly discussed below with pertinent references.

Monoliths are single-unit polymeric material having networks of large porous interconnections based on which the operations are performed at much higher flow rates and moderate pressures as opposed to the resin beads. Monoliths are prepared using different materials and are available in wide range of shapes [20], sizes, and porosity and therefore suitable for processing of different biological molecules [21,22]. Monolithic separations in analytical and preparative monoclonal antibody (mAb) purifications is widely seen over the literature and the transition from research to industry has already commenced [21,23]. Due to providing higher porosity, they are highly suitable for clearance of larger molecules such as viruses. [24]. Nevertheless, when compared to adsorptive membranes, commercialized monoliths are excessively more expensive (by an order of magnitude) which is considered as their main disadvantage.

Mixed matrix membrane chromatography has emerged as a technique which combines the membrane and resins in one stationary media. The preparation is through mixing the adsorptive resin with the membrane polymer solution. The suspension is then made into flat sheet membranes or hollow fibers. Mixed matrix chromatography was initially developed for ion exchange (IEX) membrane chromatography [25-27] and more recently for hydrophobic interaction chromatography in separation of whey proteins [28]. This is while they have not found wide commercial applications.

## 1.2. Membrane Chromatography

Adsorptive membranes include a wide range of functionalized microporous (i.e. controlled pore sizes with diameters within the range of 0.03-10  $\mu\text{m}$ ) membranes which bind the target molecule based on the ligand chemistry [29, 30]. The main advantage of membrane chromatography is the dominance of convective mass transfer as opposed to the diffusion limited solute transport within the resin beads. This feature translates to an order of magnitude higher speed of operation as the resolution of separation is independent of flow rate over a wide range [13,30].

The most commonly used support material for adsorptive membranes are regenerated cellulose (RC), nylon, polycarbonate (PC), polyethersulfone (PES), and polyvinylidene fluoride (PVDF). The support should provide high mechanical strength, high internal surface area which meets the required ligand density, enough resistance to different solvents, and hydrophilic surfaces to avoid non-specific binding [30]. The pore size and distribution are normally in the same range with microfiltration membranes. Relatively large pore sizes make adsorptive membranes highly suitable for processing of large molecules while it is unfavorable from the binding capacity point of view. The bed height in membrane chromatography is provided by stacking certain number of membrane layers which is highly advantageous in moderating the effect of pore distribution [13,14].

The ligand chemistries are commonly similar to the ones used with resin beads [31,32]. Widely used ligands in membrane chromatography include both strong and weak anionic and cationic exchangers including quaternary ammonium (Q), diethylaminoethyl (DEAE), sulfonated (S), and carboxyl (C) [14]. While alkyl chains are normally used with resins, there is not much interest in using them for membrane chromatography. Application of Sartobind phenyl in bind and elute chromatography showed acceptable binding capacity and scalability [33].

The adsorption of material on ion exchange membranes is normally carried out at relatively low conductivity, followed by elution with high salt buffer [34]. The high

concentration of electrolytes in the eluting buffer decreases the Debye length which results in the decrease in the retention factor of the protein [35]. The adsorption of proteins on hydrophobic membranes is carried out under high salt concentrations. That makes it an ideal separation after high salt elution ion exchange separation [28]. This is highly reliant on the salt type and concentration [36]. The antichaotropic salts in the beginning of the Hofmeister series, mostly  $\text{NH}_4^+$ , due to having high salting out effects are suitable for hydrophobic interaction membrane chromatography (HIMC). High concentration of these salts would expose the hydrophobic patches of the protein molecule to the ligands available on the porous support of the membrane, determining the binding capacity of the chromatographic system.

Membrane chromatography devices or membrane adsorbers eliminate the packing and unpacking stages which is a significant advancement in large-scale purification [37]. The advantages of single-use membrane chromatography in polishing include the reduction in capital requirements, increasing the process flexibility, minimizing the risk of cross contamination, and elimination of the cleaning and regeneration steps [38,39]. The most attractive reason for moving towards the disposable technology is the elimination of such validation steps. FDA regulations involve maintenance, cleaning, and sanitization of the equipment including the streamline development, housing, and the vessels. This should be carried out at an appropriate interval so that to protect the operation unit from contamination [40]. From the manufacturing cost point of view, although the consumable cost for membrane chromatography is higher owing to the single-use operations; however, the extensively lower cost of buffer and utility as well as the lower capital and labor costs compensate for that [38,41]. In addition, the elimination of diffusion factors make the scale-up of membrane chromatography linear.

The features of membrane chromatography processes make the process development much simpler compared to columns. However, owing to the

relentless pressure on biomanufacturing companies to reduce the overall manufacturing costs, high-throughput process development (HTPD) is essential. This requirement has been met through miniaturization and automation in which low sample volumes can be used to study diverse experimental conditions. [1,42,43].

### **1.3. Membrane Chromatography Devices**

Membrane chromatography has found broad application in the flow-through operations in which the target molecule does not bind to the membrane stack as opposed to the impurities. This is while currently developed membrane adsorbers fail to give acceptable resolution for bind-and-elute operations with very few commercialized large-scale applications [44]. While inherently lower binding capacity of adsorptive membranes has been the perceived cause of their failure to provide satisfactory resolutions in membrane adsorbers, the device design plays an important role. Although this has been the primary motivation for this work, it is necessary to know the drawbacks of the currently available devices [45]. Membrane chromatography devices are available in two different formats: stacked-disk and radial flow (spiral-wound). Hollow fiber membrane adsorbers have also been studied.

Stacked-disk devices resemble the syringe micro-filters and perform well in lab scale operations. However, their performance drastically fails in larger scale. The flow path lengths for the solute flowing through the center of the device is much shorter than the solutes flowing through the peripheral regions. This is owing to the high radial to axial dimension aspect ratio [46]. Therefore, the breakthrough from the center regions is normally commenced before the saturation occurs at the outer radial regions of the membrane stack [47-49]. The poor utilization of binding capacity in stacked disk devices was initially addressed by tapering in both inlet and outlet of the capsules. Later, the application of flow distributors containing plural channels helped with increasing the uniformity of the flow over the cross

section of the membrane. The channel depths were higher in the center and lower closer to the peripheral regions [48].

Radial flow devices, also referred to as spiral wound, are fabricated by wrapping a sheet of membrane around a cylindrical core. This configuration provides great scalability in which the binding capacity is proportional to the membrane surface area and normally the bed height is kept constant [17]. Nevertheless, the design is associated with severe shortcomings, including variation of membrane area over the bed height and large dead volumes. Therefore, there is a huge variability over the flow path lengths and solute residence times. The superficial velocity is also disturbed over the bed height and is not uniform. These dispersion effects are aggravated by the considerable dead volumes. In consequence, they give broad elution peaks which makes them unsuitable for bind and elute applications [13,14]. In other words, the intrinsic resolution of such short membrane bed heights is very high; however, this is highly affected by the flow maldistribution [50]. Very recently, radial flow devices were used for fractionation of lysozyme and ovotransferrin from chicken egg white through binding the target molecule in two cation-exchange steps [51]. The radial flow device offered good yields and purification factors; nevertheless, the possibility of separation was due to the pI value difference of the two proteins. However, these devices would not be suitable for performing more challenging bind and elute separations.

Hollow fiber membrane device have also been studied for membrane chromatography applications owing to their interesting features which would suit the large-scale applications, majorly the high surface area in a small module which offers high capacity. The tubes mostly have diameters of 0.25 to 2.5 mm [13]. In scale-up of hollow-fiber devices parameters such as transmembrane pressure and residence time are kept constant. However, they are not suitable for pulse-inputs and therefore have not found acceptance in the industry [30,45,52]

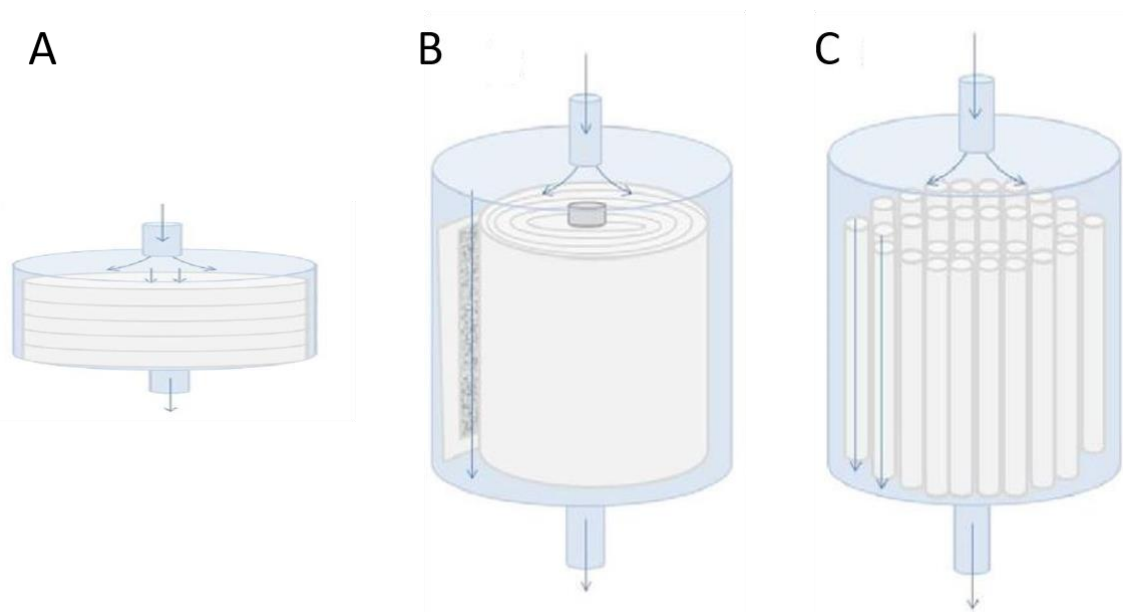


**Fig. 1.2:** Membrane chromatography devices: stacked-disk (A) radial-flow (B) hollow-fiber (C) (adapted from [14])

Modeling of membrane adsorbers requires detailed knowledge on the adsorption kinetics of the solute on the membrane as well as the flow convection and diffusion parameters. Different adsorption isotherms have been used in the modeling studies based on the type of binding [30,47,53].

The performance of the binding capacity utilization is studied by breakthrough curves [54,55]. Ideally, breakthrough curves should demonstrate a step change from no solute in the permeate to the point that the permeate concentration is equal to the feed concentration. However, due to such flow non-idealities the breakthrough curves are S shaped, the extent of which demonstrates the ligand binding utilization of the system.

A detailed model has to consider for the dispersion effects within the system including the module and the fittings. The dispersion effects comprise of the flow non-idealities, void volume of the membranes, flow distributors both in the distribution head and collection head, and the mixing as a result of the void

volumes [30]. Such non-idealities are the major source of band broadening [30]. The fittings also play a role in dispersion effects.

Two types of time lag effects have been mostly taken into account in the models. The delay due to the volume and the lag as a result of mixing effects which are modelled by PFR (zero order) and CSTR (first order) reactors respectively [53,56]. In another model, the use of CSTR/PFR was considered after the membrane module to account for the dispersion effects in the collection region [49]. This is while it was later shown that this approach is not sufficient for the stacked-disc devices in quantitative modeling of the breakthrough curves [57]. Such one-dimensional models assume that the flow is homogenous over the cross section of the membranes which is practically untrue based on the device features.

In addition, a zonal rate model (ZRM) was described to address the deficiency of the previous approach on the effect of dispersion [46,47]. The semi-empirical model (i.e. involving a combination of measurement and theory) discusses the non-binding conditions based on zones with homogeneous velocity in which the axial dispersion is neglected. The study of internal flow patterns independent of the binding kinetics is essential in studying the breakthrough and module design as well as the scale-up [46]. The ZRM studies were followed by computational flow dynamics (CFD) modeling of membrane chromatography capsules which considered for the binding parameters at the same time with offering a mechanistic understanding of the flow non-idealities. This was made possible through having precise information on the internal geometry of both stacked-disk and radial flow capsules [58].

#### **1.4. Application of membrane chromatography**

##### **1.4.1. Protein capture and intermediate purification**

Frontal affinity chromatography in which the device is fed with continuous flow of the material to the point of saturation and breakthrough has been studied for the adsorptive membranes [59]. One of the major limitations associated with

membrane chromatography is the lower inherent binding capacity of adsorptive membranes compared to resins which is owing to their lower surface area per volume. This has been addressed through developing membranes with higher binding capacity by polymer grafting to the existing membranes [58,60] or by development of new membrane technologies [18]. Also, ion-exchange chromatography is the most widely studied technique with adsorptive membranes. This is while in intermediate stages the separations are carried out in the bind-and-elute mode with gradient elution. However, none of the currently available membrane chromatography devices are suitable to be used in the large-scale bind and elute unit operations.

#### **1.4.2. Late-stage polishing**

The main parameter in late-stage polishing is the speed of processing large volumes of material and because the impurities are available in low concentrations the adsorptive capacity is not a limiting parameter.

Conventional resin columns operate at 100-150 cm/hr linear flow rate and thus in order for the columns to process high volumes of material, the column diameter should be larger than a meter which results in large column volumes. Considering the high binding capacity and low titers of the contaminants, columns are significantly underused [38]. On the contrary, membrane adsorbers offer high-surface area and low bed heights based on which the polishing is carried out at significantly higher flow rates. Accordingly, the footprint for the membrane device is much lower as a the equivalent membrane device would have two orders of magnitude lower bed volume [61].

#### **1.4.3. Monoclonal antibody purification**

Monoclonal Antibodies (mAbs) are the biggest class of biopharmaceutical with a \$40 billion market in 2010 which are used as therapeutic agents for cancer, autoimmune, and infectious diseases with numerous others in the pre-clinical studies. Owing to the advances in the recombinant technology in the past three

decades, mAbs are generated with high-expressing cell lines [12,19,62,63]. It is notable that many mAbs are generated from the same framework due to the similarities between different products.

Protein A affinity resins are the most widely used in capture chromatography of monoclonal antibodies. The binding is based on the affinity of the  $F_c$  region of the mAb and the protein A ligand. The main advantages include relatively high capacity, significant volume reduction and robustness to purification of different variations of the molecules. However, the elution occurs at low pH which is considered as harsh condition for the proteins, often leading to aggregation. The drawback is the leaching of the protein A which should not exceed 10 ppm. The other concern is the lifetime of the resins. However, membrane chromatography has not found industrial application in this section owing to the binding capacity limitations discussed earlier [14,64].

Following capture chromatography, mAbs normally go through a three column and seldom two-column ion exchange separation [63]. The separation of mAb aggregates is normally carried out in this stage. Substitution of IEX membrane chromatography in this section has been considered [19,66-69].

The intermediate purification steps are followed by late-stage polishing which are carried out in the flow-through mode where membrane chromatography has found the most commercial applications [19]. The impurities include viruses, endotoxins, DNA, and other host cell proteins (HCPs) which are mostly negatively charged and would bind to the anion-exchange (AEX) chromatographic media during flow-through operations. While weak anion-exchangers have been also looked into [60], Q membrane chromatography is the most famous technique [37]. Most host cell proteins (HCPs) have low pI values compared to the mAbs (target molecules) which mostly have pI of 8-9. Among the impurities which are in anion-exchange polishing, host cell proteins would require low conductivity buffers compared to others [34]. In some cases, the presence of considerable amounts of aggregates

may cause membrane fouling and lead to high pressure drops. This has shown to affect the lifetime of the membranes with relatively lower porosity (Mustang Q) in small scale studies of the AEX membrane chromatography [69,70]

The other contaminants are mostly large molecules which in case of using resin columns will not diffuse in the pores and therefore adsorptive membranes are highly advantageous [38,72]. Higher log reduction value (LRV) has been reported for membrane chromatography devices (5-7) [30]. In operation with Q membranes it should be considered that the salt can be problematic as the LRV values are greatly sensitive to salt concentration [73] dropping drastically from 50-150 mM salt concentrations. The performance of other ligands has been studied towards having more salt-tolerant membrane adsorbers for viral clearance. It has been demonstrated that the high binding capacity at high concentrations is due to other interactions such as hydrophobic and hydrogen bonds [74]. The increase in the binding capacity is not only through increasing the ligand density as it may result to steric hindrance. However, the pore structure and three dimensional arrangement of the ligands are highly effective [75].

Performance of different commercially available devices including Mustang Q, Sartobind Q, and ChromaSorb were compared for virus purification [75,76]. The challenges involve the sensitivity of binding capacity on the conductivity and pH of the feed which requires adjustment prior to the unit operations.

The downstream purification includes stages for viral inactivation as well as chromatographic and size-based removals [76]. Often pre-filter are used prior to the viral filters to decrease the frequency of their replacement [63]. Finally, ultrafiltration (UF) or diafiltration (DF) techniques are employed for volume reduction which is followed by formulation.

#### **1.4.4. Purification of large biomolecules**

While packed-bed columns remain as the state of the art in purification of mAbs except for polishing stages, in separation of plasmid DNA [78-80] and viruses

lower-cost alternatives have taken over [4,81]. The capture of virus vectors from mammalian cell culture for gene therapy such as retro-, adeno-, and lenti- viruses is where AEX membrane chromatography is highly advantageous [70,82,83]. Using Mustang Q membranes researchers were able to concentration lentivirus by 140 folds, an order of magnitude higher than other techniques [84]. The AEX membrane chromatography showed to have 20-25 times higher binding capacity for Plasmid DNA and 55-550 time higher flow rates when compared to bead chromatography [78].

### **1.5. Laterally-Fed Membrane Chromatography**

This thesis discusses the development of novel devices for membrane chromatography applications. The laterally-fed membrane chromatography devices houses a stack of rectangular membranes with identical rectangular channels for lateral distribution of the feed and collection of the permeate [85,86]. The device has shown to be highly suitable for high resolution separation of multiple proteins in the bind and elute mode. The advancement in the resolution is due to the uniform solute flow path length and residence time within the device.

LFMC devices offer high throughput, cost effective, and single-use processes similar to the currently available membrane adsorbers. In addition, they provide resolutions which are comparable with resin columns. The combination of high throughput and high resolution perfectly meets the current requirements in downstream purification of biopharmaceuticals. The devices are highly scalable for large-scale applications and have also shown to be very suitable for analytical separations.

It is notable that the Sartobind membranes which are widely used in this dissertation are flat sheet membranes from Sartorius (Goettingen, Germany). When they were first commercialized, they had nylon support with 0.45  $\mu\text{m}$  nominal pore size. However, they were soon changed to regenerated cellulose support with 3-5  $\mu\text{m}$  pore size which have high stability and low non-specific binding [87]. Based

on the information reported by the manufacturer the Sartobind ion exchange membrane have the ligand density of 2-5  $\mu\text{eq}/\text{cm}^2$  and porosity of 80%. The same membranes with phenyl ligands has been studied for the hydrophobic interaction membrane chromatography (HIMC) of proteins [28].

## **1.6. Structure of the Thesis**

This thesis consists of eight chapters including the current one. Chapter 1, gives an introduction on downstream purification of proteins and chromatographic separation which is followed by a comprehensive literature review on membrane chromatography. As membrane chromatography is a relatively new area, the references are majorly from the past twenty years. Chapters 2 to 7 cover six full projects which were accomplished towards the device design and development of the laterally-fed membrane chromatography (LFMC) technology with focus on application case studies. The last chapter summarizes the contribution of this work on the field of membrane chromatography and discusses the future opportunities and deliverables.

The principles of the LFMC is discussed in chapter 2 through comparing the performance of a LFMC module with a conventional circular module using one layer of Sartobind Q AEX membranes. Tracer experiments using both dye and a model protein under non-binding conditions were used to study and compare the flow distribution and collection within the modules. This was followed by obtaining the breakthrough curves and studying the binding capacity of the devices and pulse binding experiments using bovine serum albumin (BSA). The use of identical membranes with the same surface area and bed volume greatly showed the effect of module design.

Based on the primary findings, a LFMC device was designed which housed a stack of Sartobind S CEX membranes. Fabricated by 3D printing, the performance of the device was head-to-head compared with the equivalent commercially available radial flow membrane chromatography device containing the same membrane

(Sartobind SingleSep mini, 7 mL). With the focus on the performance of the devices in bind and elute separation of multiple proteins, chapter 3 includes the study of flow distribution within the devices using tracer experiments which were followed by single- and multiple- protein bind and elute separation.

The resolutions obtained with the LFMC device were greatly motivating to the point that they were compared with resin columns in chapter 4. Initially, the device design was modified towards simpler fabrication and lower dead volumes. Then, the performance of the CEX-LFMC was head-to-head compared with HiTrap HP SP columns from GE life sciences. Three model proteins were used for multiple component separations in the bind and elute mode at both 1 mL and 5 mL bed volumes. The resolutions were compared at different operating flow rates and the results were argued. Finally the two systems were compared in separation of IgG1 charge variants.

Chapter 5 discusses the first application case study of the LFMC devices for purification of PEGylated proteins. PEGylation is one of the most widely studied post-translational modification of therapeutic proteins which is accompanied by impurities [88]. Cation exchange chromatography has shown to be one of the most promising techniques in purification of the mono-PEGylated proteins which is the target molecule [89,90]. PEGylation of lysozyme was carried out using methoxy-polythyleneglycol propionaldehyde (or m-PEG propionaldehyde) in the batch mode. Preparative CEX-LFMC was used to separate the mono-PEGylated lysozyme (the target) from higher PEGylated proteins and unreacted lysozyme in a single step. The elution conditions were then optimized for resolution and speed and efficient recovery of the unreacted protein.

The other application case study is the separation of monoclonal antibody aggregates. Cation exchange resin columns have been widely used for large-scale purification of mAb aggregates [91]. However, currently available membrane adsorbers would perform poorly for this application. In chapter 6 we investigated

the application of CEX-LFMC devices containing Sartobind S membranes in three different scales for separation of aggregates from different mAb samples.

It is notable that separation of mAb aggregates by hydrophobic interaction membrane chromatography using hydrophilic environmental responsive membranes has been previously studied in our group [92]. The same PVDF membranes were housed in a modified version of LFMC devices adapted to analytical scale separations (chapter 7). The goal was to develop an ultra-fast assay with cost-effective and single-use devices for analytical mAb aggregate separation.

### 1.7. References

- [1] R. Bhambure, K. Kumar, A.S. Rathore, High-throughput process development for biopharmaceutical drug substances., *Trends Biotechnol.* 29 (2011) 127–35.
- [2] N. Singh, A. Arunkumar, S. Chollangi, Z.G. Tan, M. Borys, Z.J. Li, Clarification technologies for monoclonal antibody manufacturing processes: Current state and future perspectives, *Biotechnol. Bioeng.* 113 (2015) 698–716.
- [3] A.T. Hanke, M. Ottens, Purifying biopharmaceuticals: Knowledge-based chromatographic process development, *Trends Biotechnol.* 32 (2014) 210–220.
- [4] E.N. Lightfoot, J.L. Coffman, F. Lode, Q.S. Yuan, T.W. Perkins, T.W. Root, Refining the description of protein chromatography, *J. Chromatogr. A.* 760 (1997) 139–149.
- [5] A.C. a Roque, C.S.O. Silva, M.A. Taipa, Affinity-based methodologies and ligands for antibody purification: advances and perspectives., *J. Chromatogr. A.* 1160 (2007) 44–55.

- [6] S. Fekete, A. Beck, J.L. Veuthey, D. Guillarme, Ion-exchange chromatography for the characterization of biopharmaceuticals, *J. Pharm. Biomed. Anal.* 113 (2015) 43–55.
- [7] J.F. Kramarczyk, B.D. Kelley, J.L. Coffman, High-throughput screening of chromatographic separations: II. Hydrophobic interaction, *Biotechnol. Bioeng.* 100 (2008) 707–720.
- [8] K. Zhang, X. Liu, Mixed-mode chromatography in pharmaceutical and biopharmaceutical applications, *J. Pharm. Biomed. Anal.* 128 (2016) 73-88.
- [9] J. Chen, J. Tetrault, Y. Zhang, A. Wasserman, G. Conley, M. DiLeo, E. Haimes, A. E. Nixon, A. Ley, The distinctive separation attributes of mixed-mode resins and their application in monoclonal antibody downstream purification process. *J. Chromatogr. A.* 1217 (2010) 216-224.
- [10] T.M. Przybycien, N.S. Pujar, L.M. Steele, Alternative bioseparation operations: life beyond packed-bed chromatography., *Curr. Opin. Biotechnol.* 15 (2004) 469–78.
- [11] A.L. Zydney, Continuous downstream processing for high value biological products: A Review, *Biotechnol. Bioeng.* 113 (2016) 465–475.
- [12] U. Gottschalk, Bioseparation in antibody manufacturing: The good, the bad and the ugly, *Biotechnol. Prog.* 24 (2008) 496–503.
- [13] R. Ghosh, Protein separation using membrane chromatography: opportunities and challenges., *J. Chromatogr. A.* 952 (2002) 13–27.
- [14] V. Orr, L. Zhong, M. Moo-Young, C.P. Chou, Recent advances in bioprocessing application of membrane chromatography., *Biotechnol. Adv.* 31 (2013) 450–65.
- [15] F.G. Lode, A. Rosenfeld, Q.S. Yuan, T.W. Root, E.N. Lightfoot, Refining the scale-up of chromatographic separations, *J. Chromatogr. A.* 796 (1998) 3–14.

- [16] S. Gerontas, M. Asplund, R. Hjorth, D.G. Bracewell, Integration of scale-down experimentation and general rate modelling to predict manufacturing scale chromatographic separations, *J. Chromatogr. A.* 1217 (2010) 6917–6926.
- [17] T.N. Warner, S. Nochumson, Innovations of Membrane Chromatography, *Pharma. Tech.* (2002) 36-42.
- [18] B. V Bhut, K. a Christensen, S.M. Husson, Membrane chromatography: protein purification from *E. coli* lysate using newly designed and commercial anion-exchange stationary phases., *J. Chromatogr. A.* 1217 (2010) 4946–57.
- [19] J.H. Chon, G. Zarbis-Papastoitsis, Advances in the production and downstream processing of antibodies, *N. Biotechnol.* 28 (2011) 458–463.
- [20] R.D. Arrua, T.J. Causon, E.F. Hilder, Recent developments and future possibilities for polymer monoliths in separation science, *Analyst.* 137 (2012) 5179.
- [21] T. Barroso, A. Hussain, A.C.A. Roque, A. Aguiar-Ricardo, Functional monolithic platforms: Chromatographic tools for antibody purification, *Biotechnol. J.* 8 (2013) 671–681.
- [22] F. Svec, Y. Lv, Advances and recent trends in the field of monolithic columns for chromatography, *Anal. Chem.* 87 (2015) 250–273.
- [23] T. Barroso, M. Temtem, A. Hussain, A. Aguiar-Ricardo, A.C.A. Roque, Preparation and characterization of a cellulose affinity membrane for human immunoglobulin G (IgG) purification, *J. Memb. Sci.* 348 (2010) 224–230.
- [24] M.R. Etzel, W.T. Riordan, Viral clearance using monoliths, *J. Chromatogr. A.* 1216 (2009) 2621–2624.
- [25] M.-E. Avramescu, Z. Borneman, M. Wessling, Dynamic behavior of adsorber membranes for protein recovery., *Biotechnol. Bioeng.* 84 (2003) 564–72.

- [26] M.E. Avramescu, Z. Borneman, M. Wessling, Particle-loaded hollow-fiber membrane adsorbers for lysozyme separation, *J. Memb. Sci.* 322 (2008) 306–313.
- [27] S.M. Saufi, C.J. Fee, Fractionation of  $\beta$ -Lactoglobulin from whey by mixed matrix membrane ion exchange chromatography, *Biotechnol. Bioeng.* 103 (2009) 137–148.
- [28] S.M. Saufi, C.J. Fee, Mixed matrix membrane chromatography based on hydrophobic interaction for whey protein fractionation, *J. Memb. Sci.* 444 (2013) 157–163.
- [29] T.B. Tennikova, F. Svec, B.G. Belenkii, High-Performance Membrane Chromatography. A Novel Method of Protein Separation, *J. Liq. Chromatogr.* 13 (1990) 63–70.
- [30] C. Boi, Membrane adsorbers as purification tools for monoclonal antibody purification., *J. Chromatogr. B. Analyt. Technol. Biomed. Life Sci.* 848 (2007) 19–27.
- [31] C. Charcosset, Review Purification of Proteins by Membrane Chromatography, 71 (1998) 95-110.
- [32] A. Saxena, B.P. Tripathi, M. Kumar, V.K. Shahi, Membrane-based techniques for the separation and purification of proteins: an overview., *Adv. Colloid Interface Sci.* 145 (2009) 1–22.
- [33] M. Kuczewski, N. Fraud, R. Faber, G. Zarbis-Papastoitsis, Development of a polishing step using a hydrophobic interaction membrane adsorber with a PER.C6-derived recombinant antibody, *Biotechnol. Bioeng.* 105 (2010) 296–305.
- [34] R. van Reis, A. Zydney, Bioprocess membrane technology, *J. Memb. Sci.* 297 (2007) 16–50.

- [35] E. Hallgren, F. Kalman, D. Farnan, C. Horvath, J. Stahlberg, Protein retention in ion-exchange chromatography: effect of net charge and charge distribution. *J. Chromatogr. A.* 877 (2000) 13-24.
- [36] A. Kosior, M. Antořová, R. Faber, L. Villain, M. Polakovič, Single-component adsorption of proteins on a cellulose membrane with the phenyl ligand for hydrophobic interaction chromatography, *J. Memb. Sci.* 442 (2013) 216–224.
- [37] J.X. Zhou, T. Tressel, Membrane Chromatography as a Robust Purification System for Large-Scale Antibody Production, (2005) 33–35.
- [38] J.A.C. Lim, A. Sinclair, D.S. Kim, U. Gottschalk, Economic benefits of single-use membrane chromatography in polishing, *Bioprocess Int.* (2007) 48–56.
- [39] A. a. Shukla, U. Gottschalk, Single-use disposable technologies for biopharmaceutical manufacturing, *Trends Biotechnol.* 31 (2013) 147–154.
- [40] J. Mora, A. Sinclair, N. Delmdahl, U. Gottschalk, Disposable Membrane Chromatography, *Bioprocess Int.* (2006) 38–43.
- [41] S. Muthukumar, T. Muralikrishnan, R. Mendhe, A.S. Rathore, Economic benefits of membrane chromatography versus packed bed column purification of therapeutic proteins expressed in microbial and mammalian hosts, *J. Chem. Technol. Biotechnol.* (2016).
- [42] O. Kökpınar, D. Harkensee, C. Kasper, T. Scheper, R. Zeidler, O.-W. Reif, R. Ulber, Innovative modular membrane adsorber system for high-throughput downstream screening for protein purification., *Biotechnol. Prog.* 22 (2006) 1215–9.
- [43] S. Muthukumar, A.S. Rathore, High throughput process development (HTPD) platform for membrane chromatography, *J. Memb. Sci.* 442 (2013) 245–253.

- [44] J.H. Vogel, H. Nguyen, R. Giovannini, J. Ignowski, S. Garger, A. Salgotra, J. Tom, A new large-scale manufacturing platform for complex biopharmaceuticals, *Biotechnol. Bioeng.* 109 (2012) 3049–3058.
- [45] E. Klein, D. Yeager, R. Seshadri, U. Baurmeister, Affinity adsorption devices prepared from microporous poly ( amide ) hollow fibers and sheet membranes, *J. Memb. Sci.* 129 (1997) 31–46.
- [46] E. von Lieres, J. Wang, M. Ulbricht, Model Based Quantification of Internal Flow Distributions from Breakthrough Curves of Flat Sheet Membrane Chromatography Modules, *Chem. Eng. Technol.* 33 (2010) 960–968.
- [47] P. langmi, E. von Lieres, C. a Haynes, Zonal rate model for stacked membrane chromatography. I: characterizing solute dispersion under flow-through conditions., *J. Chromatogr. A.* 1218 (2011) 5071–8.
- [48] R. Ghosh, T. Wong, Effect of module design on the efficiency of membrane chromatographic separation processes, *J. Memb. Sci.* 281 (2006) 532–540.
- [49] D.K. Roper, E.N. Lightfoot, Separation of biomolecules using adsorptive membranes, *J. Chromatogr. A.* 702 (1995) 3–26.
- [50] M. a Teeters, T.W. Root, E.N. Lightfoot, Performance and scale-up of adsorptive membrane chromatography., *J. Chromatogr. A.* 944 (2002) 129–39.
- [51] J. Brand, E. Dachmann, M. Pichler, S. Lotz, U. Kulozik, A novel approach for lysozyme and ovotransferrin fractionation from egg white by radial flow membrane adsorption chromatography: Impact of product and process variables, *Sep. Purif. Technol.* 161 (2016) 44–52.
- [52] K. Hagiwara, S. Yonedu, K. Saito, T. Shiraishi, T. Sugo, T. Tojyo, E. Katayama, High-performance purification of gelsolin from plasma using anion-exchange porous hollow-fiber membrane, *J. Chromatogr. B Anal. Technol. Biomed. Life Sci.* 821 (2005) 153–158.

- [53] S.E. Bower, S.R. Wickramasinghe, Elimination of non-uniform, extra-device flow effects in membrane adsorbers, *J. Memb. Sci.* 330 (2009) 379–387.
- [54] K.H. Gebauer, M.R. Kula, I. Enzymtechnologie, H. Dfisseldorf, P.O. Box, Breakthrough performance of high-capacity membrane adsorbers in protein chromatography, *J. Chromatogr. A* 52 (1997) 405-419.
- [55] S.Y. Suen, M.R. Etzel, Sorption kinetics and breakthrough curves for pepsin and chymosin using pepstatin A affinity membranes., *J. Chromatogr. A* 686 (1994) 179–92.
- [56] C. Boi, S. Dimartino, G.C. Sarti, Modelling and simulation of affinity membrane adsorption, *J. Chromatogr. A* 1162 (2007) 24–33.
- [57] D. He, M. Ulbricht, Preparation and characterization of porous anion-exchange membrane adsorbers with high protein-binding capacity, *J. Memb. Sci.* 315 (2008) 155–163.
- [58] P. Ghosh, K. Vahedipour, M. Lin, J.H. Vogel, C. Haynes, E. von Lieres, Computational fluid dynamic simulation of axial and radial flow membrane chromatography: mechanisms of non-ideality and validation of the zonal rate model., *J. Chromatogr. A* 1305 (2013) 114–22.
- [59] a Tejeda-Mansir, R.M. Montesinos, R. Guzmán, Mathematical analysis of frontal affinity chromatography in particle and membrane configurations., *J. Biochem. Biophys. Methods* 49 (2001) 1–28.
- [60] B. V Bhut, K. a Christensen, S.M. Husson, Membrane chromatography: protein purification from E. coli lysate using newly designed and commercial anion-exchange stationary phases., *J. Chromatogr. A* 1217 (2010) 4946–57.
- [61] J. Mora, A. Sinclair, N. Delmdahl, U. Gottschalk, Disposable Membrane Chromatography, *Bioprocess Int.* (2006) 38–43.

- [62] P.A. Marichal-Gallardo, M.M. Alvarez, State-of-the-art in downstream processing of monoclonal antibodies: Process trends in design and validation, *Biotechnol. Prog.* 28 (2012) 899–916.
- [63] A.A. Shukla, B. Hubbard, T. Tressel, S. Guhan, D. Low, Downstream processing of monoclonal antibodies-Application of platform approaches, *J. Chromatogr. B Anal. Technol. Biomed. Life Sci.* 848 (2007) 28–39.
- [64] O.P. Dancette, J.L. Taboureau, E. Tournier, C. Charcosset, P. Blond, Purification of immunoglobulins G by protein A/G affinity membrane chromatography, *J. Chromatogr. B Biomed. Sci. Appl.* 723 (1999) 61–68.
- [65] A.A. Shukla, J. Thommes, Recent advances in large-scale production of monoclonal antibodies and related proteins, *Trends Biotechnol.* 28 (2010) 253–261.
- [66] H.L. Knudsen, R.L. Fahrner, Y. Xu, L. a Norling, G.S. Blank, Membrane ion-exchange chromatography for process-scale antibody purification., *J. Chromatogr. A.* 907 (2001) 145–54.
- [67] X. Santarelli, F. Domergue, G. Clofent-Sanchez, M. Dabadie, R. Grissely, C. Cassagne, Characterization and application of new macroporous membrane ion exchangers., *J. Chromatogr. B. Biomed. Sci. Appl.* 706 (1998) 13–22.
- [68] F.T. Sarfert, M.R. Etzel, Mass transfer limitations in protein separations using ion-exchange membranes., *J. Chromatogr. A.* 764 (1997) 3–20.
- [69] K. Suck, J. Walter, F. Menzel, A. Tappe, C. Kasper, C. Naumann, R. Zeidler, T. Scheper, Fast and efficient protein purification using membrane adsorber systems., *J. Biotechnol.* 121 (2006) 361–7.
- [70] A.R. Lajmi, S. Nochumson, A. Berges, Impact of antibody aggregation on a flowthrough anion-exchange membrane process, *Biotechnol. Prog.* 26 (2010) 1654–1661.

- [71] J.X. Zhou, T. Tressel, U. Gottschalk, F. Solamo, A. Pastor, S. Dermawan, T. Hong, O. Reif, J. Mora, F. Hutchison, M. Murphy, New Q membrane scale-down model for process-scale antibody purification, *J. Chromatogr. A.* 1134 (2006) 66–73.
- [72] J. Thömmes, M. Etzel, Alternatives to chromatographic separations, *Biotechnol. Prog.* 23 (2007) 42–45.
- [73] M.R. Etzel, W.T. Riordan, Viral clearance using monoliths, *J. Chromatogr. A.* 1216 (2009) 2621–2624.
- [74] W. Riordan, S. Heilmann, K. Brorson, K. Seshadri, Y. He, M. Etzel, Design of salt-tolerant membrane adsorbers for viral clearance, *Biotechnol. Bioeng.* 103 (2009) 920–929.
- [75] J. Weaver, S.M. Husson, L. Murphy, S.R. Wickramasinghe, Anion exchange membrane adsorbers for flow-through polishing steps: Part I. clearance of minute virus of mice, *Biotechnol. Bioeng.* 110 (2013) 491–499.
- [76] J. Weaver, S.M. Husson, L. Murphy, S.R. Wickramasinghe, Anion exchange membrane adsorbers for flow-through polishing steps: Part II. Virus, host cell protein, DNA clearance, and antibody recovery, *Biotechnol. Bioeng.* 110 (2013) 500–510.
- [77] R. van Reis, a Zydney, Membrane separations in biotechnology., *Curr. Opin. Biotechnol.* 12 (2001) 208–11.
- [78] H.N. Endres, J. a C. Johnson, C. a Ross, J.K. Welp, M.R. Etzel, Evaluation of an ion-exchange membrane for the purification of plasmid DNA., *Biotechnol. Appl. Biochem.* 37 (2003) 259–266.
- [79] P. Guerrero-Germán, D.M.F. Prazeres, R. Guzmán, R.M. Montesinos-Cisneros, A. Tejeda-Mansir, Purification of plasmid DNA using tangential flow

filtration and tandem anion-exchange membrane chromatography, *Bioprocess Biosyst. Eng.* 32 (2009) 615–623.

[80] M. a Teeters, S.E. Conrardy, B.L. Thomas, T.W. Root, E.N. Lightfoot, Adsorptive membrane chromatography for purification of plasmid DNA., *J. Chromatogr. A.* 989 (2003) 165–73.

[81] B. Kalbfuss, M. Wolff, L. Geisler, A. Tappe, R. Wickramasinghe, V. Thom, U. Reichl, Direct capture of influenza A virus from cell culture supernatant with Sartobind anion-exchange membrane adsorbers, *J. Memb. Sci.* 299 (2007) 251–260.

[82] D.J. McNally, D. Darling, F. Farzaneh, P.R. Levison, N.K.H. Slater, Optimised concentration and purification of retroviruses using membrane chromatography, *J. Chromatogr. A.* 1340 (2014) 24–32.

[83] K. Zimmermann, O. Scheibe, A. Kocourek, J. Muelich, E. Jurkiewicz, A. Pfeifer, Highly efficient concentration of lenti- and retroviral vector preparations by membrane adsorbers and ultrafiltration., *BMC Biotechnol.* 11 (2011) 55.

[84] R.H. Kutner, S. Puthli, M.P. Marino, J. Reiser, Simplified production and concentration of HIV-1-based lentiviral vectors using HYPERFlask vessels and anion exchange membrane chromatography., *BMC Biotechnol.* 9 (2009) 10.

[85] R. Ghosh, P. Madadkar, Q. Wu, On the workings of laterally-fed membrane chromatography, *J. Memb. Sci.* 516 (2016) 26–32.

[86] R. Ghosh, P. Madadkar, Laterally-fed membrane chromatography device, 62304379, 2016.

[87] W. Demmer, D. Nussbaumer, Large-scale membrane adsorbers., *J. Chromatogr. A.* 852 (1999) 73–81.

[88] C.J. Fee, J.M. Van Alstine, PEG-proteins: Reaction engineering and separation issues, *Chem. Eng. Sci.* 61 (2006) 924–939.

- [89] M. Abe, P. Akbarzaderaleh, M. Hamachi, N. Yoshimoto, S. Yamamoto, Interaction mechanism of mono-PEGylated proteins in electrostatic interaction chromatography, *Biotechnol. J.* 5 (2010) 477–483.
- [90] D. Yu, R. Ghosh, Method for studying immunoglobulin G binding on hydrophobic surfaces, *Langmuir.* 26 (2010) 924–929.
- [91] Z. Xu, J. Li, J.X. Zhou, Process Development for Robust Removal of Aggregates Using Cation Exchange Chromatography in Monoclonal Antibody Purification With Implementation of Quality By Design, *Prep. Biochem. Biotechnol.* 42 (2012) 183–202.
- [92] L. Wang, G. Hale, R. Ghosh, Non-size-based membrane chromatographic separation and analysis of monoclonal antibody aggregates., *Anal. Chem.* 78 (2006) 6863–7.

## **Chapter 2**

### **A Laterally-Fed Membrane Chromatography Module**

Reprinted with permission. Copyright 2015 ELSEVIER Journal

## 2.1. Abstract

Module design is of critical importance in membrane chromatography as the efficiency of separation is highly dependent on fluid flow distribution and collection within the membrane device. We discuss a novel, laterally-fed module, designed specifically for flat-sheet membrane chromatography. The performance of the novel module was compared with that of a conventional, centrally-fed, circular membrane module. Experiments were carried out with both devices using anion-exchange membrane sheets having the same surface area and thickness, and thereby the same bed volume. Tracer experiments using either a dye or a protein (lysozyme) under non-binding condition clearly indicated superior flow distribution and collection within the novel module. This could be attributed to greater uniformity in solute flow path length. The protein binding capacities of membrane sheets of identical surface area and bed volume housed in the novel and conventional modules were compared in the breakthrough and pulse modes, using bovine serum albumin (or BSA) as the model adsorbed protein. The breakthrough experiments showed that at the same experimental conditions, the 1% breakthrough binding capacity of the membrane housed in the novel module was 5.12 times higher than that housed in the conventional module. Moreover, flow-through and elution peaks obtained with the novel membrane module were significantly sharper and more symmetrical, with lower peak width.

**Keywords** Membrane chromatography; Protein; Module Design; Flow distribution

## 2.2. Introduction

Membrane chromatography is a relatively new purification technique which involves the use of a stack of synthetic membrane as chromatographic media [1–9]. The most attractive feature of membrane chromatography is the speed of separation. As solute transport is largely based on convection, the time taken for solute to reach its binding site during adsorption and away from it during elution is significantly lower than in column chromatography, where such transport is diffusion-limited. Membrane chromatography could therefore be faster by more than one order of magnitude, a factor which contributes towards higher productivity and decrease in product degradation by proteolysis, denaturation and aggregation. The predominance of convection also makes it easier to model membrane chromatography as the diffusion based terms in the equations could be eliminated. It is also much easier to develop thumb-rules for scaling up separation processes. Membrane chromatography is frequently scaled-up in a modular fashion, i.e. by using multiple devices either in series or in parallel. The disposable nature of membrane chromatography devices eliminates the need for equipment cleaning and revalidation is one of the main factors behind its acceptance by users in recent years.

The efficiency of membrane chromatography is critically dependent on the fluid flow distribution within the membrane device [5, 8–12]. Membrane chromatography devices are commonly available in two formats: (a) stacked disks, and (b) radial flow. Both types of devices suffer from poor flow distribution which leads to shallow breakthrough and consequently poor binding capacity utilization [13–17]. Hollow fiber membrane chromatography devices are also available [7,16] but they are less commonly used. The stacked disk devices which resemble a syringe-type micro-filters are relatively easy to fabricate, and are used for preliminary process development work. However, stacked disk devices with large bed volumes are impractical and the circular shape of the membrane results in significant material wastage. Stacked disks typically have small bed heights with

relatively large radial dimension (see Fig. 2.1). The feed enters at a location corresponding to the center of the first disk, while the flow-through is collected from the center of the last membrane in the stack. Consequently, the central region of the stack gets saturated with solute much earlier than the peripheral regions leading to poor breakthrough binding capacities. Radial flow devices have complicated design, and are used for large-scale purification. They have large dead volumes on both feed and permeate sides, and a large central core for supporting the membrane, and therefore extremely poor device volume utilization [13]. The availability of devices with better design would increase the efficiency of membrane chromatography based separation processes, and this in turn could potentially make this technology more attractive to potential users. A good membrane device should give a sharp solute breakthrough; have low void volume and be based on a simple design with well-defined flow path. While there is significant potential for research and development work on efficient membrane devices, mathematical modeling, operational aspects, and process optimization of membrane chromatography, relatively less has been published in the above-mentioned areas [18–23].

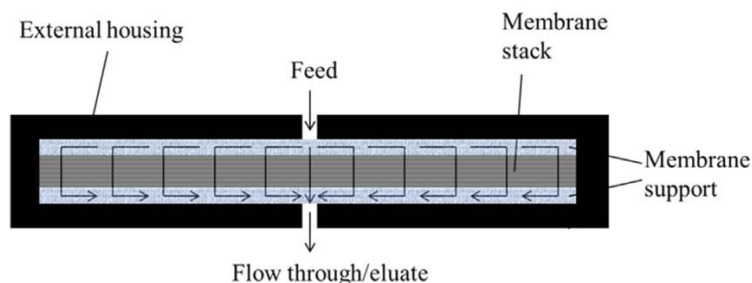


**Fig. 2.1:** Flow distribution in conventional, centrally-fed circular membrane adsorber

In this paper, we discuss a novel membrane chromatography module [24] which addresses some of the issues highlighted in the previous paragraph. The module which is shown in Fig. 2.2 houses a stack of rectangular flat sheet adsorptive membranes. Fluid entering the device is distributed in a lateral manner over the

side of the membrane stack closer to the inlet. The fluid then enters the membrane stack at different locations along its length, flow normal to the membrane surface, and eventually emerges at the other side of the membrane stack. The fluid then flow laterally with respect to the surface of the last membrane in the stack and is collected at the device outlet. The lateral-flows on both sides of the membrane stack are parallel and in the same direction. As shown in Fig. 2.2, the flow path lengths are uniform which is expected to improve the efficiency of membrane utilization and thereby result in a higher breakthrough binding capacity. The performance of the novel device was compared with that of an equivalent centrally-fed, disk-based membrane module. Anion- exchange membrane sheets having the same surface area and thickness, and thereby same bed volume were used in both devices. Tracer experiments were carried out using a dye as well as a protein (lysozyme) under non-binding condition. Bovine serum albumin (or BSA) was used as model binding protein to determine the binding capacities of membrane sheets of identical surface area and bed volume housed in the novel and conventional modules were compared in the breakthrough and pulse modes. The results obtained are discussed.

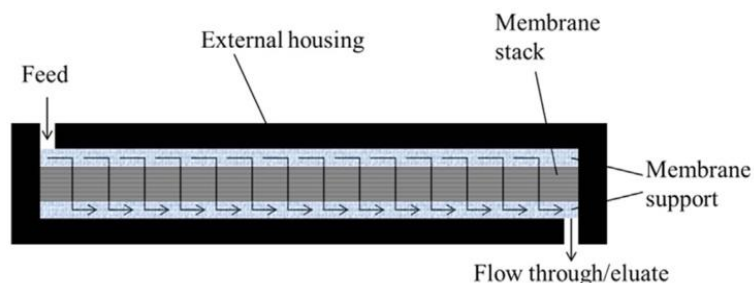


**Fig. 2.2:** Flow distribution in novel, laterally-fed rectangular membrane adsorber

### 2.3. Materials and Methods

Bovine serum albumin (A2153), lysozyme (L6876), sodium phosphate monobasic (S0751), sodium phosphate dibasic (S0876), and sodium chloride (S7653) were purchased from Sigma-Aldrich (St. Louis, MO, USA). Red food dye was purchased

from (McCormick, Sparks, MD, USA). Sartobind Q anion-exchange membrane sheet (94IEXQ42-001, 275 mm thickness) was purchased from Sartorius (Gottingen, Germany). Hydrophilized PVDF membrane (0.22 mm; GVWP) was purchased from Millipore (Billerica, MA, USA). All buffers and sample solutions were prepared using ultra-pure water (18.2 MΩcm) obtained from a SIMPLICITY 185 water purification unit from Millipore (Molsheim, France). The detailed design of the conventional circular module for housing disk-shaped membrane is shown in Fig. 2.3 while that of the novel module is shown in Fig. 2.4. The circular module had an outer diameter of 75mm while the novel module had an external dimension of 200 mm × 40 mm. As shown in Figs. 2.3 and 2.4 membrane assemblies consisting of the adsorptive membrane sandwiched between two Teflon spacers (each of 0.508 mm thickness) was held between the top and bottom plates. The circular or rectangular spaces within the Teflon spacers on both sides of a membrane were filled with woven wire meshes which served as membrane support and liquid distributor. Appropriately positioned screws were used to hold the top and bottom plates together. The effective membrane area in both of these devices was 12.57 cm<sup>2</sup>. The effective diameter of membrane used in the circular module which corresponded to the area of the space within the Teflon spacer was 40 mm whereas the effective length and breadth of the membrane housed within the novel device was 157 mm × 8 mm. The dimensions of the inlet and outlet were minimized as much as possible to reduce the dead volume of these devices to reduce sample dilution and thereby improve separation efficiency. Similar tubings and connectors were used for both devices. The effective dead volumes including that within the device and connectors for the conventional and the novel device were 1.45 and 1.35mL respectively. These values were obtained by measuring the volume of water required to fill the module and associated fittings. In addition to the inlet and outlet, the modules were provided with additional ports for priming and removal of bubbles prior to each run.

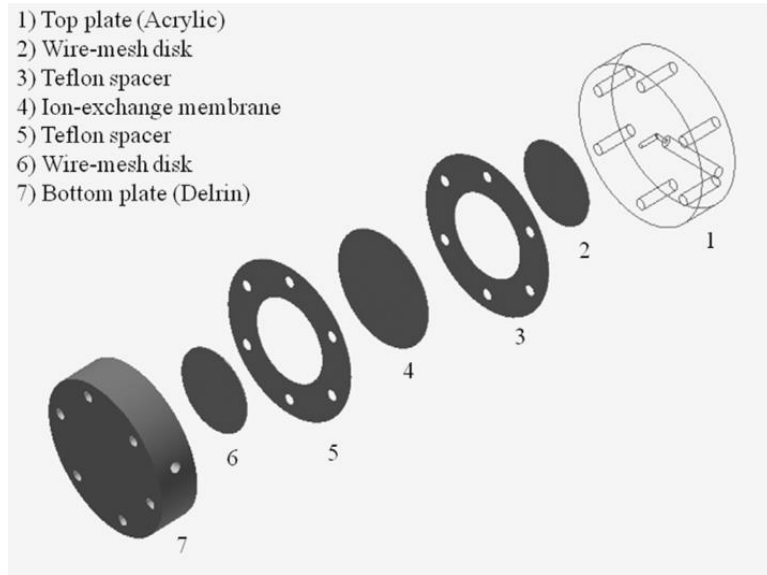


**Fig. 2.3:** Blowout diagram of conventional, centrally-fed circular membrane module (from right to left: transparent acrylic top plate, woven wire mesh support/ distributor, membrane spacer, membrane disk, membrane spacer, woven wire mesh support/distributor, bottom plate)

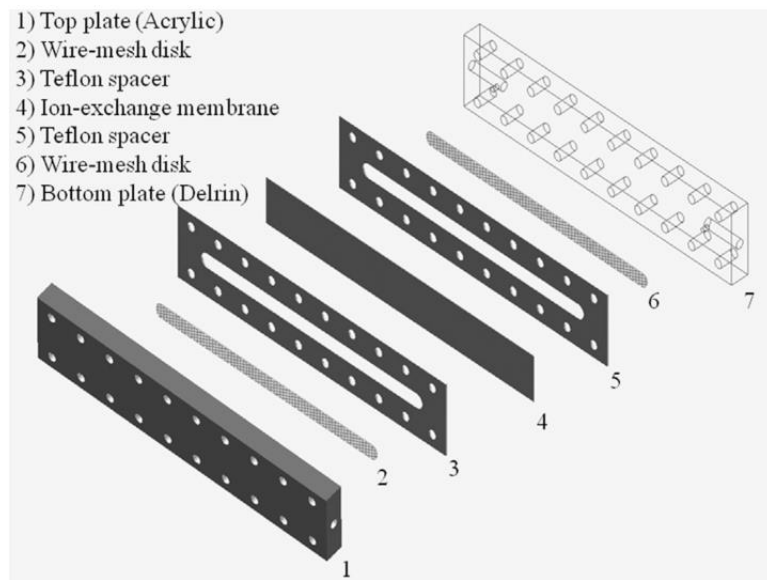


**Fig. 2.4:** Blowout diagram of novel, laterally-fed rectangular membrane module (from right to left: transparent acrylic top plate, woven wire mesh support/ distributor, membrane spacer, rectangular membrane sheet, membrane spacer, woven wire mesh support/distributor, bottom plate)

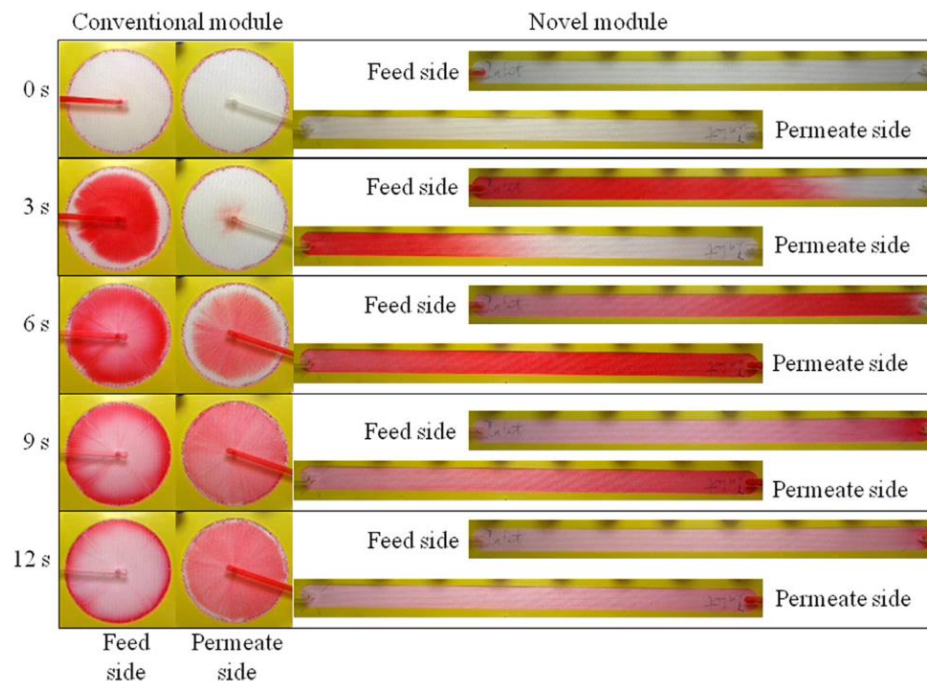
The dye tracer experiments were performed using ten times diluted food color solutions. The dye was found to bind strongly to the Sartobind Q membrane and so hydrophilized PVDF membranes having 0.22 mm pore size was used in the dye experiments. Degassed micro-filtered water was pumped at a flow rate of 10 mL/min from a reservoir to the membrane modules using a HiLoad P-50 pump (GE Healthcare, Piscataway, NJ, USA). A sample injector fitted with a 250 mL loop, installed between the pump and module was used to introduce the food dye into the devices. The transparent (acrylic) side of the membrane module was illuminated using a table lamp. A digital camera (Sony Cyber-shot, Model DSC-WX7, Japan) was used to take video clips of the membrane surface during the dye experiments. Video clips were recorded in MTS format and the extent of zooming together with the location of the camera relative to the module was kept the same in all the experiments. Snapshots were obtained from the video files at the rate of one every second using Windows Live Movie Maker and processed using Image J freeware (<http://imagej.nih.gov/ij/>). The gray scale intensities of the snapshots were measured by coding macros. For the circular membrane module, intensities of pixels on the radius from the center to the periphery (73 pixels in all) were recorded for all 30 frames and were multiplied by the area of the circular increment corresponding to the distance of the pixel from center. For the novel module, intensities of the pixels were measured along the length of the membrane (570 pixels in all) and were multiplied by the width of the membrane. To avoid any discrepancies owing to the experiment-to-experiment variations, the intensities were normalized by subtracting the base line intensity for each pixel, this being the intensity at time zero. For the protein experiments, the modules fitted with Sartobind Q membrane were integrated with an Akta Prime liquid chromatography system (GE Healthcare Bioscience, QC, Canada) using PEEK tubings. Phosphate buffer (20 mM, pH 7.0) was used as the binding buffer as well as for preparing the feed protein solutions. The eluting buffer consisted to the binding buffer containing in addition, 0.5M NaCl. All buffers were degassed and filtered using PVDF filters

(VVLP04700, 0.1 mm pore size, Millipore, Billerica, MA, USA) just before running the membrane chromatography experiments which were carried out at 10 mL/min flow rate. Unbound tracer molecule experiments were carried out with lysozyme solution using three different sample loops having volumes of 250 mL, 1 mL, and 2 mL. Breakthrough experiments were carried out by injecting BSA solutions of appropriate concentration prepared in the binding buffer. A 50 mL superloop was used to inject the protein solution into the modules. The BSA bound to the membrane was eluted using buffer containing 0.5 M sodium chloride. The void volume of the membrane modules was determined using lysozyme which did not bind to the Sartobind Q membrane and the breakthrough curves were corrected accordingly. BSA binding experiments were also carried out in the pulse mode by injecting 100 mL of BSA solution.

#### **2.4. Results and Discussion**

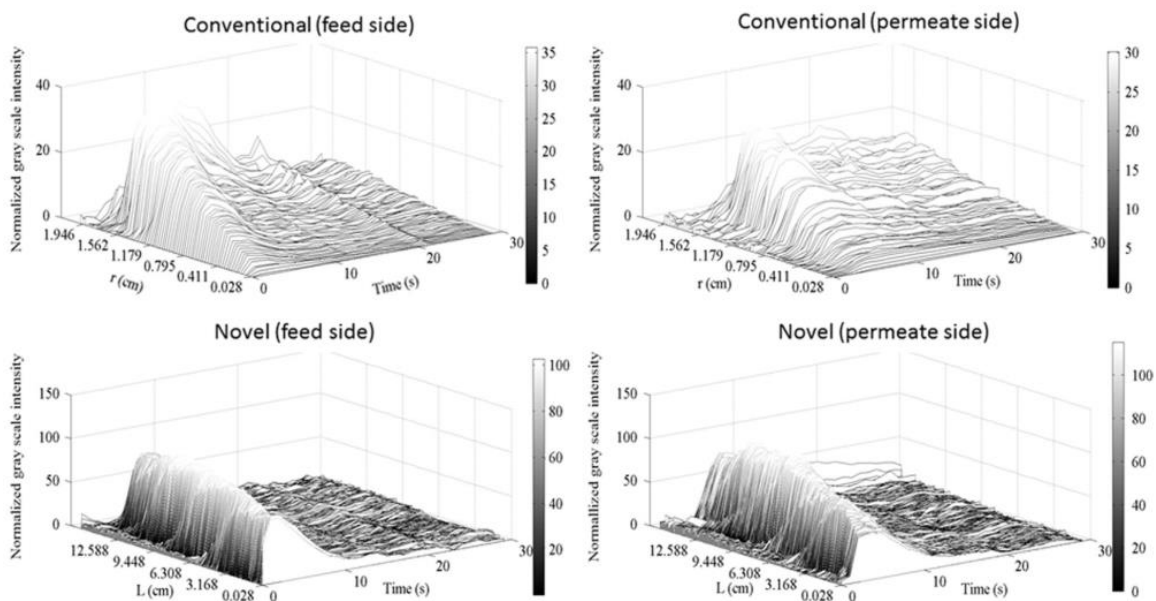
Fig. 2.5 shows snapshots from the first twelve seconds of the dye experiments carried out with the conventional and novel modules. The aim of these dye experiments was to visually compare the flow distribution on the feed side as well as the effluent collection on the permeate side of the membrane modules. As already stated, only the top acrylic plates of the modules were transparent. The inlet and outlet connections were therefore swapped around to make either the feed side or the permeate side transparent. This was feasible as top and bottom plates, though made of different materials, were identical in design. The time zero in each case was designated to the instant at which the dye just entered the module. The snapshots of the conventional module showed the dye breaking through the central region of the module after three seconds, with the peripheral region of the feed side of the membrane still free of dye. After six seconds, the central region on the feed side started getting depleted of dye while the dye breakthrough in the peripheral region was yet to happen. After twelve seconds, the feed side of the membrane was largely free of dye except for the periphery and the uniform coloration on the permeate side was due to the dye breaking through the

peripheral region and migrating to the outlet located at the center of the module. Overall, the snapshots obtained with the conventional module clearly indicate acute maldistribution of dye. At the initial stages, most of the dye went through the central regions of the membrane disk and the dye reached the peripheral regions much later. Also, by the time the dye reached the periphery, it had almost disappeared from the central regions. Therefore, the breakthrough binding capacity with this device would be expected to be low and flow-through and eluate peaks would be broad. The snapshots obtained with the novel device show very good correlation in dye intensity on the feed and permeate side with excellent lateral distribution. Therefore, the fluid flow and distribution was exactly as shown in Fig. 2.2, i.e. the variability in solute flow path length was low. Based on this, it could be anticipated that the efficiency of separation using the novel module would be high.



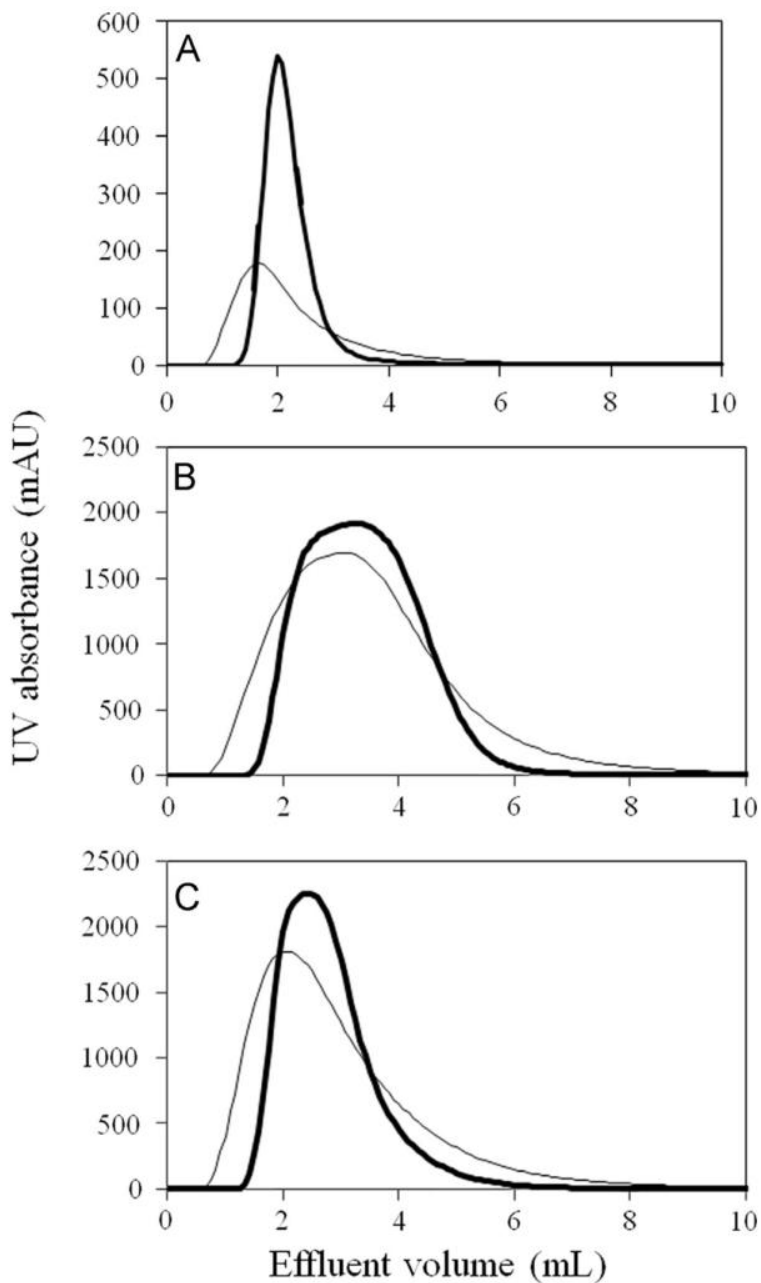
**Fig. 2.5:** Snapshots of the feed and permeate sides of the conventional and novel membrane modules obtained during dye tracer experiments at 0, 3, 6, 9, and 12 s (membrane: hydrophilized PVDF; pore size: 0.22  $\mu\text{m}$ ; feed: 10 times diluted McCormick red food dye in water; volume injected: 250 mL; flow rate: 10 mL/min)

Fig. 2.6 shows the quantitative analysis of dye experiments. The 3D graphs in Fig. 2.6 show the variations of normalized gray scale intensity with time and location within the two membrane modules. The normalized gray scale intensity could be considered to be proportional to the amount of dye at a given location. The time lag between dye passing through the central and peripheral regions of the circular membrane is clearly evident from the graphs for the conventional module shown in Fig. 2.6. The graphs also show that it took long for the dye to reach the periphery and once this happened, the dye lingered in the peripheral regions of the membrane for a long time. On the other hand, the graphs for the novel module showed a much more gradual shift of the peak which had a largely constant height, from the inlet to the outlet side, clearly indicating a far more uniform solute path length. These results once again predict higher efficiency of separation with the novel module.



**Fig. 2.6:** Representation of gray scale intensity data obtained from snapshots shown in Fig. 5 using Image J (membrane: hydrophilized PVDF; pore size: 0.22  $\mu\text{m}$ ; feed sample: 10 times diluted McCormick red food dye; volume injected: 250 mL; flow rate: 10 mL/min)

Tracer experiments were carried out by Sartobind Q membrane using lysozyme as non-binding protein. Fig. 2.7 shows the flow-through peak curves obtained with the two modules using lysozyme solution under non-binding condition (i.e. at pH=7.0). Three different combinations of loop size and protein concentration were used in these experiments. The peaks obtained with the novel module were significantly sharper and more symmetrical. With the conventional module, lysozyme appeared in the effluent earlier, even though the dead volume of the conventional module was slightly greater than that of the novel module. This was consistent with the results of the dye experiments discussed earlier, where very early breakthrough at the central region of the membrane was observed. The broadening of the peaks with the conventional module, which is indicative of flow maldistribution, was consistent with the dye experiments where the dye lingered on in the peripheral regions for quite some time before reaching the outlet. The widths at half-height, asymmetry parameter, and the tailing factor of the flow-through peaks obtained with the two modules are shown in Table 2.1. Asymmetry parameter was calculated at 10% of the peak height whereas the tailing factor was measured for the 5% of the peak height as defined by Moldoveanu and David [25]. The lower the values of the asymmetry parameter and tailing factor indicate that the flow distribution and thereby the uniformity of solute path length were significantly superior with the novel membrane module.



**Fig. 2.7:** Flow through lysozyme peaks obtained at non-binding condition with conventional (thin line) and novel (thick line) membrane modules (membrane: Sartobind Q; membrane area: 12.57 cm<sup>2</sup>; buffer: 20 mM sodium phosphate; pH=7.0; flow rate: 10 mL/min; A: 250 mL, 2 mg/mL; B: 5mL, 2 mg/ml, C: 10 mL, 1 mg/mL)

**Table 2.1:** Characteristics of flow-through peaks obtained from experiments carried out using lysozyme in non-binding condition with conventional and novel modules as shown in Fig. 2.7 (membrane: Sartobind Q; membrane area: 12.57 cm<sup>2</sup>; buffer: 20 mM sodium phosphate; pH=7.0; flow rate: 10 mL/min; A: 250 mL, 2mg/mL; B: 5 mL, 2 mg/ml, C: 10 mL, 1 mg/mL)

Figure	Loop size (mL)	Concentration (mg/mL)	Module	Peak width at half height (mL)	Asymmetry parameter	Tailing factor
2.7A	0.250	2.0	Conventional	1.37	3.16	2.30
			Novel	0.74	1.84	1.56
2.7B	5.0	2.0	Conventional	0.31	1.65	1.53
			Novel	0.26	1.38	1.25
2.7C	10.0	1.0	Conventional	2.27	3.09	2.26
			Novel	1.58	2.27	1.83

Fig. 2.8 shows the breakthrough curves for the novel and conventional membrane modules, obtained by injecting 30 mL of 2 mg/mL BSA solution using a superloop. The volume axes of the breakthrough curves were corrected to factor in the void volumes of the two devices, these being 1.45 mL and 1.35 mL respectively for the conventional and novel modules. The Sartobind Q membrane had identical bed volumes of 0.346 mL in the two devices. The 1% and 10% breakthrough BSA binding capacity obtained with the two membrane modules are shown in Table 2.2. These results clearly demonstrate how the design of the membrane module could have a profound impact on the utilization of membrane binding capacity. The quick saturation of the central regions of the membrane housed in the conventional membrane module by BSA molecules resulted in an early breakthrough. By contrast, the breakthrough took place a lot later with the novel membrane module, the resultant 1% breakthrough BSA binding capacity being almost five times higher. The 10% breakthrough binding capacity obtained with the novel membrane module was 30.73 mg/mL which is an extremely high value for a single layer of

membrane. The BSA elution peaks obtained in the above break-through experiments along with the corresponding conductivity profiles are shown in Fig. 2.9. The areas of the two eluted peaks were almost identical for the two devices with the BSA recovery with the novel module being 98.5% of that obtained with the conventional device. The width at half-height data for the BSA elution peaks obtained with the two modules are shown in Table 2.3. As expected, the novel module gave sharper and more symmetrical peak. Moreover, the sharper conductivity profile observed with the novel module indicates its superior design. Broadening of peaks, in addition to being undesirable in multi-component separation processes, results in product dilution which increases bioseparation cost in large-scale separation processes.

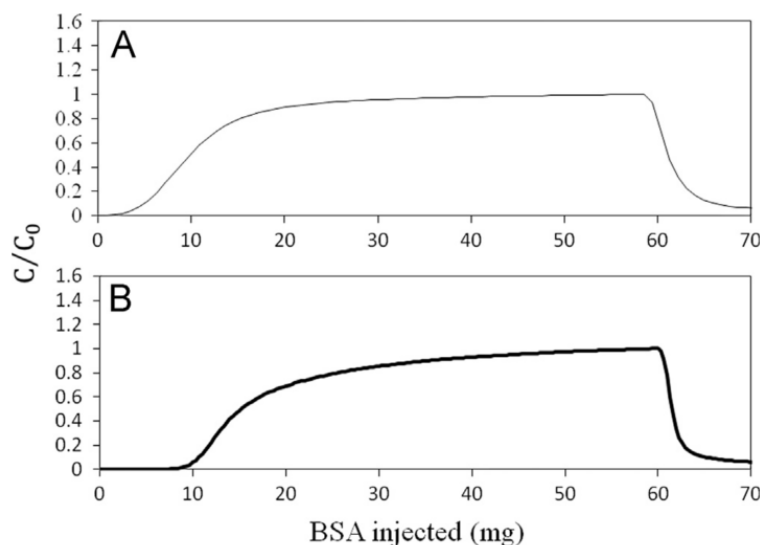


**Fig. 2.8:** Breakthrough curves for adsorption of BSA on the anion-exchange membrane obtained using A: conventional (thin line) and B: novel (thick line) membrane modules (membrane: Sartobind Q; membrane area: 12.57 cm<sup>2</sup>; feed concentration: 2 mg/mL; volume injected: 30 mL; binding buffer: 20 mM phosphate; pH=7.0; flow rate: 10 mL/min)

**Table 2.2:** Bovine serum albumin (BSA) binding capacity of the Sartobind Q anion-exchange membrane at two different breakthrough points designation for conventional and novel modules (membrane: Sartobind Q; membrane area: 12.57 cm<sup>2</sup>; feed concentration: 2 mg/mL; volume injected: till saturation ~30 mL; binding buffer: 20 mM phosphate; pH=7.0; flow rate: 10 mL/min)

	1% breakthrough binding capacity (mg/mL)	10% breakthrough binding capacity (mg/mL)
Conventional	4.87	15.46
Novel	24.95	30.73
Ratio	5.12	1.99

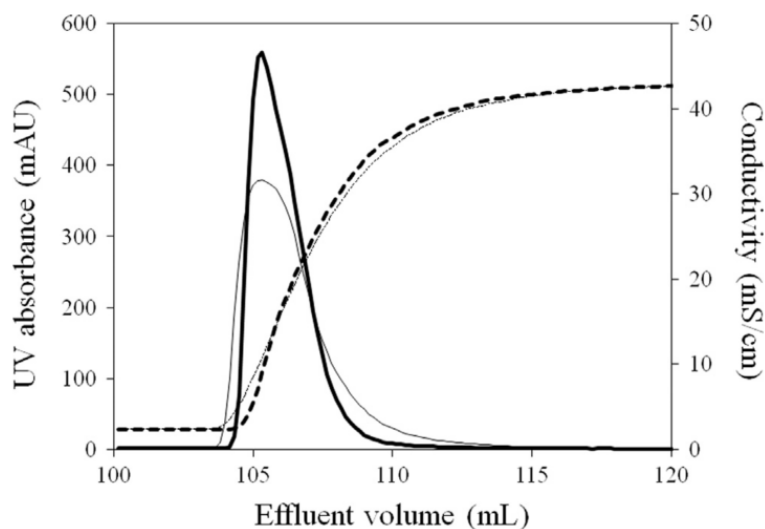


**Fig. 2.9:** BSA elution peaks and conductivity profiles obtained using conventional (thin line and thin dashed line respectively) and novel (thick line and thick dashed line respectively) modules (membrane: Sartobind Q; membrane area: 12.57 cm<sup>2</sup>; feed concentration: 2 mg/mL; volume injected: 30 mL; binding buffer: 20 mM sodium phosphate, pH 7.0; eluting buffer: binding buffer+0.5 M sodium chloride; flow rate: 10 mL/min)

**Table 2.3:** Characteristics of the elution curves obtained from the breakthrough experiments using bovine serum albumin (BSA) for conventional and novel modules as shown in Fig. 9 (membrane: Sartobind Q; membrane area: 12.57 cm<sup>2</sup>; feed concentration: 2 mg/mL; volume injected: ~30 mL; binding buffer: 20 mM sodium phosphate, pH 7.0; eluting buffer: binding buffer+0.5 M sodium chloride; flow rate: 10 mL/min)

	Peak width at half-height (mL)
Conventional	2.84
Novel	2.05

Fig. 2.10 shows the chromatograms obtained in pulse binding experiments carried out with both modules using 100 mL of 1 mg/mL BSA solution. While there was very little BSA flow-through with the novel module, a significant peak, indicating incomplete protein capture was observed with the conventional module. Table 2.4 shows the width at half-height values for the BSA elution peaks obtained with the two modules. As in the experiments described in the previous paragraph, the BSA peak was sharper and more symmetric with the novel module.

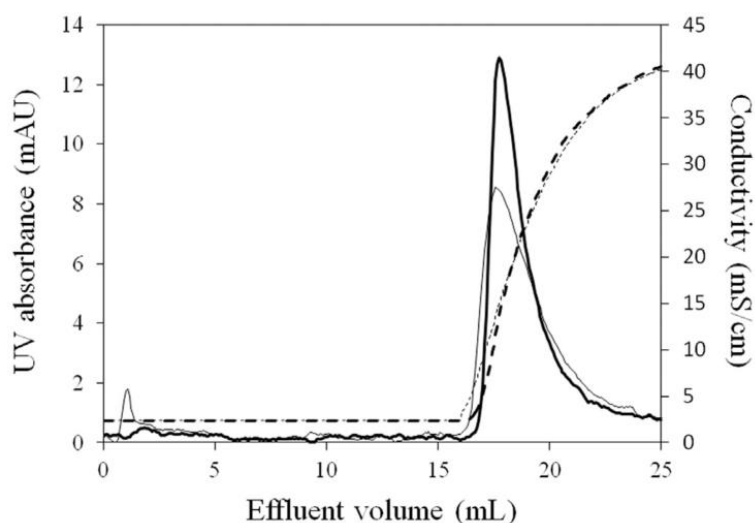


**Fig. 2.10:** BSA elution peaks and conductivity profiles obtained from pulse binding experiments carried out using conventional (thin line and thin dashed line respectively) and novel (thick line and thick dashed line respectively) modules (membrane: Sartobind Q; membrane area: 12.57 cm<sup>2</sup>; feed concentration: 1 mg/mL; volume injected: 100 mL; binding buffer: 20 mM sodium phosphate, pH 7.0; eluting buffer: binding buffer+0.5 M sodium chloride; flow rate: 10 mL/min)

**Table 2.4:** Characteristics of the elution curves obtained from the breakthrough experiments using bovine serum albumin (BSA) for conventional and novel modules as shown in Fig. 9 (membrane: Sartobind Q; membrane area: 12.57 cm<sup>2</sup>; feed concentration: 2 mg/mL; volume injected: ~30 mL; binding buffer: 20 mM sodium phosphate, pH 7.0; eluting buffer: binding buffer+0.5 M sodium chloride; flow rate: 10 mL/min)

	Peak width at half-height (mL)
Conventional	2.75
Novel	1.65

The above results clearly demonstrate the superiority of the novel laterally-fed, rectangular membrane module over a conventional, centrally-fed, circular membrane module. They also highlight the critical role played by the membrane module design on the efficiency of membrane binding capacity utilization. The novel laterally-fed design examined in the current study reduces the variability in solute path length within the device and thereby leads in more uniform usage of membrane. In order for the novel design feature to be effective, the following conditions have to be met. Firstly, the hydraulic resistance offered support material (woven wire mesh in this case) within which lateral flow distribution and collection takes place has to be lower than that offered by the membrane. Secondly, the resistance to lateral flow in the support material on both sides of the membrane has to be identical. A higher resistance on the feed side would result in greater flow in the membrane closer to the inlet while a higher resistance on the permeate side would result in greater flow closer to the outlet. Finally, the aspect (i.e. length to width) ratio of the device is quite important. A low aspect ratio could result in maldistribution with more lateral flow of feed taking place closer to the centerline of the support material. A very high aspect ratio on the other hand would result in poor utilization of membrane closer to the outlet due to increase in lateral resistance. This work is intended to stimulate research and activities in the area of module development for membrane chromatography. As the next step, a scaled-up, laterally fed membrane module that can be fitted with a stack of membranes is being designed and its performance will be compared with equivalent circular disk-stack and radial flow membrane modules. With a stack of membranes, the ratio of hydraulic resistance offered by the membrane relative to the lateral resistances offered on the two sides of the membrane stack would be significantly greater than in the single layered device used in the current study. Therefore the enhancement in separation efficiency could be anticipated to be even greater with such a device. Such laterally fed membrane modules, addition to being suitable for separations, could also be used as membrane reactors and dead-end microfiltration devices.

## 2.5. Conclusions

The efficiency of membrane binding capacity utilization in a membrane module depends greatly on the fluid flow distribution and collection within the device. Tracer experiments carried out using dye and the protein lysozyme under non-binding conditions demonstrate acute maldistribution of solute within a conventional, centrally fed, circular membrane module. One of the major problems resulting from such maldistribution was the very early solute breakthrough at the center of the membrane. The other problem was that solute molecules reached the peripheral regions quite late and stayed there even longer. Consequently, the breakthrough binding capacity obtained with this device was low and the flow-through and eluate peaks were broad. The novel laterally-fed, rectangular membrane module addressed these issues by maintaining the solute path lengths within the device more uniform. This aspect was clearly demonstrated by tracer experiments, carried out using dye and unbound protein. The breakthrough binding capacity of bovine serum albumin was almost five times that obtained with an equivalent conventional, centrally fed, circular membrane module. The uniformity of solute path length along with more uniform solute binding on the membrane housed within the novel module also resulted in sharper and more symmetric elution peaks.

## 2.6. Acknowledgment

We thank the Natural Science and Engineering Research Council of Canada (NSERC) for funding this study and Paul Gatt for fabricating the membrane modules used in this project.

## 2.7. References

[1] T.B. Tennikova, F. Svec, B.G. Belenkii, High-performance membrane chromatography. A novel method of protein separation, *J. Liq. Chromatogr.* 13 (1990) 63–70.

- [2] M.E. Avramescu, Z. Borneman, M. Wessling, Dynamic behavior of adsorber membranes for protein recovery, *Biotechnol. Bioeng.* 84 (2003) 564–572.
- [3] S.M. Saufi, C.J. Fee, Mixed matrix membrane chromatography based on hydrophobic interaction for whey protein fractionation, *J. Membr. Sci.* 444 (2013) 157–163.
- [4] N. Singh, J. Wang, M. Ulbricht, S.R. Wickramasinghe, S.M. Husson, Surface-initiated atom transfer radical polymerization: a new method for preparation of polymeric membrane adsorbers, *J. Membr. Sci.* 309 (2008) 64–72.
- [5] R. Ghosh, Protein Separation using membrane chromatography: opportunities and challenges, *J. Chromatogr. A* 952 (2002) 13–27.
- [6] S. Brandt, R.A. Goffe, S.B. Kessler, J.L. O'Connor, S. Zale, Membrane-based affinity technology for commercial scale purifications, *Bio/Technol* 6 (1988) 779–782.
- [7] R. Ghosh, Separation of proteins using hydrophobic interaction membrane chromatography, *J. Chromatogr. A* 923 (2001) 59–64.
- [8] C. Charcosset, Purification of proteins by membrane chromatography, *J. Chem. Technol. Biotechnol.* 71 (1998) 95–110.
- [9] D.K. Roper, E.N. Lightfoot, Separation of biomolecules using adsorptive membranes, *J. Chromatogr. A* 702 (1995) 3–26.
- [10] B.V. Bhut, K.A. Christensen, S.M. Husson, Membrane chromatography: protein purification from *E. coli* lysate using newly designed and commercial anion-exchange stationary phases, *J. Chromatogr. A* 1217 (2010) 4946–4957.
- [11] H.H. Liu, J.R. Fried, Breakthrough of lysozyme through an affinity membrane of cellulose-Cibacron blue, *AIChE J.* 40 (1994) 40–49.
- [12] S.Y. Suen, M.R. Etzel, A mathematical analysis of affinity membrane bioseparations, *Chem. Eng. Sci.* 47 (1992) 1355–1364.

- [13] K.D. Program, Affinity adsorption devices prepared from microporous poly (amide) hollow fibers and sheet membranes, *J. Membr. Sci.* 129 (1997) 31–46.
- [14] K.H. Gebauer, J. Thommes, M.R. Kula, Breakthrough performance of high-capacity membrane adsorbers in protein chromatography, *Chem. Eng. Sci.* 52 (1997) 405–419.
- [15] R. van Reis, A. Zydney, Membrane separations in biotechnology, *Curr. Opin. Biotechnol.* 12 (2001) 208–211.
- [16] J. Thömmes, M.-R. Kula, Membrane chromatography – an integrative concept in the downstream processing of proteins, *Biotechnol. Prog.* 11 (1995) 357–367.
- [17] W. Demmer, D. Nussbaumer, Large-scale membrane adsorber, *J. Chromatogr. A* 852 (1999) 73–81.
- [18] R. Ghosh, T. Wong, Effect of module design on the efficiency of membrane chromatographic separation processes, *J. Membr. Sci.* 281 (2006) 532–540.
- [19] F.T. Sarfert, M.R. Etzel, Mass transfer limitations in protein separations using ion-exchange membranes, *J. Chromatogr. A* 764 (1997) 3–20.
- [20] P. Francis, E. von Lieres, C.A. Haynes, Zonal rate model for stacked membrane chromatography. I: characterizing solute dispersion under flow-through conditions, *J. Chromatogr. A* 1218 (2011) 5071–5078.
- [21] P. Ghosh, K. Vahedipour, M. Lin, J.H. Vogel, C. Haynes, E. von Lieres, Computational fluid dynamic simulation of axial and radial flow membrane chromatography: mechanisms of non-ideality and validation of the zonal rate model, *J. Chromatogr. A* 1305 (2013) 114–122.
- [22] R. Ghosh, Membrane adsorber module, Canadian Patent Application, PCT/CA2005/000468.

[23] S. Dimartino, C. Boi, G.C. Sarti, Influence of protein adsorption kinetics on breakthrough broadening in membrane affinity chromatography, *J. Chromatogr, A* 1218 (2011) 3966–3972.

[24] R. Ghosh, Laterally-fed membrane chromatography module, US Patent Application No. 62074858 filing date November 4, 2014.

[25] S.C. Moldoveanu, V. David, *Essentials in Modern HPLC Separations*, Elsevier, Waltham, 2013.

## **Chapter 3**

### **High-Resolution Protein Separation Using a Laterally-Fed Membrane Chromatography Device**

Reprinted with permission. Copyright 2016 ELSEVIER Journal

### 3.1 Abstract

Radial-flow membrane chromatography devices which are used for flow-through separation are generally unsuitable for bind-and-elute chromatography, particularly where multiple components need to be separated. We discuss a laterally-fed membrane chromatography device, suitable for high-resolution, multi-component protein separation in the bind-and-elute mode. In the current study, a stack of cation exchange membranes was housed within the membrane device and its performance was compared with an equivalent commercial radial-flow device having the same membrane bed volume and bed height. Tracer experiments were carried out using sodium chloride solution to compare their residence time distributions. The laterally-fed device showed superior flow distribution characteristics, which could be attributed to a lower variability in solute-flow path-lengths, and a smaller dead volume. Single protein bind-and-elute experiments carried out using lysozyme showed that the peaks obtained with the laterally-fed device were significantly sharper and more symmetrical. Excellent separation of three model proteins ovalbumin, conalbumin and lysozyme demonstrated that the laterally-fed membrane chromatography device was indeed suitable for carrying out high-resolution multi-component protein purification. These proteins could be fractionated in about 10 membrane bed volumes using the laterally-fed device as opposed to 25 bed volumes with the radial-flow device. The design of the laterally-fed device is simple and its flat shape gives it significantly lower footprint and offers additional advantages such as stackability and ease of multiplexing.

**Keywords** Membrane chromatography; Protein; Device; Membrane adsorber; Bioseparation

### 3.2 Introduction

Downstream processing capacity in the biotechnology industry has struggled to keep up with the remarkable improvements in both bioreactor titer and volume. Chromatography, which is the linchpin in most purification processes, has become the major bottleneck in bio-manufacturing [1]. Economy of scale does not exist for large columns due to the high resin cost. Also, the resolution decreases with increase in scale. Membrane chromatography has long been suggested as a fast and cost-effective alternative to resin-based column chromatography [2-7]. The predominantly convection-based transport of target biomolecules to and from their binding sites on a membrane, as opposed to the largely diffusion-limited mass transport of these molecules within the resin bed makes membrane chromatography significantly faster [2-7]. Speed of separation translates to both higher productivity and lower product degradation. Also, in membrane chromatography, the efficiency of binding of even large solutes such as monoclonal antibodies is relatively independent of the superficial velocity. This offers significant flexibility in process design. Other advantages include lower buffer usage and pressure drops, and the absence of problems such as channeling and fracturing of resin beds. Moreover, the disposable nature of membrane devices eliminates the need for cleaning and validation steps, and thereby contributes toward practicality and ease of use [8, 9].

Devices for membrane chromatography are commonly available in the stacked-disk and radial-flow formats [10, 11]. The use of hollow-fiber membrane devices has also been reported but they are not very commonly used, and are not suitable for pulse chromatography [12, 13]. Stacked-disk membrane devices are most commonly used for laboratory-scale separations and process development. However, it is impractical to use these devices in large-scale processes as when their diameter is increased, the radial to axial dimension aspect ratio, and thereby the variability of flow path lengths become large enough to severely affect separation performance. Stacked-disc devices which incorporate efficient flow-

distribution features have been shown to be suitable for high-resolution protein fractionation [14]. However, even with these improved devices, the separation efficiency decreases when the diameter exceeds 50–60 mm. Radial-flow devices which are made by wrapping long pieces of flat-sheet membranes over central collection channels are commonly used in large-scale applications [15–17]. These devices offer large cross-sectional area to bed volume ratios, can be operated at low back pressures, and are scalable. They perform quite well in flow-through separations where the target bio-molecules are typically collected as unbound material going through the device, while impurities that are present in relatively small amounts are adsorbed. Major applications of radial-flow devices include polishing of monoclonal antibodies (mAbs), i.e. removal of impurities such as host cell proteins (HCPs), endotoxins, and viruses [18–22].

While membrane chromatography is widely used for polishing applications in the biotech industry, there has been very limited use of this technique for large-scale purification in the bind-and-elute mode, particularly where multiple components need to be separated [23]. As shown in Fig. 3.1, a radial-flow device has a complicated design and thereby a complicated flow-path. The liquid is first distributed in a radially outward direction to the annular space surrounding the membrane roll. It is then forced into the membrane in a radially inward direction and collected on the outer surface of the central core which supports the membrane roll. As demonstrated in this paper, such complexity creates large variability in flow path lengths within the device, resulting in dispersion effects such as peak broadening and loss of peak resolution. It is also difficult to balance the pressure drop in the axial direction on both sides of the membrane. The feed space is typically an open channel while the permeate collection space consists of either a porous or grooved structure. Pressure balancing is critically important for efficient membrane utilization as is discussed at the end of the paper. The effective membrane area in a membrane roll changes along the bed height, i.e. decreases in a radially inward direction. This results in an increase in superficial velocity in a

radially inward direction, which could adversely affect chromatographic separation. Radial-flow devices have large dead volumes, both on the feed and the permeate sides, which could aggravate the above dispersion effects. Also, the large supporting central core does not play any active role in the separation process, and therefore device volume utilization is poor. While none of the above factors are perhaps critically limiting in separations carried out in the flow-through mode, these could adversely affect high-resolution, multi-component separations carried out in the bind-and-elute mode. Elution chromatography is a very subtle process where desorption of bound species from an adsorbent bed is dependent on the uniformity of species binding and sensitive to the manner in which the eluent composition changes within the bed.

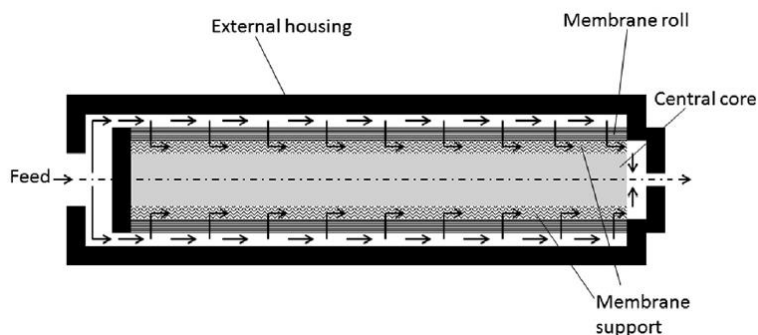


**Fig. 3.1:** Radial-flow membrane chromatography device

We feel that availability of membrane devices which address the above issues would contribute to the wider acceptance and use of membrane chromatography in the biotechnology industry. In our recent studies, we have compared the performance of such a laterally-fed device with a stacked-disc membrane device [24, 25]. The laterally-fed device outperformed the stack-disc device in terms of all the attributes examined, i.e. flow distribution, membrane binding capacity utilization, and peak resolution. In the current paper, we discuss how a laterally-fed membrane chromatography device could be used to carry out high-resolution, multiple-component protein separation in the bind-and-elute mode. The device

(see Fig. 3.2) is designed to house a stack of rectangular flat sheet adsorptive membranes. Liquid is laterally distributed over the feed side of the device and thereby enters the membrane stack at different locations along its length, eventually emerging at corresponding locations on the permeate side, where it flows laterally to the outlet of the device. This configuration makes it possible to balance the pressure-drop on the feed side with that on the permeate side, thereby ensuring uniformity of flow along the length of the membrane stack. Also, unlike in a radial-flow device, where the superficial velocity within the bed increases in a radially inward direction, the flow of liquid is anticipated to be more uniform in the laterally-fed membrane chromatography device. As idealized in Fig. 3.2, the flow path lengths are similar throughout the device. This is expected to improve both, the efficiency of membrane utilization, and the resolution of eluted peaks in chromatographic separation.

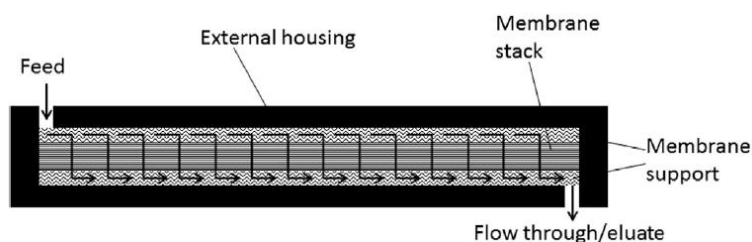


**Fig. 3.2:** Radial-flow membrane chromatography device

In this paper, we discuss the design, fabrication and use of a laterally-fed membrane chromatography device, within which a stack of rectangular flat sheet cation exchange membranes, having a bed volume of 7 mL was housed. The performance of this device was compared with that of an equivalent commercial radial-flow device having the same bed volume and bed height. Tracer experiments were carried out using sodium chloride in both pulse- and step-input modes to investigate their residence time distributions. Single protein, bind-and-elute experiments were then carried out using lysozyme and peaks thus obtained were compared. Protein separation experiments were then carried out in the pulse-

mode using ovalbumin as the model unbound protein, and conalbumin and lysozyme as model bound proteins, to demonstrate the suitability of the laterally-fed device for carrying out high-resolution, multi-component, protein purification. The results obtained are discussed.

### 3.3. Materials and Methods

Lysozyme (L6876), conalbumin (C7786), ovalbumin(A5503), sodium phosphate monobasic (S0751), sodium phosphate dibasic (S0876), citric acid (C0759), sodium citrate dehydrate (S4641), sodium chloride (S7653), hydrochloric acid (258148), ammonium persulfate (A3678), 30% acrylamide solution (A3699), glycerol (G2025), bromophenol blue (B0126), Brilliant Blue R concentrate (B8647), glycine (G8898), sodium dodecyl sulfate (L3771), Trizma- hydrochloride (T3253), Trizma base (T1503), N,N,N',N'-tetramethyl ethylenediamine (T9281), and DL-dithiothreitol (43817) were purchased from Sigma-Aldrich (St.Louis, MO, USA). Acetic acid (1000-1) and methanol (6700-1) were purchased from Caledon Laboratories LTD. (Georgetown, ON, Canada). Ultra-4centrifugal filters (3 kDa MWCO, UFC800324) were purchased from EMD Millipore Co. (Billerica, MA, USA). RTV 108 silicon-based adhesive was purchased from MOMENTIVE (Columbus, OH, USA). Sartobind S cation-exchange membrane sheets (94IEXS42-001) and Sartobind Single Sep Mini (92IEXS42D4-SS-A, 7 mL bed volume) were purchased from Sartorius Stedim Biotech (Gottingen, Germany). All buffers and the solutions were prepared using water obtained from a SIMPLICITY 185 water purification unit Millipore (Molsheim, France).

The schematic design of the laterally-fed membrane chromatography device used in this study is shown in Fig. 3.3. The device is consisted of two acrylic plates (numbered 1 and 3) which provided the rectangular feed and permeate channels for lateral flow on the two sides of the membrane stack, and a plate (numbered 2), which housed the membrane stack. The plates were fabricated by 3-D printing using a ProJet HD3000 printer purchased from 3D Systems (Rock Hill, SC, USA).

VisiJet EX200 acrylic-based polymer was used as the printing material. The detailed design of the plates and the frame used to assemble the laterally-fed membrane chromatography device is shown in Fig. 3.4. The plates featured slanted tapered channels for distribution of the liquid over the width of the lateral channel on the feed side and collection of the liquid from the lateral channel on the permeate side. The rectangular feed and permeate channels were 70 mm (length)  $\times$  20 mm (width) with 0.5 mm depth. Before assembling the device, these channels were filled with 70 mm  $\times$  20 mm pieces of woven wire mesh (approximately 0.5 mm thick) which served both as liquid distributor and membrane support. These wire mesh pieces also helped reduce the dead volume of the device. The plates were provided with vents as shown in Figs. 3.3 and 3.4. These were essential for priming the device and for removal of air bubbles trapped in the channels. The dimensions of the distribution and flow channels, and the inlet and outlet ports were minimized to reduce the dead volume of the device. The frame which had a thickness of 5 mm (corresponding to the membrane bed height) was made of delrin. The outer dimension of the frame was 130 mm  $\times$  40 mm and it was provided with a tapered slot within which the membrane stack was glued in place. The dimension of the slot at the smaller end was 70 mm  $\times$  20 mm, which corresponded to the length and width of the membrane stack. The larger end of the slot had a dimension of 75 mm  $\times$  25 mm. Rectangular pieces (70 mm  $\times$  20 mm) of cation-exchange membranes (18 nos.) were cut out using a metal stamp cutter, assembled as a stack, and placed within the frame. A metal block having the same length and width as the membrane pieces was placed over the stack to hold it in place, and also to mask it during the gluing process. RTV 108 adhesive was dispensed into the tapered space around the membrane stack till it was completely filled. The adhesive was allowed to cure for 48 h before assembling the device.

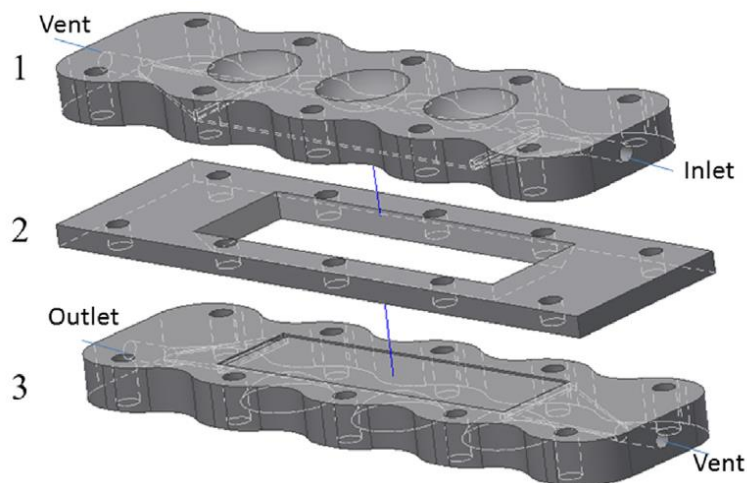


**Fig. 3.3:** Diagram of the prototype laterally-fed membrane chromatography device used in the current study (1: acrylic top plate; 2: delrin frame; 3: acrylic bottom plate)

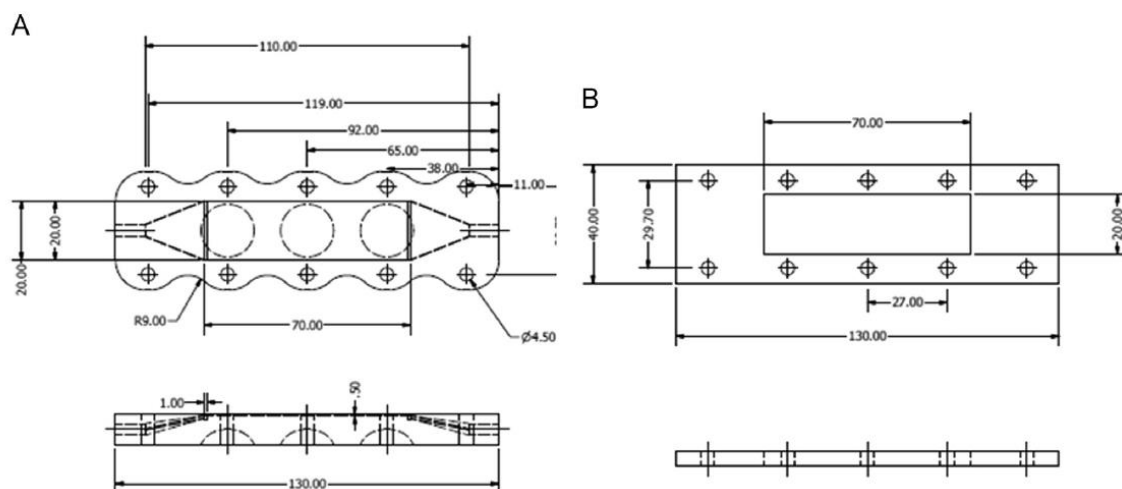


**Fig. 3.4:** Figure showing the top- and side-views of the plates (A) and the frame (B) used to assemble the laterally-fed membrane chromatography device used in this study. All dimensions are in mm

Standard PEEK fittings were employed to integrate the membrane chromatography devices with an AKTA Prime liquid chromatography system (GE Healthcare Bioscience, QC, Canada). The sanitary connectors on the inlet and outlet of the radial-flow de-vice were modified using delrin inserts to make them

compatible with the PEEK fittings. This alteration helped reduce the dead volume of the device from its rated value of 25 mL to 21.0 mL. The dead volume of both devices was accurately measured by weighing the volume of water required to fill them up. These were found to be 4.8 mL and 21.0 mL respectively, for the laterally-fed and radial-flow devices.

Salt tracer experiments were carried out using sodium phosphate buffer (20 mM, pH 7.0) as the running buffer, and sodium chloride solution (0.5 M) as tracer. These experiments were performed both in the pulse- and step-input modes. Pulse experiments were carried out using 2 mL and 5 mL sample loops while the step-input experiment was carried out by using a 150 mL super loop.

All membrane chromatography experiments were carried out at 10 mL/min flow rate using appropriate micro-filtered and degassed buffers. Single protein bind-and-elute experiments were carried out by injecting 2 mL or 5 mL of 8 mg/mL lysozyme solution prepared in the binding buffer (20 mM sodium phosphate, pH 7.0). The eluting buffer consisted of 0.5 M sodium chloride solution prepared in binding buffer, with the elution being carried out in the step-change mode. Multi-component protein separation experiments were carried out by injecting 2 mL of protein solution prepared using ovalbumin (pI 4.5), conalbumin (pI 6.1), and lysozyme (pI 11.0), the respective concentrations being 0.25 mg/mL, 0.5 mg/mL, and 0.25 mg/mL. Citrate buffer (20 mM, pH 5.5) was used as the binding buffer as well as for sample preparation. Sodium chloride solution (0.5 M NaCl) prepared in binding buffer was used to elute the bound proteins. Samples obtained from the multi-component separation experiments were collected and de-salted using 3 kDa MWCO centrifugal filters (30 min, 3750 rpm). These were then analyzed by 10% non-reducing sodium dodecyl sulfate polyacrylamide gel electrophoresis (SDS-PAGE) [26] using a miniVE vertical electrophoresis system (GE Healthcare Life Sciences, Baie d'Urfe, QC, Canada). The gel was stained using Coomassie Brilliant Blue R dye and imaged using a Bio-imaging MiniBis Pro system (DNR-Imaging Systems, Jerusalem, Israel).

### 3.4. Results and Discussion

Figs. 3.5A and B show the conductivity peaks obtained from the pulse tracer experiments carried out with sodium chloride solution using 2 mL and 5 mL sample loops respectively. For both pulse volumes examined, the conductivity peaks obtained with the laterally-fed device were significantly sharper than those obtained with the radial-flow device. Also, the peaks obtained with the laterally-fed device were quite symmetrical while those obtained with the radial-flow device showed significant tailing. The peak width at half height, asymmetry parameter, and tailing factor of these conductivity peaks are summarized in Table 3.1. The asymmetry parameter was measured at 10% of peak height while the tailing factor was calculated at 5% of the peak height as recommended in the literature [27]. Peak broadening and asymmetry are both signs of poor flow distributions within a device, and indicate that the efficiency in chromatographic separations carried out using these devices would be poor. With the laterally-fed device, sodium chloride was observed at the outlet (as evident from change in conductivity) at about 4.7 mL with both sample loops, which corresponded very well with the measured dead volume (i.e. 4.8 mL). With the radial-flow device, the salt appeared at the outlet at around 8.8 mL which was significantly lower than its measured dead volume (i.e. 21 mL). Quite clearly, there was significant variability in the solute path length within the radial flow device with the shortest path (corresponding to 8.8 mL effluent volume) being significantly lower than the average path length. On the other hand, the flow behavior observed with the laterally-fed device was quite close of that idealized in Fig. 3.2, i.e. the distribution in flow path lengths was narrow. Based on this, it may be inferred that the efficiency of chromatographic separation would be better with the latter. The large difference in the dead volumes of the two devices could also be partially responsible for the above results. Large dead volume within a device could cause back-mixing, which is undesirable in chromatographic separations.

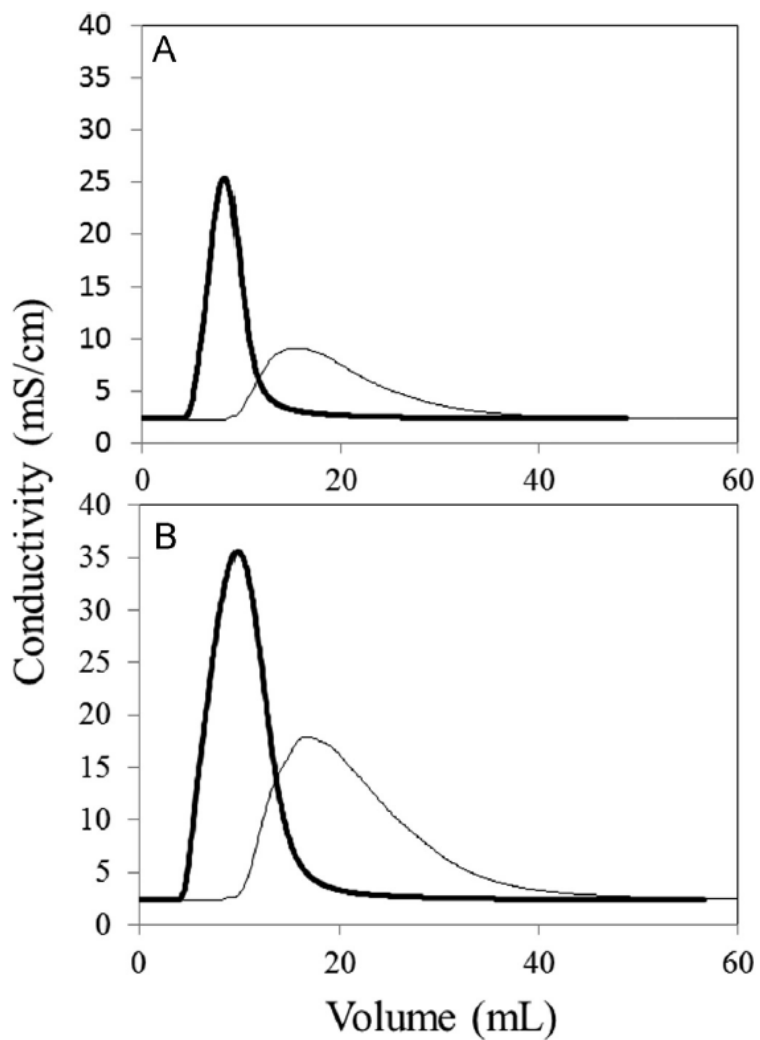
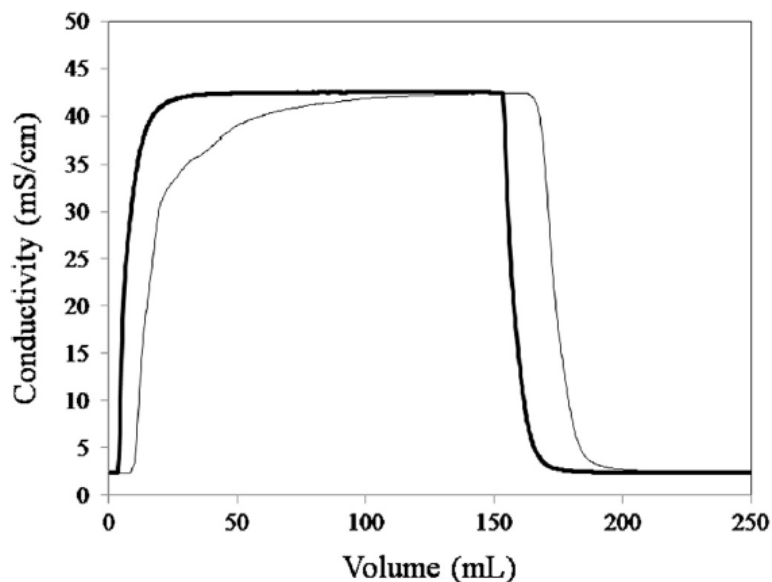


**Fig. 3.5:** Salt tracer peaks obtained with the radial-flow (thin line) and the laterally-fed (thick line) membrane chromatography devices (membrane: Sartobind S; membrane bed volume: 7mL; feed: 0.5 M NaCl; running buffer: 20 mM sodium phosphate, pH=7.0; flow rate: 10 mL/min; volume injected: 2 mL (A) and 5mL (B))

**Table 3.1:** Characteristics of pulse tracer peaks (shown in Fig. 3.5) obtained with sodium chloride using the radial-flow and the laterally-fed membrane chromatography devices (membrane: Sartobind S; membrane bed volume: 7 mL; tracer: 0.5 M NaCl; running buffer: 20 mM sodium phosphate, pH=7.0; flow rate: 10 mL/min).

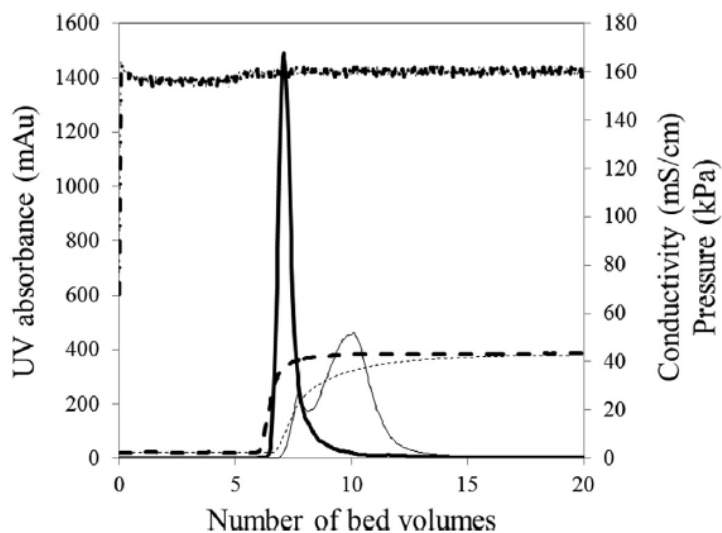
Reference figure	Loop size (mL)	Device	Peak width at half height (mL)	Asymmetry parameter	Tailing factor
3.5A	2.0	Radial-flow	12.19	3.03	2.33
		Laterally-fed	3.72	1.33	1.34
3.5B	5.0	Radial-flow	13.37	3.26	2.37
		Laterally-fed	6.54	1.29	1.28

Fig. 3.6 shows the results obtained from the step tracer experiments carried out with sodium chloride. In each of these experiments, approximately 150 mL of sodium chloride solution was injected into the module to simulate the step behavior. As observed in the pulse tracer experiments discussed in the above paragraph, the salt breakthrough with the radial-flow device took place around 8.7 mL, which was significantly lower than its measured dead volume. With the laterally-fed device, the salt break-through matched its measured dead volume almost perfectly. The latter part of the salt breakthrough curve (20–120 mL) obtained with the radial-flow device was shallow and jagged, clearly indicating poor flow distribution and possibly some degree of back-mixing. On the other hand, the breakthrough curve obtained with the laterally-fed device was sharp, indicating low variability in solute path length, and close to ideal plug flow behavior. The superior flow distribution of the laterally-fed device is also evident from a comparison of the conductivity decay profiles corresponding to the end of the sodium chloride injection. While the conductivity decreased very sharply with the laterally-fed device, the response with the radial flow device was slower.



**Fig. 3.6:** Salt breakthrough curves obtained with the radial-flow (thin line) and laterally-fed (thick line) membrane chromatography devices (membrane: Sartobind; membrane bed volume: 7 mL; feed: 0.5 M NaCl; volume injected: 150 mL; running buffer: 20 mM sodium phosphate, pH=7.0; flow rate: 10 mL/min)

Figs. 3.7 and 3.8 show the bind and elute chromatograms obtained by injecting 2 mL and 5 mL pulses respectively of 8 mg/mL lysozyme solution into the radial-flow and laterally-fed devices. In both sets of experiments, the eluted lysozyme peaks obtained with the laterally-fed device were significantly sharper and more symmetrical. With the radial-flow device, the peaks were not only broad but also contained shoulders, indicating non-uniform protein binding within the membrane bed. A broad peak, in addition to being indicative of poor resolution, also implies sample dilution. In large-scale separation processes, sample dilution in eluted peak is undesirable. Table 3.2 shows the peak width at half height data obtained from the above experiments. These results clearly indicate the likelihood of superior separation in the bind-and-elute mode with the laterally-fed device.



**Fig. 3.7:** Lysozyme elution peaks obtained with the radial-flow (thin lines) and the laterally-fed (thick lines) membrane chromatography devices (membrane: Sartobind S; membrane bed volume: 7 mL; feed concentration: 8 mg/mL; volume injected: 2 mL; binding buffer: 20 mM sodium phosphate, pH=7.0; eluting buffer: binding buffer+0.5 M NaCl; flow rate: 10 mL/min; UV absorbance: solid lines; conductivity: dashed lines; pressure: dotted lines)

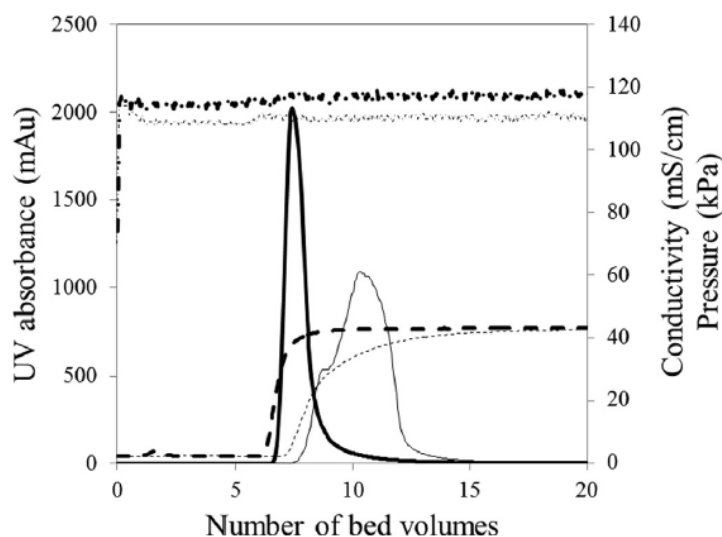


**Fig. 3.8:** Lysozyme elution peaks obtained with the radial-flow (thin lines) and the laterally-fed (thick lines) membrane chromatography devices (membrane: Sartobind S; membrane bed volume: 7 mL; feed concentration: 8 mg/mL; volume injected: 5 mL; binding buffer: 20 mM sodium phosphate, pH=7.0; eluting buffer: binding buffer+0.5 M NaCl; flow rate: 10 mL/min; UV absorbance: solid lines; conductivity: dashed lines; pressure: dotted lines).

**Table 3.2:** Characteristics of lysozyme elution peaks (shown in Figs. 3.7 and 3.8) obtained in the bind-and-elute mode with the radial-flow and the laterally-fed devices (membrane: Sartobind S; membrane bed volume: 7 mL; lysozyme concentration: 8 mg/mL; binding buffer: 20 mM sodium phosphate, pH=7.0; eluting buffer: binding buffer+0.5 M NaCl; flow rate: 10 mL/min).

Reference figure	Loop size (mL)	Device	Peak width at half height (mL)
3.7	2.0	Radial-flow	15.81
		Laterally-fed	4.21
3.8	5.0	Radial-flow	18.00
		Laterally-fed	6.43

Further single-protein experiments were carried out to assess feasibility of separating the model proteins i.e., ovalbumin, conalbumin and lysozyme. Based on their pI values, ovalbumin was expected in the flow-through while the other two other proteins were expected to bind to the membrane, with conalbumin eluting first, followed by lysozyme during salt induced elution. These experiments were also useful in determining the operating ranges for the two devices. Fig. 3.9 shows an overlay of the three chromatograms obtained in single-protein bind-and-elute experiments carried out using the radial-flow device, with 40 mL linear gradient elution. Ovalbumin was obtained as a broad single peak in the flow-through. For both conalbumin and lysozyme, the eluted peaks contained shoulders, consistent with results shown in Figs. 3.7 and 3.8. The peaks were quite jagged and broad, clearly showing the effect of uneven flow within the device, and uneven binding on the cation-exchange membrane. These results indicate that with the radial-flow device, the conalbumin and lysozyme peaks would not be properly resolved with a 40 mL linear gradient. A similar set of experiments carried out using the laterally-fed device (data not shown) showed that the three proteins could potentially be separated from each other.

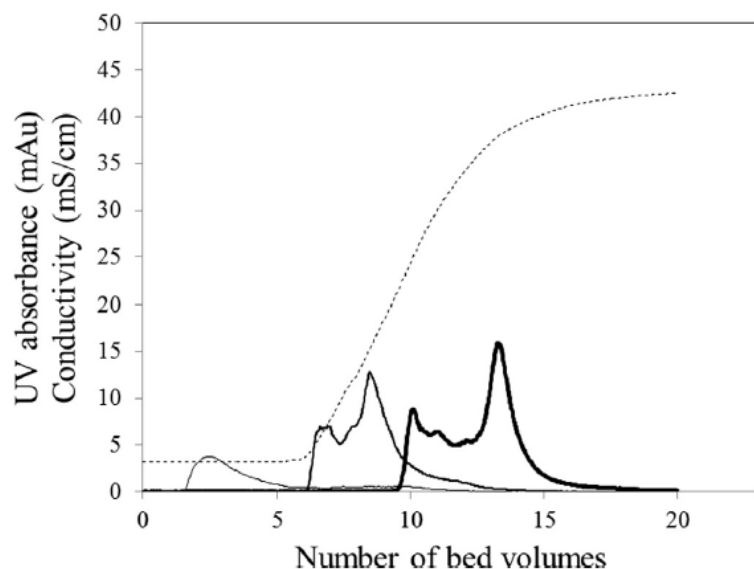


**Fig. 3.9:** Single-protein peaks obtained with ovalbumin (thin line), conalbumin (medium line), and lysozyme (thick line) using the radial-flow device (membrane: Sartobind S; membrane bed volume: 7 mL; ovalbumin concentration: 0.25 mg/mL; conalbumin concentration: 0.5 mg/mL; lysozyme concentration: 0.25 mg/mL; loop size: 2 mL; binding buffer: 20 mM citrate, pH=5.5; eluting buffer: binding buffer+0.5 M NaCl; linear gradient length: 40 mL; flow rate: 10 mL/min; solid line: UV absorbance; dashed line: conductivity).

Some preliminary three-component, protein separation experiments were carried out to determine the point at which the elution gradients could be commenced with the radial-flow and laterally-fed devices. Fig. 3.10 shows the early part of the chromatograms obtained from experiments carried out with the radial-flow device where the linear elution gradients were started 10 mL and 20 mL after sample injection. When the gradient was commenced 10 mL after sample injection, the elution of conalbumin started even before ovalbumin could be completely removed in the flow-through. Therefore the ovalbumin and conalbumin peaks were not baseline resolvable. When the elution was started 20 mL after sample injection, the quality of resolution was much better. With the laterally-fed device (data not shown), ovalbumin and conalbumin were completely resolved even when elution was started 5 mL after sample injection. The point at which elution gradients can be started is of significant importance in large-scale purification processes as this

affects buffer usage. Sterile buffers that are typically used in biopharmaceutical production can be quite expensive to prepare and their consumption may significantly affect the manufacturing cost.

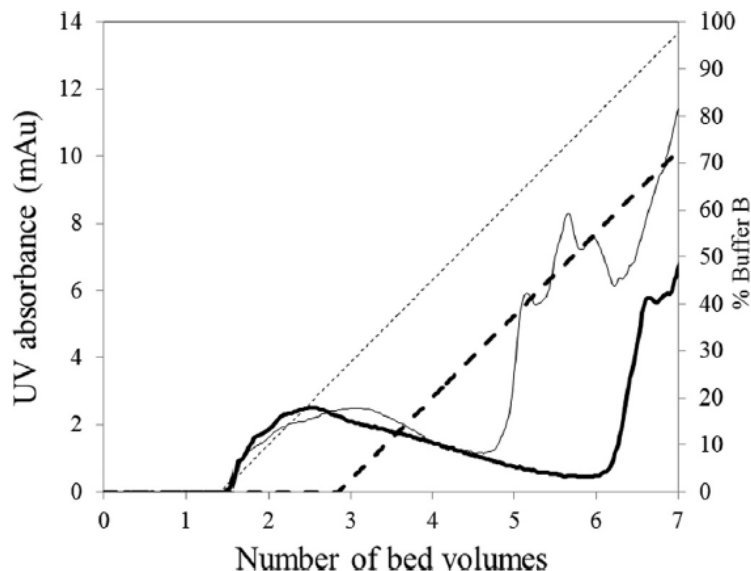


**Fig. 3.10:** Ovalbumin flow-through and eluted conalbumin peaks obtained from multi-component separation experiments carried out with the radial-flow device to determine the effect of gradient elution start volume on resolution of bound and eluted proteins (thick lines: 20 mL start; thin lines: 10 mL start; solid line: UV absorbance; dashed line: % eluting buffer; membrane: Sartobind S; membrane bed volume: 7 mL; ovalbumin concentration: 0.25 mg/mL; conalbumin concentration: 0.5 mg/mL; loop size: 2 mL; binding buffer: 20 mM citrate, pH=5.5; eluting buffer: binding buffer+0.5 M NaCl; gradient volume: 40 mL; flow rate: 10 mL/min).

Fig. 3.11 shows the chromatograms obtained from three-component protein separation experiments carried out with the radial-flow device using linear gradient lengths of 40, 60 and 80 mL respectively. In each of these experiments, the gradients were started 20 mL after sample injection. As expected based on the single-protein experiments, lysozyme and conalbumin could not be resolved using the 40 mL linear gradient. The resolution was slightly better with 60 mL gradient and near baseline re-resolution was obtained using 80 mL gradient. However, the ovalbumin peak was very broad, almost occupying almost the entire amount of flow-through. The conalbumin and lysozyme peaks, though resolved, were very

broad and jagged. Therefore, all the separated proteins were significantly diluted in the purification process and it took close to 25 bed volumes of buffer to carry out this separation.

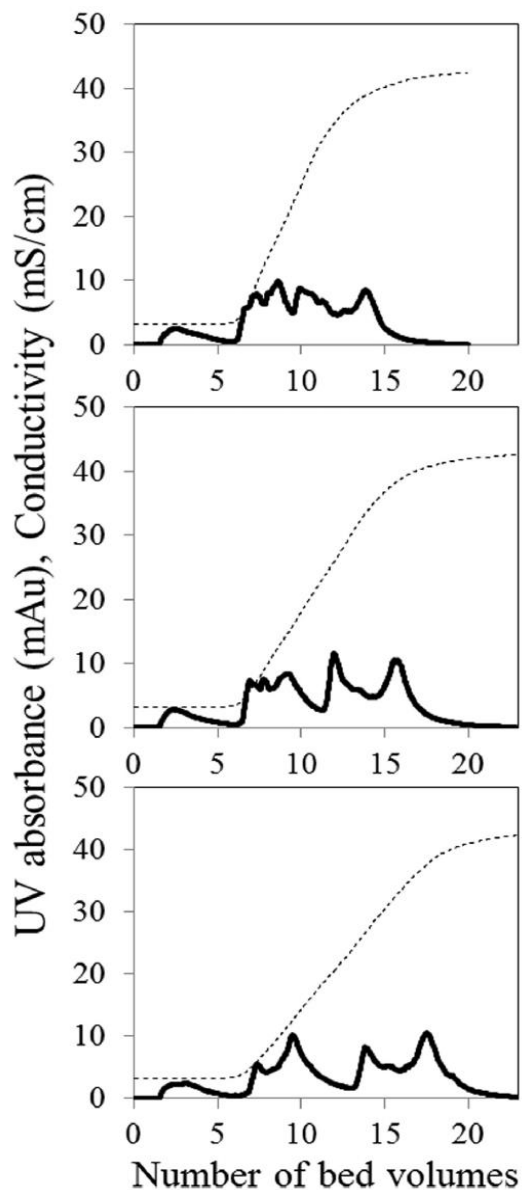


**Fig. 3.11:** Multi-component separation peaks obtained with the radial-flow device using 40 mL (A), 60 mL (B) and 80 mL (C) linear gradients (membrane: Sartobind S; membrane bed volume: 7 mL; ovalbumin concentration: 0.25 mg/mL, conalbumin concentration: 0.5 mg/mL; lysozyme concentration: 0.25 mg/mL; loop size: 2 mL; binding buffer: 20 mM citrate, pH=5.5; eluting buffer: binding buffer+0.5 M NaCl; flow rate:10 mL/min; solid line: UV absorbance; dashed line: conductivity).

Fig. 3.12 shows the chromatograms obtained from the three-component protein separation experiments carried out using the laterally-fed device using linear gradient lengths of 20, 30 and 40 mL respectively. In all three experiments, the gradient was started 5 mL after sample injection. The flow-through ovalbumin peaks were significantly sharper than those obtained with the radial flow device. Consistent with the single-protein experiments, the eluted peaks were very sharp and symmetrical at all three gradients examined. The sharpness of the eluted peaks decreased slightly, while their resolution increased as the gradient length was increased. With 20 mL gradient, the conalbumin and lysozyme peaks were not completely resolved. However, these peaks were almost completely resolved with 30 mL gradient while the resolution increased further when the gradient length was increased to 40 mL. Fractionated protein samples obtained from the experiment carried out with the laterally-fed device using 40 mL gradient were analyzed using SDS-PAGE. Fig. 13 which shows the stained gel thus obtained. The results shown in Figs. 3.12 and 3.13 clearly demonstrate that the three model proteins could be efficiently separated using the cation exchange membrane stack housed within the laterally-fed device. The three model proteins examined in this study could be fractionated in about 10 bed volumes using the laterally-fed device as opposed to 25 bed volumes with the radial-flow device. In a large-scale separation process, such difference would have a huge impact on the difference in processing cost. Also, with the laterally-fed device, the fractionated proteins were not diluted to the extent with the radial-flow device.

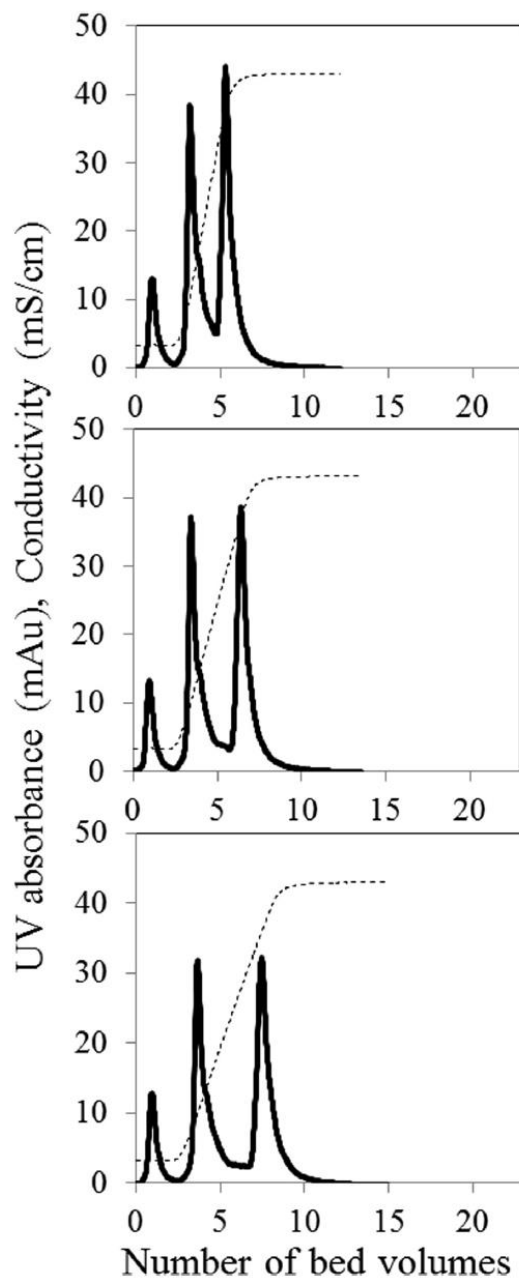


**Fig. 3.12:** Multi-component separation peaks obtained with the laterally device using 20 mL (A), 30 mL (B) and 40 mL (C) linear gradients (membrane: Sartobind S; membrane bed volume: 7 mL; ovalbumin concentration: 0.25 mg/mL, conalbumin concentration: 0.5 mg/mL; lysozyme concentration: 0.25 mg/mL; loop size: 2 mL; binding buffer: 20 mM citrate, pH=5.5; eluting buffer: binding buffer+0.5 M NaCl; flow rate:10 mL/min; solid line: UV absorbance; dashed line: conductivity).

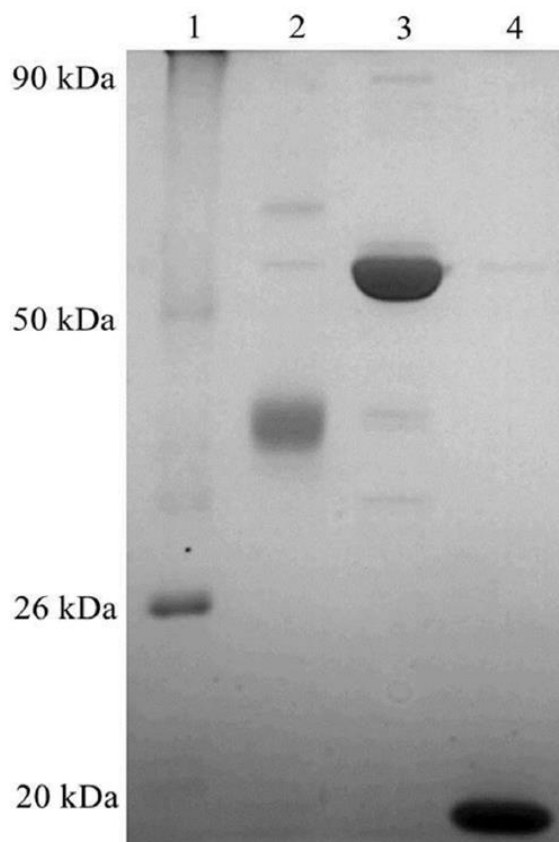


**Fig. 3.12:** SDS-PAGE analysis of samples obtained from the multi-component protein separation experiment carried out with the laterally-fed device using 40 mL linear gradient elution (1: protein molecular weight markers; 2: flow-through peak, i.e. ovalbumin; 3: first eluted peak, i.e. conalbumin; 4: second eluted peak, i.e. lysozyme).

The above results clearly demonstrate the suitability of the laterally-fed device for carrying out high-resolution, multi-component protein purification. Its design is simple and such devices are relatively easy to fabricate. The prototype device used in this study was fabricated by 3-D printing. However, similar devices could easily be mass-produced by polymer molding. The flat shape of the laterally-fed device as opposed to the cylindrical shape of the radial-flow device is of significant advantage as the former can be placed or mounted vertically with significantly lower footprint. Other advantages include their stackability which makes it convenient to assemble multiplexed systems for complex separations. Laterally-

fed devices housing membrane stacks in the subliter bed volume range are being designed for further studies. Some of the design features in the prototype device used in the current study were based on those recommended in our previous paper [25]. Firstly, the hydraulic resistance offered in the lateral flow channels had to be lower than that offered by the membrane stack. This was to ensure that the entire length of the membrane stack was utilized in a uniform manner. Secondly, the resistances in these lateral flow channels had to be identical. A higher resistance on the feed side would result in greater flow of liquid in the portions of the membrane stack closer to the membrane inlet. On the other hand, a higher resistance on the permeate side would have the opposite effect, i.e. greater flow of liquid in the portions of the membrane stack closer to the outlet. Both these conditions would lead to poor membrane utilization. The aspect (i.e. length to width) ratio of the lateral channel is likely to be quite important and will be investigated in further studies.

### **3.5. Conclusions**

Radial-flow membrane chromatography devices while being widely used in the biotechnology industry for large-scale polishing applications are unsuitable for bind and elute chromatography. The laterally-fed membrane chromatography device was found to be suitable for carrying out high-resolution, multi-component protein purification in the bind-and-elute mode. It outperformed its equivalent radial-flow device in terms of all the attributes examined, i.e. flow distribution, peak shape, and resolution of eluted peaks. The superior performance of the laterally-fed device could be attributed to lower variability in solute-flow path-length, and smaller dead volume. Tracer experiments carried out using salt in the pulse and step modes clearly demonstrated the superior hydraulic characteristics and narrower residence time distribution of the laterally-fed device. Single-protein experiments carried out in the bind-and-elute mode showed that the eluted peaks obtained with the laterally-fed device were significantly sharper and more symmetrical. Also, the elution step could be commenced much earlier, implying significantly lower buffer

usage. Three-component protein separation experiments carried out with the radial-flow device resulted in broad and jagged peaks, leading to poor resolution and protein dilution. The eluted peaks obtained with the laterally-fed device were very sharp and symmetrical at all three gradients examined. The sharpness of the eluted peaks de-creased slightly, while their resolution increased as the gradient length was increased. Three model proteins could be fractionated in about 10 bed volumes using the laterally-fed device as opposed to 25 bed volumes with the radial-flow device. The design of the laterally-fed device is simple and could potentially be mass-produced by polymer molding. The flat shape of the laterally-fed device gives it significantly lower footprint and offers additional advantages such as stackability and ease of multiplexing.

### **3.6. Acknowledgements**

We thank the Natural Science and Engineering Research Council (NSERC) of Canada for funding this study. We thank Paul Gatt and Mark MacKenzie for fabricating the membrane devices based on design provided by RG.

### **3.7. References**

- [1] U. Gottschalk, K. Brorson, A.A. Shukla, The need for innovation in biomanufacturing, *Nat. Biotechnol.* 30 (2012) 489–492.
- [2] R. Ghosh, Protein separation using membrane chromatography: opportunities and challenges, *J. Chromatogr. A* 952 (2002) 13–27.
- [3] T.B. Tennikova, F. Svec, B.G. Belenkii, High-performance membrane chromatography. A novel method of protein separation, *J. Liq. Chromatogr.* 13 (1990) 63–70.
- [4] C. Charcosset, Review Purification of proteins by membrane chromatography, *Chem. Technol. Biotechnol.* 71 (1998) 95–110.
- [5] D.K. Roper, E.N. Lightfoot, Separation of biomolecules using adsorptive membranes, *J. Chromatogr. A* 702 (1995) 3–26.

- [6] R. Van Reis, A. Zydney, Membrane separations in biotechnology, *Curr. Opin. Biotechnol.* 12 (2001) 208–211.
- [7] R. Ghosh, Separation of proteins using hydrophobic interaction membrane chromatography, *J. Chromatogr. A* 923 (2001) 59–64.
- [8] V. Orr, L. Zhong, M. Moo-Young, C.P. Chou, Recent advances in bioprocessing application of membrane chromatography, *Biotechnol. Adv.* 31 (2013) 450–465.
- [9] A. Saxena, B.P. Tripathi, M. Kumar, V.K. Shahi, Membrane-based techniques for the separation and purification of proteins: an overview, *Adv. Colloid. Interface. Sci.* 145 (2009) 1–22.
- [10] U. Klein, E. Yeager, D. Seshadri, R. Baurmeister, Affinity adsorption devices, *J. Membr. Sci.* 129 (1997) 31–46.
- [11] P. Ghosh, K. Vahedipour, M. Lin, J.H. Vogel, C.A. Haynes, E. von Lieres, Computational fluid dynamic simulation of axial and radial flow membrane chromatography: mechanisms of non-ideality and validation of the zonal rate model, *J. Chromatogr. A* 1305 (2013) 114–122.
- [12] J. Thommes, M.R. Kula, Membrane chromatography-An integrative concept in the downstream processing of proteins, *Biotechnol. Prog.* 11 (1995) 357–367.
- [13] K.D. Program, Affinity adsorption devices prepared from microporous poly (amide) hollow fibers and sheet membranes, *J. Membr. Sci.* 129 (1997) 31–46.
- [14] R. Ghosh, T. Wong, Effect of module design on the efficiency of membrane chromatographic separation processes, *J. Membr. Sci.* 281 (2006) 532–540.
- [15] M. Kuczewski, N. Fraud, R. Faber, G. Zarbis-Papastoitsis, Development of a polishing step using a hydrophobic interaction membrane adsorber with a PER.C6-derived recombinant antibody, *Biotechnol. Bioeng.* 105 (2010) 296–305.
- [16] L. Raiado-Pereira, J.D. La Vega, D.M.F. Prazeres, M. Mateus, Development of a phenyl membrane chromatography-based process yielding pharmaceutical

grade plasmid deoxyribonucleic acid for mammalian cells transfection, *J. Chromatogr. A* 1337 (2014) 67–74.

[17] L. Voswinkel, U. Kulozik, Fractionation of all major and minor whey proteins with radial flow membrane adsorption chromatography at lab and pilot scale, *Int. Dairy. J.* 39 (2014) 209–214.

[18] B.V. Bhut, K.A. Christensen, S. M. Husson, Membrane chromatography: protein purification from *E. coli* lysate using newly designed and commercial anion-exchange stationary phases, *J. Chromatogr. A* 1217 (2010) 4946–4957.

[19] J. Weaver, S.M. Husson, L. Murphy, A.R. Wickramasinghe, Anion-exchange membrane adsorbers for flow-through polishing steps: part I. Clearance of minute virus of mice, *Biotechnol. Bioeng.* 110 (2013) 491–499.

[20] J.H. Vogel, H. Nguyen, R. Giovannini, J. Ignowski, S. Garger, A. Salgotra, J. Tom, new large-scale manufacturing platform complex for biopharmaceuticals, *Biotechnol. Bioeng.* 109 (2012) 3049–3058.

[21] J.H. Chon, G. Zarbis-Papastoitis, Advances in the production and downstream processing of antibodies, *New. Biotechnol.* 25 (2001) 458–463.

[22] J.X. Zhou, T. Tressel, Basic concepts in Q membrane chromatography for large-scale antibody production, *Biotechnol. Prog.* 22 (2006) 341–349.

[23] H.L. Knudsen, R.L. Fahrner, Y. Xu, L.A. Norling, G.S. Blank, Membrane ion-exchange chromatography for process-scale antibody purification, *J. Chromatogr. A* 907 (2001) 145–154.

[24] R. Ghosh, Laterally-fed membrane module, US Patent Application No. 62074858 filing date November 4, 2014.

[25] P. Madadkar, Q. Wu, R. Ghosh, A laterally-fed membrane chromatography module, *J. Membr. Sci.* 487 (2015) 173–179.

[26] U.K. Laemmli, *Nature* 227 (1970) 680–685.

[27] S.C. Moldoveanu, V. David, Essentials in Modern HPLC Separations, Elsevier, Waltham, 2013

## **Chapter 4**

### **Performance Comparison of Laterally-fed Membrane Chromatography (LFMC) Devices with Commercial Packed Resin Columns: Application Case Study for Preparative Separation of IgG1 Charge Variants**

#### 4.1. Abstract

The application of the currently available membrane adsorbers has been only limited to operations carried out in flow-through format as they fail to give acceptable resolution in bind-and-elute processes. The recently developed laterally-fed membrane chromatography (LFMC) devices have shown to be an efficient solution, greatly suitable for high-resolution membrane chromatography. In this study, the performance of LFMC devices is head-to-head compared with commercial packed resin columns. The comparison was carried out between LFMC devices containing Sartobind S membranes and HiTrap SP high-performance (HP) columns in 1 mL and 5 mL scale using a three model protein system. The cation-exchange separation of ovalbumin, conalbumin, and lysozyme were carried out using linear salt gradients at different flow rates. The results confirmed comparable resolution for both systems with LFMC devices being highly consistent at much higher flow rates. The two systems were then compared for an application case study in preparative separation of HIgG1-CD4 charge variants with salt gradients. The LFMC device gave immaculate separation of the variants at the extensively shallow linear gradients used, whereas in case of the HiTrap column, the separations were messy resulting from jagged conductivity profiles.

**Keywords:** Membrane chromatography; Laterally-fed; HiTrap; resin chromatography; lysozyme; charge variant

## 4.2. Introduction

Chromatography is the linchpin in separation of biopharmaceuticals as far as high-resolution of separation is concerned. This is while conventional packed-bed column chromatography has remained as the state of the art in downstream purification of biological molecules despite its major shortcomings [1-4]. The main drawback associated with resin columns is the strong correlation of the resolution with the operating flow rate which is due to the diffusion based solute transport to the binding sites within the porous resin beads. Operation at low flow rates highly affects the productivity whereas increasing the flow rate results in drastic decline in the resolution of separation [5,6]. Considering the cleaning and regeneration also at limited flow rates, the processes are very low-throughput. The other downside of packed-bed chromatography is the high pressure drops which is directly proportional to the bed height of the column. Therefore, scale-up of the columns is commonly through increasing the column diameter at similar bed height based on which the resulting larger cross-sectional area keeps the pressure drops below the limiting values. However, in columns with such aspect ratios, problems such as uneven packing and insufficient header design yet contribute to broad and poorly resolved peaks, the effects which are aggravated at higher flow rates [7,8].

In the past few decades, the use of membranes [9-11], monoliths [12,13], and mix-matrix [14] has been suggested to substitute the conventional resin-based stationary phase. Membrane chromatography which uses a stack of adsorptive membranes provides an order of magnitude higher productivity. As opposed to resin beads, solute mass transport within adsorptive membranes is dominated by convection which is the chief advantage of this techniques. Accordingly, the performance of membrane chromatography is consistent over a wide range of flow rates, offering significantly greater throughputs. Moreover, the pressure drops are much lower and devices are used in a single-use manner, eliminating the cleaning and validation steps, all contributing to lower overall processing cost [15-17]. In spite of all the benefits, membrane adsorbers have been accepted only in niche

applications where dilute impurities are removed at high flow rates in flow-through operation format [18]. Such applications include late-stage polishing of monoclonal antibody (mAb) and therapeutic proteins as well as purification of large biomolecules such as viruses and plasmid DNA [19]. In other applications where bind-and-elute separations are involved, currently available membrane chromatography devices give poor resolutions. The reason lies behind the severe design deficiency which results in flow maldistribution within the devices, namely, non-uniformity in the solute flow path, uneven solute residence time, and large dead volumes which exacerbates the related dispersion effects [20]. Hence, a combined high-productivity and high-resolution technology would be a great fit in the future downstream processing in the fast-growing commercial environment of biopharmaceuticals [9].

Recently, we have introduced a membrane chromatography technology through development of new devices which are very much suitable for high-resolution separations in the bind-and-elute format with great potential to expand the application of membrane chromatography [20-22]. The Laterally-fed membrane chromatography (LFMC) devices house a stack of rectangular membrane sheets with identical lateral channels on both sides of the stack. The design and fabrication of the latest embodiment of the devices is described in details in our previous study [23]. Owing to the novel device design, the solute flow path lengths within the device is highly uniform and the pressure is well-balanced over the sides of the membranes [24]. These features result in uniformity of permeate flux and therefore solute residence times and result in sharp, symmetrical peaks. Thus far, the LFMC devices have extensively outperformed the commercially available radial-flow devices for bind-and-elute separations [20] and showed excellent resolution when used for challenging separation case studies, being purification of mono-PEGylated proteins [23] and separation of mAb aggregates. The encouraging results, i.e. high resolutions at high flow rates, called for head-to-head comparison of the performance of LFMC devices with commercial packed resin

columns. In this study, we compare the performance of cation-exchange LFMC with the commercially available resin columns having similar ligand chemistries. The separation of three model proteins is investigated with major focus on resolution at different flow rates. The intentions were to investigate the benefits of the LFMC technology when high-resolution of separation is required.

The performance of the two chromatography systems were examined with model proteins were then compared for preparative separation of mAb charge variants using linear salt gradients as an application case study [16]. Previous studies have shown that charge variants of therapeutic antibodies can have diverse bioactivity [25]. More specifically, in mAbs, the intrinsic micro-heterogeneity often as a result of spontaneous and non-enzymatic protein degradation might result in undesirable reactions in patients [26,27]. Other alterations in the final mAb products may be due to intended post-translational modifications. Complete characterization of the mAb charge variants requires a combination of techniques commonly involving enzyme digestion to study the mAb fragments followed by mass spectroscopy [28,29]. However, cation-exchange chromatography is a non-denaturing technique which is sensitive to the variations in the charge of the mAb molecules [30,31]. This is while diverse parameters should be optimized in order to achieve the separation as the structural diversities are very minor and the separation is considered rigorously challenging [29,32-34]. All things considered, conventional CEX with salt gradients offers great resolving power. Furthermore, cation exchange chromatography using pH gradients either by pre-column mixing of two buffers or by chromatofocusing has shown to be promising for separation of mAb variants [30,35,36]. While elution by pH gradient methods are considered to offer multi-product charge sensitive separation as opposed to the product-specific typical salt-gradient techniques, it is very challenging to control the slope of the pH gradients and the methods often involve extensive column regeneration times [37].

The LFMC devices used in this study contained Sartobind S membranes from Sartorius which were head-to-head compared with HiTrap columns from GE

Healthcare Life Sciences commercially packed with SP sepharose high-performance (SP HP) resins [38]. The comparison was carried out in two different scales of 1 mL and 5 mL bed volume using three model proteins. It is notable that sepharose HP resins having particle size of 34  $\mu\text{m}$  (24  $\mu\text{m}$ -44  $\mu\text{m}$ ) are specifically designed for high-resolution applications due to their relatively small particle size. This was followed by comparing the performance of the systems at 5 mL bed volume for preparative separation of HIgG1-CD4 (campath-9 [39]) charge variants. HIgG1-CD4 is a humanized IgG1-type antibody against CD4 antigen which has been used in human clinical trials towards rheumatoid arthritis and psoriasis.

### **4.3. Materials and Methods**

#### **4.3.1. Materials**

Ovalbumin (A5503), conalbumin (C7786), lysozyme (L6876), citric acid (C0759), sodium citrate dihydrate (S4641), sodium phosphate monobasic (S0751), sodium phosphate dibasic (S0875), and sodium chloride (S7653) were purchased from Sigma-Aldrich (St. Louis, MO, USA). Humanized monoclonal antibody HIgG1-CD4 (campath-9) was kindly donated by the Therapeutic Antibody Centre, University of Oxford, UK. HiTrap sepharose SP HP strong cation exchange columns (5 mL and 1 mL) were purchased from GE healthcare Life Sciences (Piscataway, NJ, USA). Sartobind S cation-exchange membrane sheets (94IEXS42-001) were purchased from Sartorius Stedim Biotech (Gottingen, Germany). Lepage epoxy glue was purchased from Henkel (Dusseldorf, Germany). Weld-on 16 glue was purchased from IPS Corporation (Compton, CA, USA). All buffers and the solutions were prepared using water obtained from a SIMPLICITY 185 water purification unit by Millipore (Molsheim, France).

#### **4.3.2. LFMC device design and fabrication**

The details of the design of the LFMC devices has been previously reported in a recently published article [23]. The devices are made of two acrylic plates which contain rectangular channels with an array of pillars having the same height of the

channel. The plates also contain two ports one for inlet/outlet and one for priming the system which is blocked during the chromatographic operations. The plates sandwich the middle frame within which the stack of rectangular membrane sheets are glued. The LFMC devices fabricated for this study had the bed volume of 4.7 mL and 1 mL. The design specifications is summarized in Table. 1. The devices were then connected to AKTA Prime liquid chromatography system (GE Healthcare Biosciences, QC, Canada) via standard PEEK tubings and luer fittings.

**Table 4.1:** Design details of the LFMC devices

Membrane bed volume (mL)	Number of membrane layers	Bed height (mm)	Membrane dimensions (mm × mm)	Pillar array	Outer dimension of plate (mm × mm)	Dead volume (mL)
4.7	12	3.3	70 × 20	28 × 7	150 × 40	5.19
1.0	10	2.7	38 × 10	15 × 3	120 × 30	1.21

#### 4.3.3. Model protein separation

The model protein system used for this study was consisted of a solution containing three different proteins: ovalbumin (pI 4.5, 0.2 mg/mL), conalbumin (pI 6.1, 1.0 mg/mL), and lysozyme (pI 11.0, 0.5 mg/mL). The sample volume injected was 10 % of the bed volume of the system using 500 µL and 100 µL sample loops. Sodium citrate buffer (20 mM, pH 5.5) was used as the binding buffer and the eluting buffer contained 0.5 M NaCl prepared in the binding buffer. Linear gradient elution was commenced at the same time with the sample injection.

#### 4.3.4. Lysozyme oxidation and CEX separation

Lysozyme sample with 2 mg/mL concentration was oxidized with hydrogen peroxide, a strong oxidant. Stock solution of 5 mg/mL lysozyme was prepared in 20 mM sodium phosphate buffer (pH 6.0). Stock solution of 2% hydrogen peroxide

was also prepared in the same buffer. The lysozyme solution was diluted to 0.5 mg/mL with the hydrogen peroxide solution in 1.5 mL vials. The vial was then heated at 37°C water bath (Multi Temp III, Amersham Biosciences, UK) for 18 hours and then allowed to cool off at room temperature for 30 min. The sample for the control experiment contained 0.5 mg/mL lysozyme in the same buffer which was kept in the water bath along with the main sample. The control sample did not contain hydrogen peroxide.

The oxidized sample and the control sample were injected to the 4.7 mL device using a 2 mL sample loop. The binding buffer was 20 mM sodium phosphate (pH 6.0) and 0.5 M NaCl prepared in the same buffer was used to elute the bound lysozyme. The experiments were carried out at 15 mL/min using 20 mL linear gradient which was commenced at the same time with sample injection.

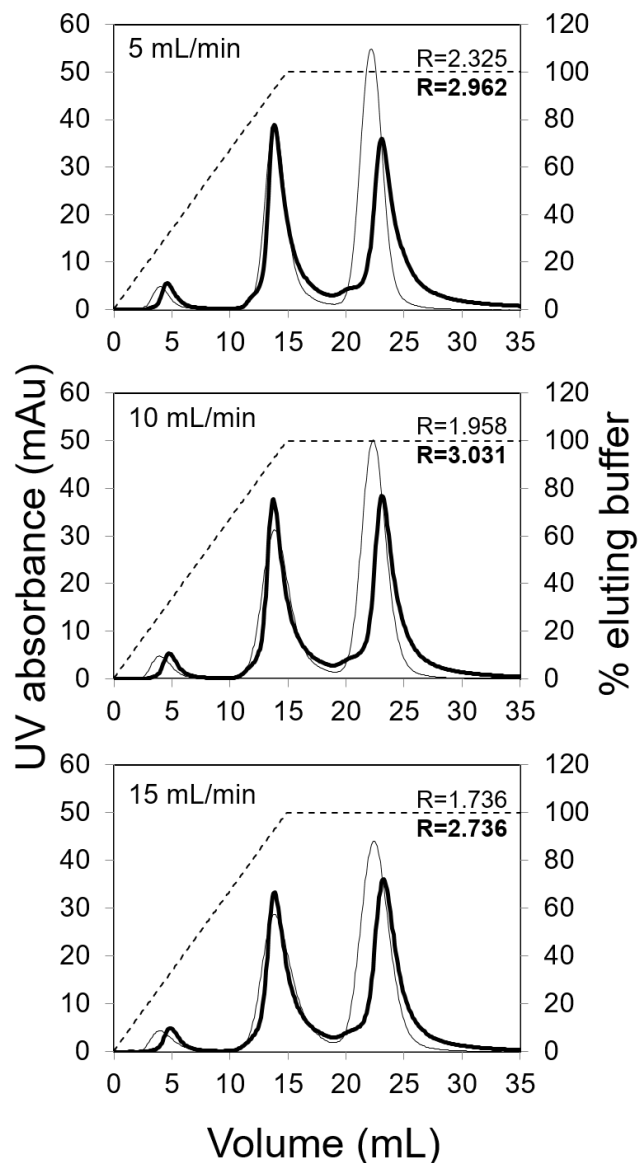
#### **4.3.5. Separation of mAb charge variants**

The HlgG1-CD4 (pI 8.7) stock solution was ~10 times diluted to 0.5 mg/mL using 20 mM sodium phosphate buffer (pH 6.0). The same buffer was also used as the binding buffer in all the experiments. The sample volume injected in every experiment was 2 mL and shallow linear gradients to the eluting buffer (0.5 M NaCl prepared in binding buffer) was performed to resolve the charge variants.

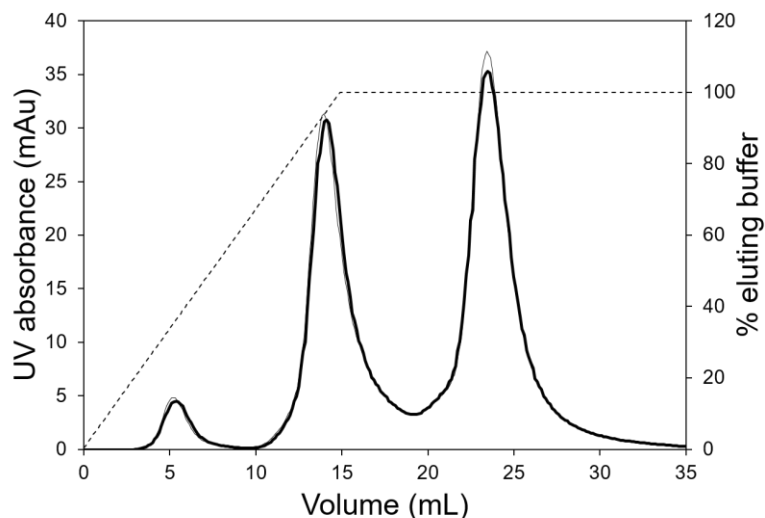
#### **4.4. Results and Discussion**

Based on the pI values of the three model proteins and the operating pH, the ovalbumin showed up in the flow through which was followed by the elution of conalbumin and lysozyme respectively. The results shown in Fig. 4.1 compare the performance of the HiTrap SP HP (5 mL) with the 4.7 mL LFMC device with 15 mL gradient at three different flow rates. Comparing the ovalbumin flow-through peaks, the LFMC device gave sharper peaks whereas the peaks obtained with the HiTrap column were broader and further tailed. The peak shapes indicated more uniform residence time for the LFMC device which is brought by the uniform solute flow path length within the device. This is while in columns the radially outward

distribution of the liquid in the inlet and radially inward collection in the outlet causes non-uniformity in the flow path lengths. Even though this affects the large-scale columns with bigger diameters more drastically [8], the effect is still observable at this scale. The results acquired from the HiTrap column showed high-resolution of separation for the two eluting proteins. This is due to the small particle diameter together with the 25 mm bed height which provides high number of theoretical plates. Nevertheless, the results were highly affected by flow rate which is an expected behavior for resin packed-bed stationary phase owing to the diffusion-dominated solute transport. The resolutions obtained with the LFMC device were greatly comparable with those attained from the HiTrap column although not resolved as nearly to the baseline. This is while the bed height of the LFMC device was almost eight time lower being 3.3 mm. It can be inferred that the LFMC devices provide a very uniform binding and elution of the solutes based on which the resolution of separation is comparable with resin columns at such low bed heights. This uniformity is in consequence of the design which gives excellent flow distribution within the devices. It is of high value that the performance over the range of the flow rates examined was highly consistent for the LFMC device which was predictable based on the dominance of convection within the membrane stack. We explored this even further by carrying out the same model protein separation at higher flow rates. Fig. 4.2 demonstrates the performance of the device for 25 and 30 mL/min. The chromatograms obtained clearly showed that the LFMC device performed consistently even at flow rates twice the ones suggested by the HiTrap column manufacturer being 15 mL/min. This is extremely advantageous from the manufacturing point of view, offering much greater productivity with trivial sacrifice on the resolution. Regardless, the resin columns are still beneficial at low flow rates from the resolution point of view.



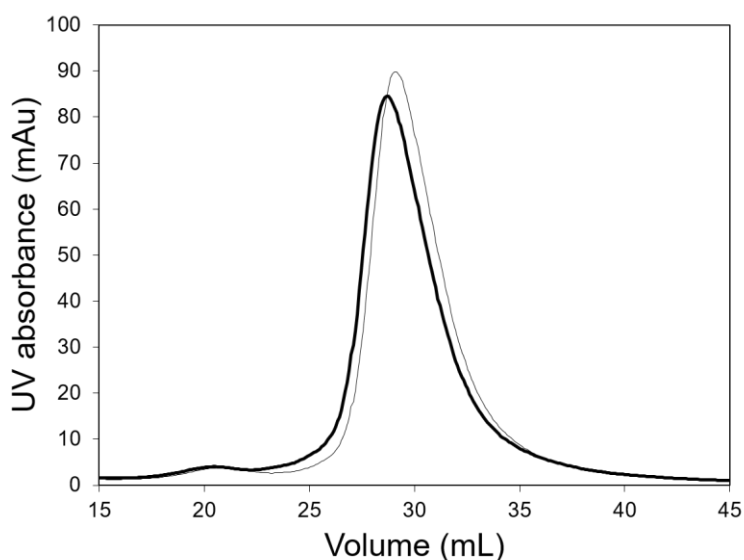
**Fig 4.1:** Performance comparison of the CEX-LFMC (thick line) and HiTrap SP HP (thin line) for separation of model proteins in 5 mL bed volume scale (membrane: Sartorius S; membrane bed volume: 4.7 mL; feed: 0.1 mg/mL ovalbumin, 1.0 mg/mL conalbumin, 0.5 mg/mL lysozyme; sample volume: 500  $\mu$ L; binding buffer: 20 mM sodium citrate pH 5.5; eluting buffer: binding buffer + 0.5 M NaCl; linear gradient volume: 15 mL (dashed line))



**Fig 4.2:** Model protein separation using the CEX-LFMC at higher flow rates of 25 mL/min (thin line) and 30 mL/min (thick line) (membrane: Sartorius S; membrane bed volume: 4.7 mL; feed: 0.1 mg/mL ovalbumin, 1.0 mg/mL conalbumin, 0.5 mg/mL lysozyme; sample volume: 500  $\mu$ L; binding buffer: 20 mM sodium citrate pH 5.5; eluting buffer: binding buffer + 0.5 M NaCl; linear gradient volume: 15 mL (dashed line))

Despite the comparable results, the peak shapes obtained from the LFMC device were quite different being wider in the base and narrower and sharper closer to the tip. Therefore, the resolution of separation ( $R$ ) which was calculated based on the resident volume and peak width at half height values were greater for the LFMC device. Looking at the eluting peaks individually, the conalbumin peaks were fairly similar for both systems but the lysozyme peaks was preceded by a prepeak which was not picked up by the resin column. The prepeak contained the variants of the molecule with lower  $pI$ , i.e. more acidic variant with lesser net positive charge at the working  $pH$ . Different retention volumes of charge variants on cation exchangers has been widely studied for antibodies of subclasses IgG1 and IgG2 as discussed earlier in this paper [32,40,41]. Nevertheless, for lysozyme, due to the higher stability of the molecule in comparison, charge variants are less of a concern. In order to investigate the separation of lysozyme charge variants by the CEX-LFMC device, samples containing oxidized lysozyme as well as the control

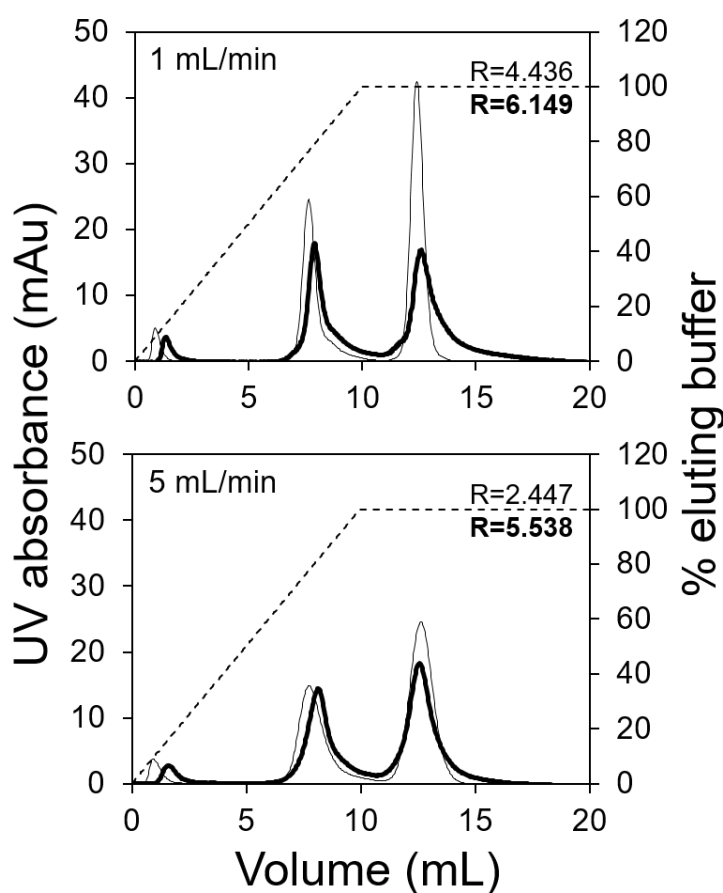
were experimented with the device. As it is shown by the chromatograms in Fig. 4.3, the oxidized lysozyme peak was shifted to left due to the presence of more acidic variants of the molecule as a result of oxidation. Based on the chromatograms, the prepeak seen preceding the lysozyme peak contained the acidic variant of lysozyme. Based on the results obtained, great resolution of separation for lysozyme charge variants was confirmed by the LFMC device in the model protein separation.



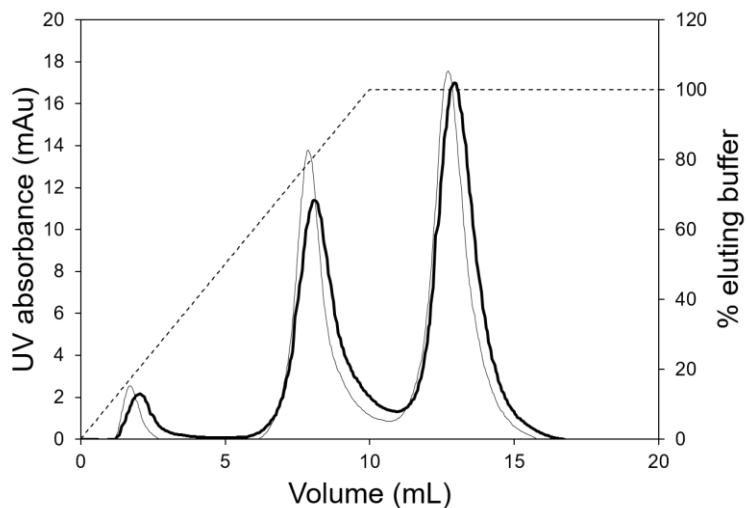
**Fig 4.3:** Elution behavior of oxidized lysozyme (thick line) and the control sample (thin line) using the CEX-LFMC (membrane: Sartorius S; membrane bed volume: 4.7 mL; feed: 0.5 mg/mL lysozyme; sample volume: 2 mL; binding buffer: 20 mM sodium phosphate pH 6.0; eluting buffer: binding buffer + 0.5 M NaCl; linear gradient volume: 20 mL; flow rate: 15 mL/min)

The performance comparison of the two systems using the same model proteins was studied in the 1 mL bed volume scale (Fig. 4.4). The same trends seen at the 5 mL scale was factual in the smaller scale: baseline resolution of separation at 1 mL/min flow rate by the HiTrap column in common with tailed flow-through peak and the flow rate dependent performance. Also, wider peak bases, separation of lysozyme charge variants, and consistency over the range of the flow rates examined, for the LFMC device. It is notable that the bed height of the 1 mL LFMC

was nine times lower than the equivalent HiTrap column. Likewise with the larger scale, the performance of the 1 mL LFMC device was studied at higher flow rate this time even as high as 10 and 20 membrane bed volume (MBV)/min (Fig. 4.5). Considering that these flow rates were much higher than the maximum flow rates suggested by the column manufacturer, the performance of the LFMC device was fairly consistent, representing the great potential of this technology in performing high-resolution and high productivity bind-and-elute processes.

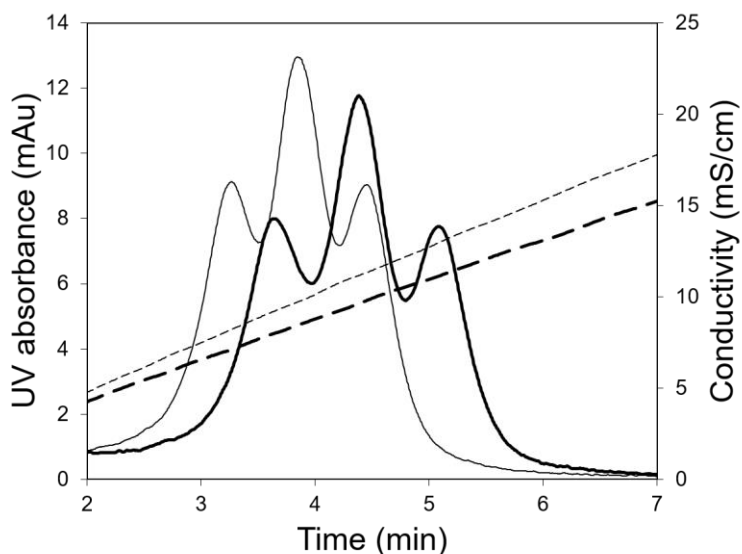


**Fig 4.4:** Performance comparison of the CEX-LFMC (thick line) and HiTrap SP HP (thin line) for separation of model proteins in 1 mL bed volume scale (membrane: Sartorius S; membrane bed volume: 1 mL; feed: 0.1 mg/mL ovalbumin, 1.0 mg/mL conalbumin, 0.5 mg/mL lysozyme; sample volume: 100  $\mu$ L; binding buffer: 20 mM sodium citrate pH 5.5; eluting buffer: binding buffer + 0.5 M NaCl; linear gradient volume: 10 mL (dashed line))



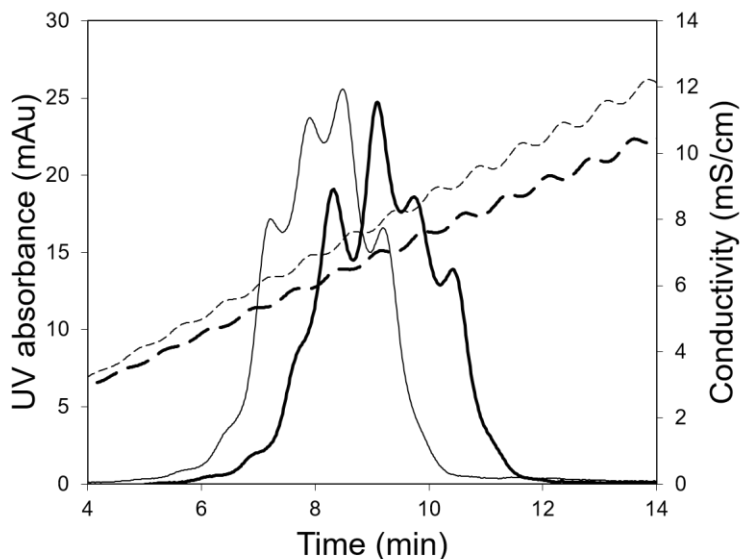
**Fig 4.5:** Model protein separation of the CEX-LFMC at higher flow rates of 10 mL/min (thin line) and 20 mL/min (thick line) (membrane: Sartorius S; membrane bed volume: 1.0 mL; feed: 0.1 mg/mL ovalbumin, 1.0 mg/mL conalbumin, 0.5 mg/mL lysozyme; sample volume: 100  $\mu$ L; binding buffer: 20 mM sodium citrate pH 5.5; eluting buffer: binding buffer + 0.5 M NaCl; linear gradient volume: 10 mL(dashed line))

Fig. 4.6 shows the performance of the 4.7 mL device in charge variant separation of HIgG1-CD4. The three peaks showed the acidic, main (neutral), and basic variants of the IgG1 molecule, the behavior which has been previously studied on cation exchangers [40,41]. Separation of IgG1 charge variants has been also attained using affinity chromatography, mostly with FcRn columns [42] as well as hydrophobic interaction chromatography (HIC) [43]. Owing to the similarities between the charge variants, the shallow gradients of 250 mL and 350 mL were used. This is while due to the high operating flow rate (15 mL/min), the separation was achieved in 7 min. The device provided very stable linear conductivity gradient which highly contributed to the immaculate separation of the variants which have trivial differences in their binding strengths to the stationary phase. This was made possible by the uniform flow distribution as a result of the device design.



**Fig. 4.6:** Charge variant separation of HlgG1-CD4 using the CEX-LFMC with 250 mL (thin line) and 300 mL (thick line) salt gradients (membrane: Sartorius S; membrane bed volume: 4.7 mL; feed: 0.5 mg/mL HlgG1-CD4; sample volume: 2 mL; binding buffer: 20 mM sodium phosphate pH 6.0; eluting buffer: binding buffer + 0.5 M NaCl; flow rate: 15 mL/min)

The same separation was performed with the 5 mL HiTrap column at 5 mL/min which is the recommended flow rate suggested by the manufacturer. As it was shown in Fig. 4.1, the column gave very high resolution at this flow rate due to which it was chosen for carrying out the challenging separation of charge variants. The results shown in Fig. 4.7 demonstrate jagged conductivity profiles obtained with the linear gradient from the binding to the eluting buffer. This is caused by the non-uniform flow distribution within the resin column. The resulting abrupt changes in the conductivity causes the jumbled elution of the mAb charge variants. Although the peak heights obtained are larger for HiTrap column, the resolution of separation is very poor. The results clearly show the unsuitability of the HiTrap column for separations in which extremely shallow gradients are required. This is while the LFMC device offered very stable linear conductivity profiles for such conditions even at three times higher flow rates.



**Fig 4.7:** Charge variant separation of HlgG1-CD4 using the HiTrap SP HP column with 250 mL (thin line) and 300 mL (thick line) salt gradients (column volume: 5.0 mL; feed: 0.5 mg/mL HlgG1-CD4; sample volume: 2 mL; binding buffer: 20 mM sodium phosphate pH 6.0; eluting buffer: binding buffer + 0.5 M NaCl; flow rate: 5 mL/min)

The results concluded that the LFMC devices are capable of performing bind-and-elute separations with comparable resolution with their equivalent commercial packed resin columns. While columns still offer improved results at lower flow rates, their performance is drastically affected by increasing the speed of operation. This is while the LFMC devices perform consistently at a wide range of speeds which is highly outstanding from the manufacturing point of view. It is notable that the great resolutions of separation were acquired at much lower bed heights compared to the equivalent resin columns. The low bed heights contribute to having significantly lower pressure drops compared to packed bed columns, making possible operating at high flow rates without the need for high-pressure pumps and sealing. The average pressure drops for all the experiments are listed in Table. 4.2 While commercially available radial-flow membrane adsorbers are also known for their low pressure drops as a result of low bed height to frontal surface area ratio, they are not suitable for bind-and-elute separations. The LFMC

device combines both features in one device, offering high-resolution and high-productivity with relatively low pressure drops.

**Table 4.2:** Pressure drops

Device	Bed volume (mL)	Flow rate (mL/min)	Pressure drop (MPa)
HiTrap SP HP	1	1	0.05
		5	0.20
	5	5	0.07
		10	0.15
		15	0.23
	LFMC	1	1
5			0.06
10			0.12
20			0.27
4.7		5	0.04
		10	0.08
		15	0.13
		25	0.26
		30	0.33

#### 4.5. Conclusions

The performance of the LFMC devices were head-to-head compared with HiTrap high-performance columns for cation-exchange chromatography in 1 mL and 5 mL bed volume scales. The three model proteins used for this study were ovalbumin

(pI 4.5), conalbumin (pI 6.1), and lysozyme (pI 11.0). Although the high-performance resins with relatively small diameters target high-resolution separations, the results obtained with the LFMC device were greatly comparable. At low flow rates, baseline resolution was only achieved with the resin column, while the LFMC device performance was consistent even at flow rates twice the maximum speed suggested by the column manufacturer. This characteristic makes these devices highly beneficial from the manufacturing point of view, offering much lower processing time with insignificant sacrifice on the resolution. Comparable resolution of separation were accomplished with the LFMC devices while the bed heights were 8 and 9 times lower which adds value to the application of these devices as they offer considerably low pressure drops even at high speed of operation. The LFMC devices also separated the acidic charge variant of lysozyme, which was not the case with the HiTrap column, highlighting the capabilities of the device in performing high-resolution bind-and-elute separations. Lastly, the performance of the two systems were compared in preparative separation of IgG1 charge variants at the 5 mL scale. Charge variant separation with CEX chromatography requires extensively shallow gradients due to similarities between the moieties. While the HiTrap column failed to provide stable conductivity profiles at 5 mL/min, the LFMC device gave greatly stable linear gradients at 15 mL/min leading to clean separation of the variants. The results absolutely highlighted the high-productivity and capability of the LFMC devices for carrying out CEX membrane chromatography also at such conditions.

#### **4.6. Acknowledgements**

We thank National Science and Engineering Research Council of Canada (NSERC) and Ontario Research Fund-Research Excellence (ORF-RE) for funding this project. We thanks Therapeutic Antibody Centre, University of Oxford, UK for donating the HIgG1-CD4 samples. We also thank Paul Gatt for fabricating the devices based on the design provided by RG and PM.

#### 4.7. References

- [1] S. Fekete, A. Beck, J.L. Veuthey, D. Guillarme, Ion-exchange chromatography for the characterization of biopharmaceuticals, *J. Pharm. Biomed. Anal.* 113 (2015) 43–55.
- [2] F. Steinebach, T. Müller-Späth, M. Morbidelli, Continuous Counter-current Chromatography for the Capture and Polishing Steps in Biopharmaceuticals Production, *Biotechnol. J.* under revi (2016) 1–16.
- [3] A.T. Hanke, M. Ottens, Purifying biopharmaceuticals: Knowledge-based chromatographic process development, *Trends Biotechnol.* 32 (2014) 210–220.
- [4] A.L. Zydney, Continuous downstream processing for high value biological products: A Review, *Biotechnol. Bioeng.* 113 (2016) 465–475.
- [5] R. Ghosh, Protein separation using membrane chromatography: opportunities and challenges., *J. Chromatogr. A.* 952 (2002) 13–27.
- [6] C. Boi, Membrane adsorbers as purification tools for monoclonal antibody purification., *J. Chromatogr. B. Analyt. Technol. Biomed. Life Sci.* 848 (2007) 19–27.
- [7] Q.S. Yuan, A. Rosenfeld, T.W. Root, D.J. Klingenberg, E.N. Lightfoot, Flow distribution in chromatographic columns 1, 831 (1999) 149–165.
- [8] R. Ghosh, Using a box instead of a column for process chromatography, *J. Chromatogr. A.* 1468 (2016) 164–172.
- [9] T.M. Przybycien, N.S. Pujar, L.M. Steele, Alternative bioseparation operations: life beyond packed-bed chromatography., *Curr. Opin. Biotechnol.* 15 (2004) 469–78.
- [10] C. Charcosset, Review Purification of Proteins b y Membrane Chromatography, *J. Chem. Biotechnol.* 71 (1998) 95-110.

- [11] D.K. Roper, E.N. Lightfoot, Separation of biomolecules using adsorptive membranes, *J. Chromatogr. A.* 702 (1995) 3–26.
- [12] M. Talebi, A. Nordborg, A. Gaspar, N.A. Lacher, Q. Wang, X.Z. He, P.R. Haddad, E.F. Hilder, Charge heterogeneity profiling of monoclonal antibodies using low ionic strength ion-exchange chromatography and well-controlled pH gradients on monolithic columns, *J. Chromatogr. A.* 1317 (2013) 148–154.
- [13] F. Svec, Y. Lv, Advances and recent trends in the field of monolithic columns for chromatography, *Anal. Chem.* 87 (2015) 250–273.
- [14] H.F. Xia, B. Bin Don, M.J. Zheng, Mixed-mode chromatography integrated with high-performance liquid chromatography for protein analysis and separation: Using bovine serum albumin and lysozyme as the model target, *J. Sep. Sci.* 39 (2016) 1900–1907.
- [15] U. Gottschalk, Disposables in Downstream Processing, *Adv. Biochem. Eng. Biotechnol.* 123 (2010) 127–141.
- [16] S. Muthukumar, T. Muralikrishnan, R. Mendhe, A.S. Rathore, Economic benefits of membrane chromatography versus packed bed column purification of therapeutic proteins expressed in microbial and mammalian hosts, *J. Chem. Technol. Biotechnol.* (2016).
- [17] V. Orr, L. Zhong, M. Moo-Young, C.P. Chou, Recent advances in bioprocessing application of membrane chromatography., *Biotechnol. Adv.* 31 (2013) 450–65.
- [18] J.X. Zhou, T. Tressel, Basic concepts in Q membrane chromatography for large-scale antibody production., *Biotechnol. Prog.* 22 (2006) 341–9.
- [19] J. Weaver, S.M. Husson, L. Murphy, S.R. Wickramasinghe, Anion exchange membrane adsorbers for flow-through polishing steps: Part II. Virus, host cell protein, DNA clearance, and antibody recovery, *Biotechnol. Bioeng.* 110

(2013) 500–510.

[20] P. Madadkar, R. Ghosh, High-resolution protein separation using a laterally-fed membrane chromatography device, *J. Memb. Sci.* 499 (2016) 126–133.

[21] R. Ghosh, P. Madadkar, Laterally-fed membrane chromatography device, 62304379, 2016.

[22] P. Madadkar, Q. Wu, R. Ghosh, A laterally-fed membrane chromatography module, *J. Memb. Sci.* 487 (2015) 173–179.

[23] P. Madadkar, S. Luna Nino, R. Ghosh, High-resolution, preparative purification of PEGylated protein using a laterally-fed membrane chromatography device, *J. Memb. Sci.* 1035 (2016) 1–7.

[24] R. Ghosh, P. Madadkar, Q. Wu, On the workings of laterally-fed membrane chromatography, *J. Memb. Sci.* 516 (2016) 26–32.

[25] W. Wang, J. Vlasak, Y. Li, P. Pristatsky, Y. Fang, T. Pittman, J. Roman, Y. Wang, T. Prueksaritanont, R. Ionescu, Impact of methionine oxidation in human IgG1 Fc on serum half-life of monoclonal antibodies, *Mol. Immunol.* 48 (2011) 860–866.

[26] S. Fekete, A. Beck, J. Fekete, D. Guillarme, Method development for the separation of monoclonal antibody charge variants in cation exchange chromatography, Part II: PH gradient approach, *J. Pharm. Biomed. Anal.* 102 (2015) 282–289.

[27] J. Vlasak, M.C. Bussat, S. Wang, E. Wagner-Rousset, M. Schaefer, C. Klinguer-Hamour, M. Kirchmeier, N. Corvaia, R. Ionescu, A. Beck, Identification and characterization of asparagine deamidation in the light chain CDR1 of a humanized IgG1 antibody, *Anal. Biochem.* 392 (2009) 145–154.

[28] G. Ponniah, A. Kita, C. Nowak, A. Neill, Y. Kori, S. Rajendran, H. Liu, Characterization of the Acidic Species of a Monoclonal Antibody Using Weak

Cation Exchange Chromatography and LC-MS, *Anal. Chem.* 87 (2015) 9084–9092.

[29] K.G. Moorhouse, W. Nashabeh, J. Deveney, N.S. Bjork, M.G. Mulkerrin, T. Ryskamp, Validation of an HPLC method for the analysis of the charge heterogeneity of the recombinant monoclonal antibody IDEC-C2B8 after papain digestion, *J. Pharm. Biomed. Anal.* 16 (1997) 593–603.

[30] A. Rozhkova, Quantitative analysis of monoclonal antibodies by cation-exchange chromatofocusing, *J. Chromatogr. A.* 1216 (2009) 5989–5994.

[31] T. Zhang, J. Bourret, T. Cano, Isolation and characterization of therapeutic antibody charge variants using cation exchange displacement chromatography, *J. Chromatogr. A.* 1218 (2011) 5079–5086.

[32] J. Kim, L. Jones, L. Taylor, G. Kannan, F. Jackson, H. Lau, R.F. Latypov, B. Bailey, Characterization of a unique IgG1 mAb CEX profile by limited Lys-C proteolysis/CEX separation coupled with mass spectrometry and structural analysis, *J. Chromatogr. B Anal. Technol. Biomed. Life Sci.* 878 (2010) 1973–1981.

[33] J.C. Rea, G.T. Moreno, Y. Lou, D. Farnan, Validation of a pH gradient-based ion-exchange chromatography method for high-resolution monoclonal antibody charge variant separations, *J. Pharm. Biomed. Anal.* 54 (2011) 317–323.

[34] H. Lau, D. Pace, B. Yan, T. Mcgrath, S. Smallwood, K. Patel, J. Park, S.S. Park, R.F. Latypov, Investigation of degradation processes in IgG1 monoclonal antibodies by limited proteolysis coupled with weak cation-exchange HPLC, *J. Chromatogr. B.* 878 (2010) 868–876.

[35] L. Shan, D.J. Anderson, Gradient Chromatofocusing . Versatile pH Gradient Separation of Proteins in Ion-Exchange HPLC : Characterization Studies Gradient Chromatofocusing . Versatile pH Gradient Separation of Proteins in Ion-Exchange HPLC : Characterization Studies, *System.* 74 (2002) 5641–5649.

- [36] D. Farnan, G.T. Moreno, Multiproduct high-resolution monoclonal antibody charge variant separations by pH gradient ion-exchange chromatography, *Anal. Chem.* 81 (2009) 8846–8857.
- [37] L. Zhang, T. Patapoff, D. Farnan, B. Zhang, Improving pH gradient cation-exchange chromatography of monoclonal antibodies by controlling ionic strength, *J. Chromatogr. A.* 1272 (2013) 56–64.
- [38] S. Gerontas, M. Asplund, R. Hjorth, D.G. Bracewell, Integration of scale-down experimentation and general rate modelling to predict manufacturing scale chromatographic separations, *J. Chromatogr. A.* 1217 (2010) 6917–6926.
- [39] S.D. Gorman, M.R. Clark, E.G. Routledge, S.P. Cobbold, H. Waldmann, Reshaping a therapeutic CD4 antibody., *Proc. Natl. Acad. Sci. U. S. A.* 88 (1991) 4181–4185.
- [40] L.A. Khawli, S. Goswami, R. Hutchinson, Z.W. Kwong, J. Yang, X. Wang, Z. Yao, A. Sreedhara, T. Cano, D. Tesar, I. Nijem, D.E. Allison, P.Y. Wong, Y.H. Kao, C. Quan, A. Joshi, R.J. Harris, P. Motchnik, Charge variants in IgG1: Isolation, characterization, in vitro binding properties and pharmacokinetics in rats, *MAbs.* 2 (2010) 613–624.
- [41] S. Gandhi, D. Ren, G. Xiao, P. Bondarenko, C. Sloey, M.S. Ricci, S. Krishnan, Elucidation of degradants in acidic peak of cation exchange chromatography in an IgG1 monoclonal antibody formed on long-term storage in a liquid formulation, *Pharm. Res.* 29 (2012) 209–224.
- [42] J. Stracke, T. Emrich, P. Rueger, T. Schlothauer, L. Kling, A. Knaupp, H. Hertenberger, A. Wolfert, C. Spick, W. Lau, G. Drabner, U. Reiff, H. Koll, A. Papadimitriou, A novel approach to investigate the effect of methionine oxidation on pharmacokinetic properties of therapeutic antibodies, *MAbs.* 6 (2014) 1229–1242.

[43] M. Haverick, S. Mengisen, M. Shameem, A. Ambrogelly, Separation of mAbs molecular variants by analytical hydrophobic interaction chromatography HPLC: Overview and applications, MAbs. 6 (2014) 852–858.

## **Chapter 5**

### **High-resolution, preparative purification of PEGylated protein using a laterally-fed membrane chromatography device**

Reprinted with permission. Copyright 2016 ELSEVIER Journal

### 5.1. Abstract

We discuss the use of a laterally-fed membrane chromatography (or LFMC) device for single-step purification of mono-PEGylated lysozyme. Recent studies have shown such LFMC devices to be suitable for high-resolution, multi-component separation of proteins in the bind-and-elute mode. The device used in this study contained a stack of rectangular cation-exchange membranes having 9.25 mL bed volume. PEGylation of lysozyme was carried out in batch mode using 5 kDa methoxy-polyethyleneglycol propionaldehyde (or m-PEG propionaldehyde) in the presence of sodium cyanoborohydride as reducing agent. Membrane chromatographic separation was carried out at 1.62 membrane bed volumes per minute flow rate, in the bind-and-elute mode. When a salt gradient was applied, the higher PEGylated forms of lysozyme (i.e. the byproducts) eluted earlier than mono-PEGylated lysozyme (the target product), while lysozyme eluted last. Under elution conditions optimized for resolution and speed, the separation could be carried out in less than 15 membrane bed volumes. High purity and recovery of mono-PEGylated lysozyme was obtained. The resolution of separation of mono-PEGylated lysozyme obtained under the above condition was comparable to that reported in the literature for equivalent cation-exchange resin columns while the flow rate expressed in bed volumes/min was 21.7 times higher. Also, the number of theoretical plates per meter was significantly higher with the LFMC device. Therefore the LFMC based purification process discussed in this paper combined high-productivity with high-resolution.

**Keywords** Membrane chromatography; Device; PEGylated proteins; Laterally-Fed membrane chromatography; Protein purification

## 5.2. Introduction

Membrane chromatography has been proposed as a fast and cost-effective alternative to resin-based packed-bed chromatography [1–4]. This technique takes significantly less processing time, uses less buffer and can be operated at significantly lower pressure drop. Moreover, the devices are disposable, which eliminates the requirement for cleaning and validation [5, 6]. However, application of membrane chromatography using currently available devices is largely restricted to flow-through polishing processes [7]. For instance, anion-exchange membrane chromatography has been successfully used for the removal of contaminants such as viruses, DNA, host cell proteins (HCPs), and endotoxins from monoclonal antibodies (mAbs) [8–10]. The impurities removed are mostly large molecules or fine particles present in dilute feed samples. Membranes, on account of their superior mass transport, outperform resin based columns in such applications. However, for applications involving high-resolution protein separation in bind- and-elute mode, column chromatography remains the technique of choice, despite significant limitations such as low productivity and poor scalability. Membrane chromatography devices are currently available in two major formats: stacked-disk and radial-flow. Stacked-disk devices are widely used in small-scale, process development type application but their separation performance deteriorates as the membrane diameter is increased, primarily on account of the high radial to axial dimension ratio which results in tailed peaks and thereby low resolutions. Incorporation of radially-aligned flow distribution channels [11] have only worked in devices less than 50 mm in diameter. Therefore stacked-disc devices are considered unsuitable for large-scale applications. Radial-flow devices are the current state-of-the-art for large-scale membrane chromatography [12–14]. However, there are some crucial design deficiencies that make these devices unsuitable for bind-and-elute separations [15]. Firstly, there is huge variability in flow path length in these devices which contributes towards broadening and even splitting of eluted peaks, and consequently very poor resolution [15, 16]. Moreover,

these devices tend to have relatively large dead volumes, with potential for back-mixing, which aggravate all the problems associated with flow path variability. In a radial-flow device, the membrane area decreases in a radially inward direction and therefore the superficial velocity increase along the bed height, a factor not conducive to high-resolution separations. Lastly, the presence of an open channel on one side of the membrane roll and a relatively constricted collection channel on the other makes pressure balancing along the length of the membrane extremely difficult and this in turn contributes to flux variability. The availability of a membrane chromatography device which addresses the above issues would make it possible to carry out high-resolution multi-component bind-and-elute separations while ensuring high-productivity. We have attempted to address these through the development of a laterally-fed membrane chromatography (or LFMC) device [15–18]. As described in our previous papers, an LFMC device houses a stack of rectangular membrane pieces with lateral channels with identical hydraulic resistances on both sides of the stack. As shown in Fig. 5.1, liquid pumped into the device is distributed laterally over the membrane stack, passes through it, emerges on the other side, and is eventually collected in the permeate channel and directed to the outlet. This arrangement reduces variability in flow path length, makes it easy to balance pressure between the two sides of the stack (and thereby ensure uniform flux), and maintain uniform superficial velocity along bed height [15, 16, 18]. In a recent paper [18] we have discussed in detail the factors responsible for the above based on theoretical and experimental analysis of hydraulic flow-paths. Also, factors likely to affect efficiency of LFMC are discussed using a simple electrical circuit analogy. Moreover, these devices can be constructed with quite low dead volume. The prototype version of the LFMC device out-performed its equivalent radial-flow device (both containing 7 mL stacks of strong cation exchange S membrane) when used for multi-component separation of model proteins in bind-and-elute mode [15]. The LFMC device gave significantly sharper flow-through and eluted peaks and thereby significantly higher resolution, with the

separation being feasible in much lower number of bed volumes. The prototype LFMC device described in our earlier study [15] was 3D printed. The LFMC device used in our current study (see Fig. 5.2) is a modified version which was fabricated by machining and is described in detail in the Materials and Methods section. Overall, it was inexpensive, easier to fabricate and assemble, and gave better separation performance than the prototype device.

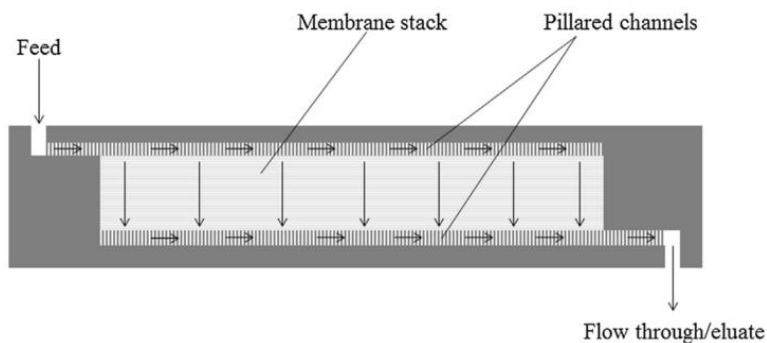


**Fig. 5.1** Schematic diagram of laterally-fed membrane chromatography (or LFMC).

Protein PEGylation [19] which involves the covalent attachment of a synthetic polymer polyethyleneglycol (or PEG) to a protein has been widely examined as a therapeutic efficacy enhancement strategy for protein biopharmaceuticals [20–23]. Generally, PEGylation increases the solubility and stability of therapeutic protein molecules, thereby making them less prone to aggregation and degradation. It also increases their biological half-life by reducing renal clearance. Therefore PEGylated protein drugs have to be administered less frequently than their non-PEGylated counterparts. Most chemical reactions for protein PEGylation result in the synthesis of a target product (generally a mono-PEGylated protein) along with several by-products (i.e. higher PEGylated protein). The mono-PEGylated protein is generally preferred for therapeutic application as it is easier to characterize (i.e. less positional isomers), and higher PEGylated forms can sometimes be less biologically active due to shielding of the active sites on a protein molecule. The separation of the mono-PEGylated protein from byproducts and the unreacted

reagents is challenging primarily because most of these substances have physical and chemical properties that are fairly similar to the target product [24, 25]. Amongst the different separation strategies for PEGylated proteins, ion exchange chromatography has been the most successful [26]. PEGylated proteins have shorter retention compared to unmodified protein due to the charge-shielding effect of the inert polymer molecule, the extent of which is affected by degree of PEGylation. Since separation and purification of PEGylated proteins is considered quite challenging, we decided to test the feasibility of carrying out such separations using our LFMC device.

In this paper, we discuss the preparative purification of mono-PEGylated lysozyme in a single-step, bind-and-elute process using an LFMC device housing a 9.25 mL stack of strong cation exchange S membrane. Lysozyme is widely used as a model protein to study protein PEGylation and purification of products obtained thereof. Strong cation-exchange S ligands have been widely studied for purification of PEGylated lysozyme [27–31]. More specifically, Moosmann et al. [29] successfully carried out single step preparative purification of mono-PEGylated lysozyme (modified with 5 kDa PEG) using a Toyopearl GigaCap S–650 M resin column having a bed volume of 13.4 mL. A linear gradient was utilized to fractionate the higher PEGylated forms, primarily di-PEGylated lysozyme from mono-PEGylated lysozyme. This gradient was followed by a step-change to 100% eluting buffer to rapidly elute unmodified lysozyme from the column to speed up the process. We used a similar approach, i.e. a linear gradient followed by step-change elution in our work using the LFMC device. The processing conditions were systematically optimized for resolution and productivity. The results obtained are discussed.

### **5.3. Materials and Methods**

#### **5.3.1. Materials**

Lysozyme (L6876), glycine (G8898), sodium cyanoborohydride (156159), acetic acid (A6283), sodium acetate trihydrate (S8625), sodium chloride (S7653), 30%

acrylamide solution (A3699) ammonium persulfate (A3678), hydrochloric acid (258148), glycerol (G2025), bromophenol blue (B0126), Brilliant blue R concentrate (B8647), sodium dodecyl sulfate (L3771), Trizma- hydrochloride (T3253), Trizma base (T1503), N,N,N',N'-tetramethyl ethylenediamine (T9281), and DL-dithiothreitol (43817) were purchased from Sigma-Aldrich (St. Louis, MO, USA). Methoxy-PEG-propionaldehyde 5000 (P1PAL-5) was purchased from Sunbio Inc. (Anyang, South Korea). Methanol (6700-1) and acetic acid (1000- 1) were purchased from Caledon Laboratories LTD. (Georgetown, ON, Canada). Ultra-4 centrifugal filters (3 kDa MWCO, UFC800324) were purchased from EMD Millipore Co. (Billerica, MA, USA). Sartobind S cation-exchange membrane sheets (94IEXS42-001) were purchased from Sartorius Stedim Biotech (Gottingen, Germany). This membrane has a rated lysozyme binding capacity of 29 mg/mL (manufacturer's data). Lepage epoxy glue was purchased from Henkel (Dusseldorf, Germany). Weld-on 16 glue was purchased from IPS Corporation (Compton, CA, USA). All buffers and the solutions were prepared using water obtained from a SIMPLICITY 185 water purification unit Millipore (Molsheim, France).

### **5.3.2. LFMC device design and fabrication**

The different components of the LFMC device used for this study are shown in Fig. 5.2A. The top and bottom plates (transparent acrylic) which were of identical design had overall dimensions of 150 mm × 40 mm. Each of these plates contained two ports as well as a pillared lateral channel (70 mm × 20 mm) which was 0.5 mm deep and contained a 28 × 7 array of pillars (1 mm diameter). The channels were tapered on both sides leading to two ports, the tapered length on one side being significantly more than the other. When used as the feed plate, the port corresponding to the longer tapered length served as the inlet while when used as the permeate plate, the port corresponding to the longer tapered length served as the outlet. The other ports which were blocked during actual chromatographic separation were used for removing bubbles and priming the device. The middle

frame which had the same length and width as the plates was made of PVC, had a rectangular slot for housing the membrane stack. The slot was tapered to provide enough space for application of the potting gluing around the membrane stack. The thickness of the middle frame which corresponded to the bed height of membrane stack was 6.6 mm. Rectangular pieces of cation exchange membranes (24 numbers) with dimensions corresponding to the rectangular channels (i.e. 70 mm × 20 mm) were cut out using a metal stamp cutter. The membrane layers were held in place within the slot in the middle frame and potted using epoxy glue. During the potting process, the membrane stack was held in place within the frame using a heavy metal block having the same dimension as the membrane. This was to ensure that epoxy did not spread into the membrane and also to reduce the intra-membrane void volume. After the epoxy was cured (24 h), the three layers of the device were glued together using Weld-on 16 adhesive. The glue was let to cure for 48 h before using the device. The resulting LFMC device which had 9.25 mL bed volume is shown in Fig. 5.2B. Prior to use in separation experiments, the number of theoretical plates of the LFMC device was measured using 0.4 M and 0.8 M sodium chloride solutions as mobile phase and tracer respectively.

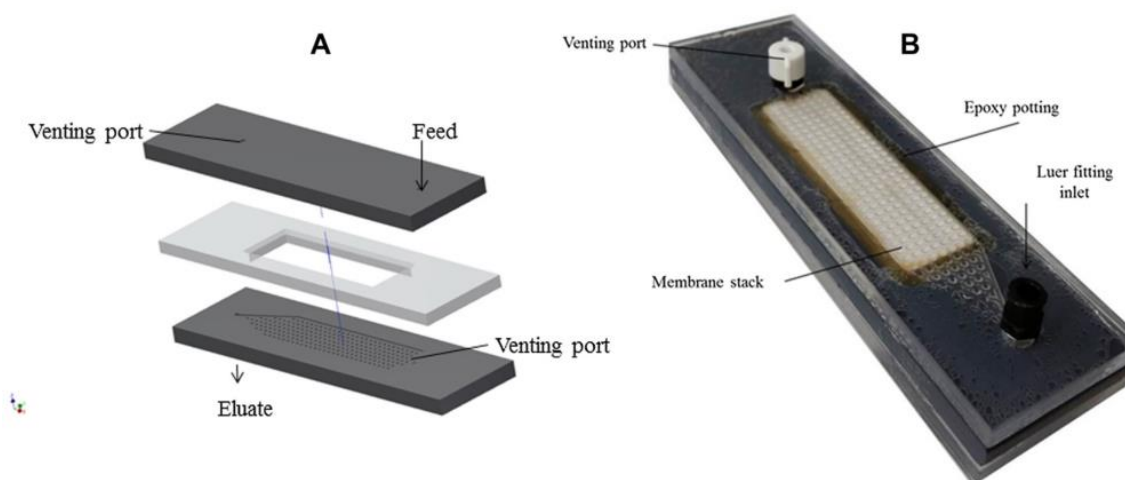


**Fig. 5.2:** A. Different components of the LFMC device: Acrylic top and bottom plates (shaded dark grey), and PVC middle frame (shaded light grey). B. Fully assembled LFMC device used in the current study (membrane bed volume: 9.25 mL; membrane: strong cation exchange S)

This measurement was carried out at 15 mL/min flow rate using a 100  $\mu$ L sample loop ( $\sim$ 1% membrane bed volume). The number of theoretical plates per meter was calculated as recommended in the literature [32] and was found to be 14444/m.

### **5.3.3. Lysozyme PEGylation**

PEGylation of lysozyme was carried out at room temperature in 100 mM sodium acetate buffer (pH 5.0) in small glass vials with constant mixing using magnetic stirrer [33]. The reaction volume was 15 mL and the reaction mixture consisted of different lysozyme concentrations (1 and 5 mg/mL), different P1PAL-5 concentration (5:2 or 4:10 PEG to protein on molar ratio in low and high molar ratio experiments respectively), and 10 mM sodium cyanoborohydride. Two reaction times, 4 h (short) and 10 h (long) were examined and at end of each reaction, the reaction mixture was quenched with glycine, its final concentration 100 mM. The quenched reaction mixture were desalted using 3 kDa MWCO centrifugal ultra-filters (3750 rpm, 30 min) and were diluted to the final required concentrations (2 mg/mL and 10 mg/mL) for cation exchange separation using 100 mM sodium acetate buffer (pH 5.0), which was also used as binding buffer.

### **5.3.4. Cation exchange LFMC**

The LFMC device was integrated with an AKTA prime liquid chromatography system (GE Healthcare Biosciences, QC, Canada) using appropriate peak tubing. The samples were injected using a 5 mL sample loop. The eluting buffer consisted of 0.5 M sodium chloride prepared in the binding buffer, i.e. 100 mM sodium acetate buffer (pH 5.0). All experiments were carried out at 15 mL/min flow rate ( $\sim$ 1.62 bed volumes per minute). The eluted peaks were collected, desalted using ultra-centrifugation, and further analyzed by sodium dodecyl sulfate polyacrylamide gel electrophoresis (SDS- PAGE) [34].

#### 5.4. Results and Discussion

Lysozyme PEGylation was carried out using different protein concentration and PEG: protein ratios in the reaction mixture, and for different lengths of reaction time. This was done to generate reaction mixtures obtained in typical protein PEGylation reactions. Initial PEGylation experiments were carried out using a low protein concentration (1 mg/mL), a high PEG: protein molar ratio (4:1), and a short reaction time (4 h) to rapidly generate samples for preliminary cation exchange LFMC experiments. The reaction mixture was desalted and concentrated to 2 mg/mL. Fig. 5.3 shows the chromatogram obtained using a linear gradient of 200 mL, starting at the same time as sample injection. The tiny flow-through peak corresponding to 1 bed volume was due to unreacted P1PAL-5, as verified by PEG staining on SDS-PAGE gel (not shown). P1PAL-5 being uncharged was not expected to bind to the membrane stack. The shoulder around 6 bed volumes corresponded to the small amount of higher-PEGylated lysozyme present in the sample. This was followed by the di-PEGylated lysozyme peak (~7 bed volumes) followed by mono-PEGylated lysozyme (~10 bed volumes), and eventually by unreacted lysozyme (~18 bed volumes). This observation is consistent with the expectation that lysozyme would bind more strongly to the S membrane stack than its PEGylated forms, and amongst these, strength of binding would decrease with degree of PEGylation [28]. Quite clearly, the elution conditions needed to be modified to increase the resolution between mono- and di-PEGylated lysozyme. Also, by reducing the considerable gap between the mono-PEGylated and unreacted lysozyme peaks, productivity of the process could be enhanced.

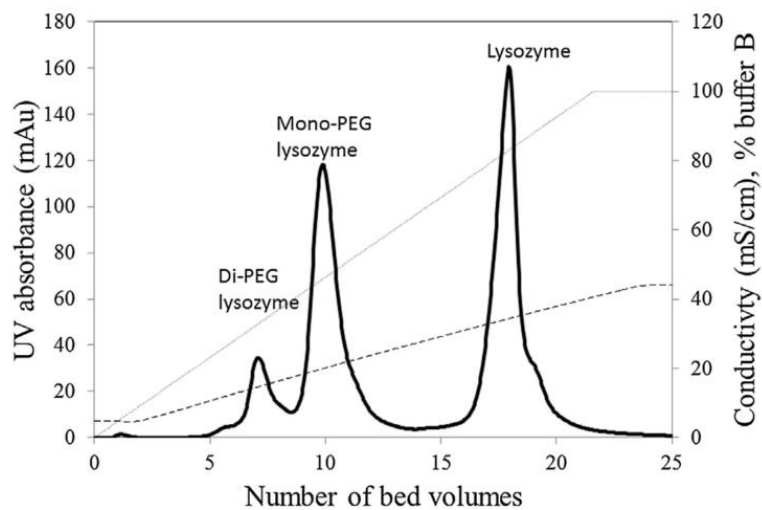


**Fig 5.3:** Single-step purification of mono-PEGylated lysozyme using 200 mL linear gradient (membrane: Sartorius S; membrane bed volume: 9.25 mL; lysozyme concentration in reaction mixture: 1 mg/mL; molar ratio: 4:1; reaction time: 4 h; protein concentration in feed: ~2 mg/mL; sample volume: 5 mL; binding buffer: 20 mM sodium acetate pH 5.0; eluting buffer: binding buffer +0.5 M NaCl; flow rate: 15 mL/min; thick line: UV absorbance; dotted line: gradient; dashed line: conductivity).

Two changes were made to increase the resolution and speed of separation: a shallower linear gradient (i.e. 150 mL) to resolve di- PEGylated and mono- PEGylated lysozyme peak, followed by a step change just after the mono- PEGylated lysozyme peak (i.e. after 50% eluting buffer). The results obtained are shown in Fig. 5.4. Using this approach, the mono- and di-PEGylated lysozyme peaks were completely resolved while unreacted lysozyme was eluted immediately after the mono-PEGylated lysozyme peak reached the baseline. This approach of using the combination of a linear gradient and step change to simultaneously increase both resolution and speed of separation of PEGylated proteins has also been in earlier studies [30, 31]. In addition to speeding up the separation process, the step change resulted in elution of the unreacted lysozyme as a sharp peak. This would make it easier to recycle the unreacted protein drug.

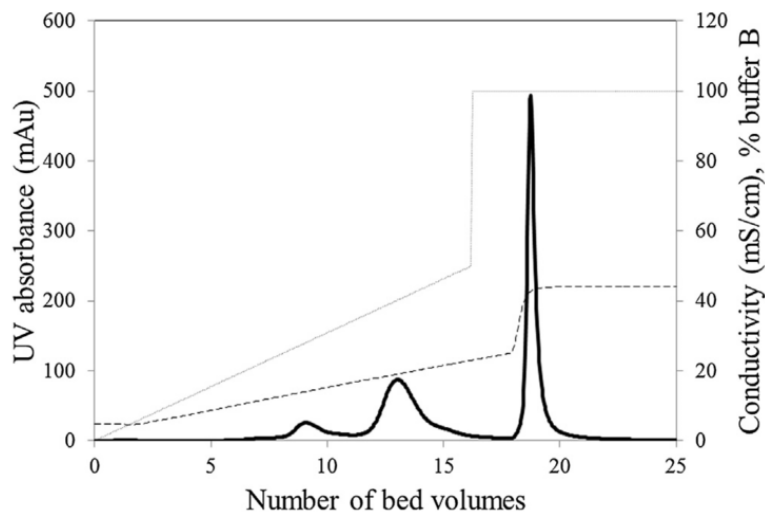


**Fig 5.4:** Single-step purification of mono-PEGylated lysozyme using 150 mL linear gradient to 50% eluting buffer followed by a step-change (membrane: Sartorius S; membrane bed volume: 9.25 mL; lysozyme concentration in reaction mixture: 1 mg/mL; molar ratio: 4:1; reaction time: 4 h; protein concentration in feed: ~2 mg/mL; sample volume: 5 mL; binding buffer: 20 mM sodium acetate pH 5.0; eluting buffer: binding buffer +0.5 M NaCl; flow rate: 15 mL/min; thick line: UV absorbance; dotted line: gradient; dashed line: conductivity).

A close inspection of chromatogram shown in Fig. 5.4 suggested that the separation time could be further reduced by using a higher salt concentration during sample injection, i.e. by moving the starting point of the salt gradient closer to the origin while maintaining its slope. Accordingly, the initial buffer consisted of 20% eluting buffer, corresponding to a conductivity of 15 mS/cm. Fig. 5.5 show two chromatograms obtained using samples for 4 and 10 h reactions respectively. As the samples were still prepared in the original binding buffer, there was a slight decrease in conductivity immediately following sample injection. However, this did not result in any PEGylated protein flow through and the conductivity recovered very rapidly and followed the gradient. The effect of reaction time on the extent of PEGylation can be clearly observed by comparing the two chromatograms in Fig. 5.5. The longer reaction time resulted in increase in the higher- and di-PEGylated lysozyme peaks and a corresponding decrease in the unreacted lysozyme peak. However, the amount of mono-PEGylated lysozyme peak remained almost

unchanged. Comparing the chromatograms in Figs. 5.4 and 5, the benefit of shifting the salt gradient is quite evident. While in the former case, the separation could be carried out in about 22 bed volumes, in the latter, the same separation could be carried out in about 15 bed volumes. The resolution obtained was comparable with those reported for preparative purification of mono-PEGylated lysozyme using 13.4 mL GigaCap 650S columns [30, 31]. However, the LFMC experiments were carried out at a flow rate of 1.62 bed volumes/min, which was 21.7 times higher than that used with the resin columns. Also, the separation could be carried out at a backpressure of 0.3 MPa which was significantly lower than that with the resin column. Figs. 5.6A and B show the SDS-PAGE results obtained with samples collected during experiments represented in Fig. 5.6. The mono-PEGylated lysozyme samples obtained in both experiments were very pure as evident from the single bands in each case. The above results clearly demonstrate that LFMC combined both high-speed and high-resolution in multi-component protein separations carried out in the bind and elute mode.

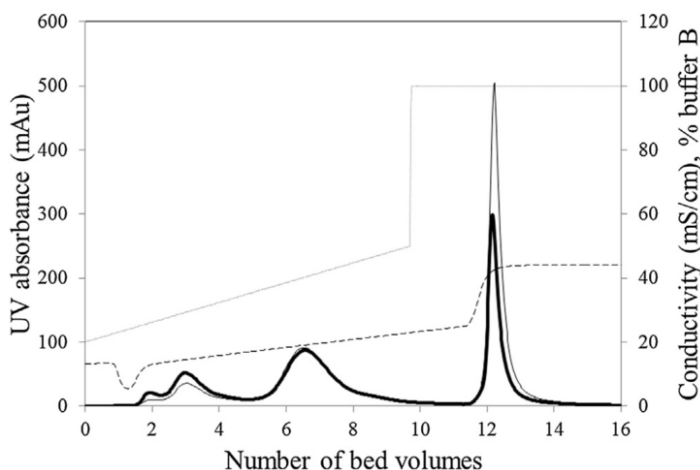


**Fig 5.5:** Single-step purification of mono-PEGylated lysozyme using 90 mL linear gradient to 50% eluting buffer followed by a step-change (sample injection condition: 20% eluting buffer; membrane: Sartorius S; membrane bed volume: 9.25 mL; lysozyme concentration in reaction mixture: 1 mg/mL; molar ratio: 4:1; protein concentration in feed: ~2 mg/mL; sample volume: 5 mL; binding buffer: 20 mM sodium acetate pH 5.0; eluting buffer: binding buffer +0.5 M NaCl; flow rate: 15 mL/min; thick line: 10 h residence time; thin line: 4 h reaction time; dotted line: gradient; dashed line: conductivity).

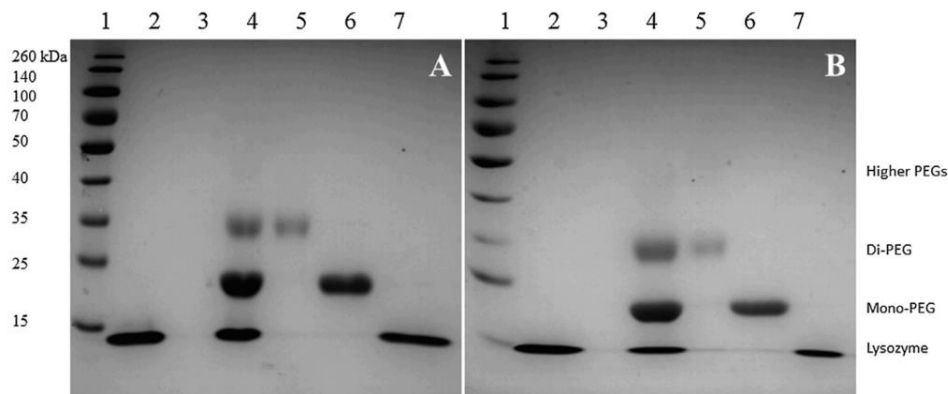


**Fig. 5.6:** SDS-PAGE analysis of samples obtained from the single-step purification of mono-PEGylated lysozyme carried out by experiment represented in Fig. 5 (A: 4 h reaction time; B: 10 h reaction time; lane 1: molecular weight marker; lane 2: pure lysozyme; lane 4: reaction mixture; lane 5: first peak with shoulder; lane 6: second peak; lane 7: third peak).

In order to assess the performance of the LFMC device with high protein concentration samples, a PEGylation experiment was carried out using 5 mg/mL lysozyme concentration, with 4:1 PEG: protein molar ratio, and 10 h reaction time. The reaction mixture was desalted and concentrated by centrifugal ultrafiltration such that the total protein concentration in the product thus obtained was 10 mg/mL. This was further purified using three different chromatographic separation protocols (see Figs. 5.7A–C). In each of these experiments, the initial buffer consisted of 20% eluting buffer, i.e. corresponding to a conductivity of 15 mS/cm. Increasing the gradient length (i.e. making it shallower) resulted in better resolution of the mono- and di-PEGylated lysozyme peaks, but led to the broadening of the product peak. Fig. 5.8 shows the SDS-PAGE results obtained with samples collected during the experiment represented by Fig. 5.7A. Quite clearly, mono-PEGylated lysozyme obtained even with the steepest gradient was very pure as evident from the single intense band on the gel. Therefore the separation could be carried out in less than 15 bed volumes. These results demonstrate that LFMC was able to deliver both high-speed and high-resolution in multi-component protein

separations even when the protein concentration in the sample to be purified was high.

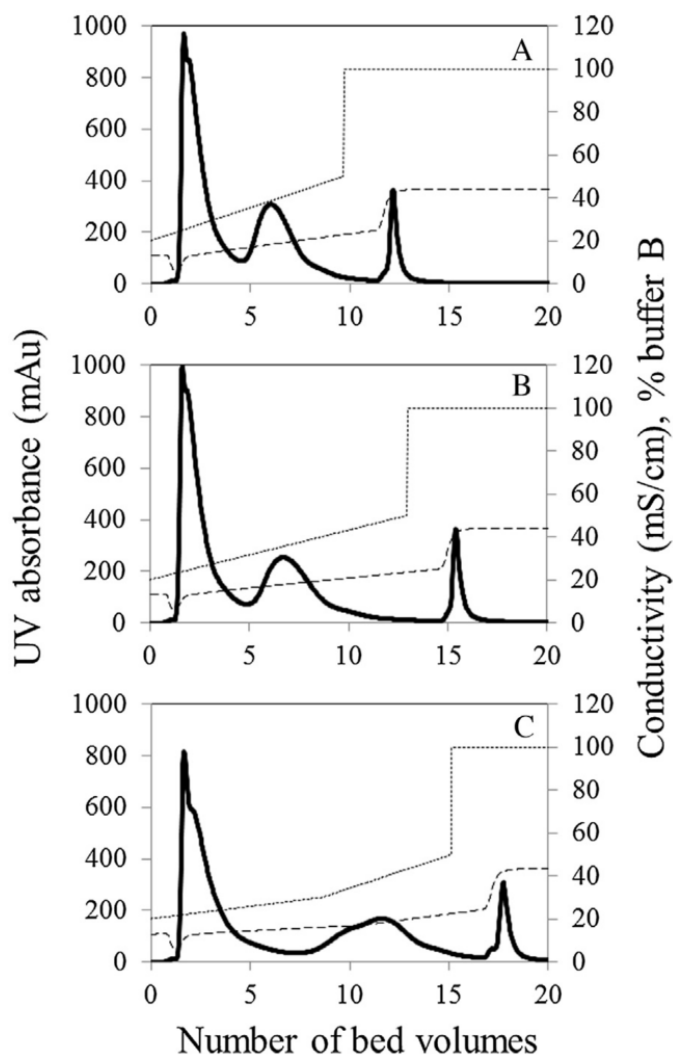


**Fig. 5.7:** Comparison of different elution conditions for single-step purification of mono-PEGylated lysozyme (sample injection condition: 20% eluting buffer; A: 90 mL linear gradient to 50% eluting buffer followed by a step-change; B: 120 mL linear gradient to 50% eluting buffer followed by a step-change; C: 80 mL linear gradient to 30% eluting buffer +60 mL linear gradient to 50% eluting buffer followed by a step-change; membrane: Sartorius S; membrane bed volume: 9.25 mL; lysozyme concentration in reaction mixture: 5 mg/mL; molar ratio: 4:1; reaction time: 10 h; protein concentration in feed: ~10 mg/mL; sample volume: 5 mL; binding buffer: 20 mM sodium acetate pH 5.0; eluting buffer: binding buffer +0.5 M NaCl; flow rate: 15 mL/min; thick line: UV absorbance; dotted line: gradient; dashed line: conductivity).

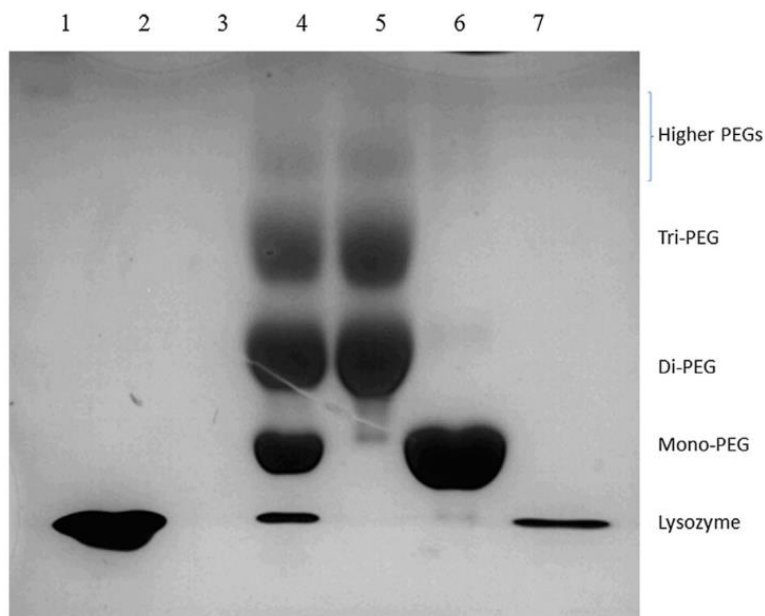


**Fig. 5.8:** SDS-PAGE analysis of samples obtained from the single-step purification of mono-PEGylated lysozyme carried out by experiment represented in Fig. 7A (lane 1: pure lysozyme; lane 4: reaction mixture; lane 5: peak 1, lane 6: peak 2; lane 7: peak 3).

PEG: protein ratio is one of the important parameters in a protein PEGylation process. The samples purified in all the experiments discussed so far were obtained using a high (i.e. 4:1) molar ratio. In order to examine the performance of the LFMC based separation with low molar ratio samples, a PEGylation experiment was carried out for 10 h using 5 mg/mL lysozyme concentration and 5:2 PEG: protein molar ratio. As in the previous set of experiments, the reaction mixture was desalted and concentrated by centrifugal ultrafiltration such that the total protein concentration in the product thus obtained was 10 mg/mL. Fig. 5.9 shows the chromatogram obtained using the same gradient as that used in experiment represented by Fig. 5.7A. Consistent with all earlier experiments, purification of mono-PEGylated lysozyme could be carried out with excellent peak resolution in less than 15 bed volumes.

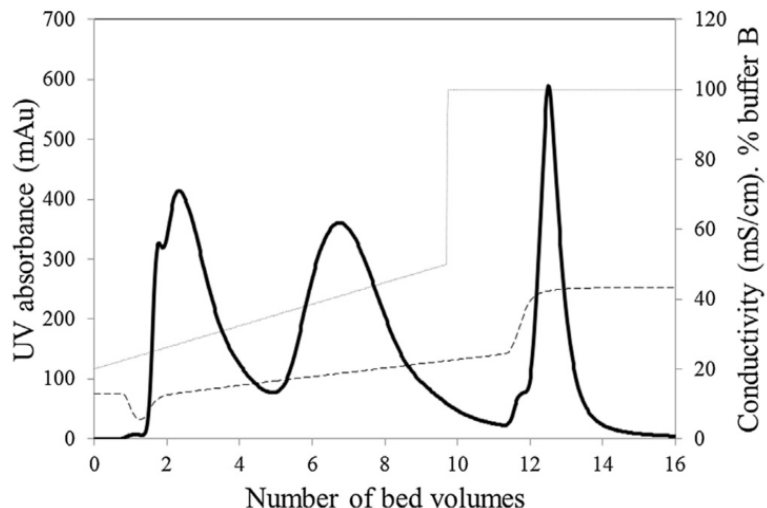


**Fig. 5.9:** Single-step purification of mono-PEGylated lysozyme using 90 mL linear gradient to 50% eluting buffer followed by a step-change (sample injection condition: 20% eluting buffer; membrane: Sartorius S; membrane bed volume: 9.25 mL; lysozyme concentration in reaction mixture: 5 mg/mL; molar ratio: 5:2; reaction time: 10 h; protein concentration in feed: 10 mg/mL; sample volume: 5 mL; binding buffer: 20 mM sodium acetate pH 5.0; eluting buffer: binding buffer +0.5 M NaCl; flow rate: 15 mL/min; thick line: UV absorbance; dotted line: gradient; dashed line: conductivity).

In our previous studies [15, 16, 18] we have demonstrated that LFMC devices give superior separation performance than other type of membrane chromatography devices. The results discussed in this paper clearly show that resolution of separation obtained with an LFMC device comparable to those obtained resin-based columns, while maintaining the high-productivity attribute of membrane chromatography. The LFMC devices therefore represent a win-win situation, i.e. combination of high-productivity with high-resolution. This is also evident from the number of theoretical plates per meter obtained with the LFMC device (14444/m) which was significantly higher than with high-performance resin columns. For instance, the Toyopearl (grade S) column used by Moosmann et al. [30] is reported to have 6000 theoretical plates per meter [35]. Based on above, we feel confident that the LFMC would find acceptance in the biotechnology industry as an efficient purification technique.

## 5.5. Conclusions

This study demonstrated that laterally-fed membrane chromatography (or LFMC) could be used to carry out high-resolution, multi-component separation of proteins in bind-and-elute mode. Purification of PEGylated proteins is challenging as the species being separated differ only very slightly in term of their physical properties. The results discussed in this paper clearly demonstrate that mono-PEGylated lysozyme could be efficiently separated from PEGylation reaction mixture as a single step purification process using an LFMC device fitted with a stack of strong cation exchange S membranes. A combination of an optimized linear salt concentration gradient followed by a step change in eluting buffer was found to be suitable for fast, high-resolution separation of mono- PEGylated lysozyme. The separation time could be further reduced by using a higher salt concentration during sample injection, i.e. by moving the starting point of the salt gradient closer to the ori- gin while maintaining its slope. The resolution of separation of mono-PEGylated lysozyme obtained under the above condition was comparable to that reported in the literature for equivalent cation-exchange resin columns. The separation could be carried out within 15 bed volumes which compared favorably to separation with resin columns. This is also supported by the significantly higher number of theoretical plates per meter offered by the LFMC device. The LFMC experiments were carried out at a flow rate of 1.62 bed volumes/min, which was 21.7 times higher than that used with resin columns. LFMC therefore combines high-productivity with high-resolution, an attribute highly desirable in a separation technique for purification of biopharmaceutical proteins.

## 5.6. Acknowledgements

We thank the Natural Science and Engineering Research Council (NSERC) of Canada and the Ontario Research Fund RE program for funding this study. We also thank Paul Gatt for fabricating the membrane devices based on design provided by R.G.

## 5.7. References

- [1] T.B. Tennikova, F. Svec, B.G. Belenkii, High-performance membrane chromatography. A novel method of protein separation, *J. Liq. Chromatogr.* 13 (1990) 63–70.
- [2] D.K. Roper, E.N. Lightfoot, Separation of biomolecules using adsorptive membranes, *J. Chromatogr. A* 702 (1995) 3–26.
- [3] R. Ghosh, Protein separation using membrane chromatography: opportunities and challenges, *J. Chromatogr. A* 952 (2002) 13–27.
- [4] R. van Reis, A. Zydney, Membrane separations in biotechnology, *Curr. Opin. Biotechnol.* 12 (2001) 208–211.
- [5] C. Charcosset, Membrane processes in biotechnology: an overview, *Biotechnol. Adv.* 24 (2006) 482–492.
- [6] V. Orr, L. Zhong, M. Moo-Young, C.P. Chou, Recent advances in bioprocessing application of membrane chromatography, *Biotechnol. Adv.* 31 (2013) 450–465.
- [7] C. Boi, Membrane adsorbers as purification tools for monoclonal antibody purification, *J. Chromatogr. B* 848 (2007) 19–27.
- [8] H.L. Knudsen, R.L. Fahrner, Y. Xu, L.A. Norling, G.S. Blank, Membrane ion-exchange chromatography for process-scale antibody purification, *J. Chromatogr. A* 907 (2001) 145–154.
- [9] J.X. Zhou, T. Tressel, Basic concepts in Q membrane chromatography for large-scale antibody production, *Biotechnol. Prog.* 22 (2006) 341–349.
- [10] J. Weaver, S.M. Husson, L. Murphy, S.R. Wickramasinghe, Anion exchange membrane adsorbers for flow-through polishing steps: part I. Clearance of minute virus of mice, *Biotechnol. Bioeng.* 110 (2013) 491–499.

- [11] R. Ghosh, T. Wong, Effect of module design on the efficiency of membrane chromatographic separation processes, *J. Membr. Sci.* 281 (2006) 532–540.
- [12] W. Demmer, D. Nussbaumer, Large-scale membrane adsorbers, *J. Chromatogr. A* 852 (1999) 73–81.
- [13] J.H. Chon, G. Zerbis-Papastoitsis, Advances in the production and downstream processing of antibodies, *New Biotechnol.* 28 (2011) 458–463.
- [14] L. Voswinkel, U. Kulozik, Fractionation of all major and minor whey proteins with radial flow membrane adsorption chromatography at lab and pilot scale, *Int. Dairy J.* 39 (2014) 209–214.
- [15] P. Madadkar, R. Ghosh, High-resolution protein separation using a laterally-fed membrane chromatography device, *J. Membr. Sci.* 499 (2016) 126–133.
- [16] P. Madadkar, Q. Wu, R. Ghosh, A laterally-fed membrane chromatography module, *J. Membr. Sci.* 487 (2015) 173–179.
- [17] R. Ghosh, Laterally-Fed Membrane Module, 2014, pp. 62074858. [18] R. Ghosh, P. Madadkar, Q. Wu, On the workings of laterally-fed membrane chromatography, *J. Membr. Sci.* 516 (2016) 26–32.
- [19] A. Abuchowski, J.R. McCoy, N.C. Palczuk, T. van Es, F.F. Davis, Effect of covalent attachment of polyethylene glycol on immunogenicity and circulating life of bovine liver catalase, *J. Biol. Chem.* 252 (1977) 3582–3586.
- [20] O. Kinstler, G. Molineux, M. Treuheit, D. Ladd, C. Gegg, Mono-N-terminal poly(ethylene glycol)-protein conjugates, *Adv. Drug Deliv. Rev.* 54 (2002) 477–485.
- [21] J.M. Harris, R.B. Chess, Effect of pegylation on pharmaceuticals, *Nat. Rev. Drug Discov.* 2 (2003) 214–221.
- [22] H. Lee, I.H. Jang, S.H. Ryu, T.G. Park, Mono-PEGylation of epidermal growth factor, *J. Pharmaceut. Res.* 20 (2003) 818–825.

- [23] A. Basu, K. Yang, M. Wang, S. Liu, R. Chintala, T. Palm, et al., Structure function engineering of interferon- $\gamma$ 1b for improving stability, solubility, potency, immunogenicity, and pharmacokinetic properties by site-selective mono-PEGylation, *Bioconjug. Chem.* 17 (2006) 618–630.
- [24] C.J. Fee, J.M. Van Alstine, PEG-proteins: reaction engineering and separation issues, *Chem. Eng. Sci.* 61 (2006) 924–939.
- [25] M.A. Gauthier, H. Klok, Peptide/protein-polymer conjugates: synthetic strategies and design concepts, *Chem. Commun.* (2008) 2591–2611.
- [26] M. Abe, P. Akbarzaderaleh, M. Hamachi, N. Yoshimoto, S. Yamamoto, Interaction mechanism of mono-PEGylated proteins in electrostatic interaction chromatography, *Biotechnol. J.* 5 (2010) 477–483.
- [27] P. Yu, G. Zhang, J. Bi, X. Lu, Y. Wang, Z. Su, Facile purification of mono-PEGylated interleukin-1 receptor antagonist and its characterization with multi-angle laser light scattering, *Process Biochem.* 42 (2007) 971–977.
- [28] D. Yu, X. Shang, R. Ghosh, Fractionation of different PEGylated forms of a protein by chromatography using environment-responsive membranes, *J. Chromatogr. A* 1217 (2010) 5595–5601.
- [29] D. Yu, R. Ghosh, Purification of PEGylated protein using membrane chromatography, *J. Pharm. Sci.* 99 (2010) 4215–4227.
- [30] A. Moosmann, J. Christel, H. Boettinger, E. Mueller, Analytical and preparative separation of PEGylated lysozyme for the characterization of chromatography media, *J. Chromatogr. A* 1217 (2010) 209–215.
- [31] B. Maiser, F. Kröner, F. Dimer, G. Brenner-Weiβ, J. Hubbuch, Isoform separation and binding site determination of mono-PEGylated lysozyme with pH gradient chromatography, *J. Chromatogr. A* 1268 (2012) 102–108.

[32] A.S. Rathore, R.M. Kennedy, J.K. O'Donnell, I. Bemberis, O. kaltenbrunner, Qualification of a chromatographic column, *Biopharm. Int.* 16 (2003) 30–40.

[33] X. Shang, D. Yu, R. Ghosh, Integrated solid-phase synthesis and purification of PEGylated protein, *Biomacromolecules* 12 (2011) 2772–2779.

[34] U.K. Laemmli, Cleavage of structural proteins during the assembly of the head of bacteriophage T4, *Nature* 227 (1970) 680–685.

[35] TOYOPEARL Instruction Manual Tosoh Bioscience

<http://www.separations.eu>.

[tosohbioscience.com/File%20Library/TBG/Products%20Download//](http://tosohbioscience.com/File%20Library/TBG/Products%20Download//)

[Instruction%20Manual/m15p73a.pdf](http://tosohbioscience.com/File%20Library/TBG/Products%20Download//Instruction%20Manual/m15p73a.pdf), (accessed 2 2016).

## **Chapter 6**

### **Preparative Separation of Monoclonal Antibody Aggregates by Cation-Exchange Laterally-Fed Membrane Chromatography**

### 6.1. Abstract

Cation exchange (or CEX) chromatography is widely used for large-scale separation of monoclonal antibody (or mAb) aggregates. The aggregates bind more strongly to CEX media and hence elute after the monomeric mAb in a salt gradient. However, monomer-aggregate resolution that is typically obtained is poor, which results in low product recovery. In the current study we address this challenge through the use of cation-exchange laterally-fed membrane chromatography (or LFMC). Three different LFMC devices, each containing a bed of strong cation-exchange (S) membranes were used for preparative-scale removal of mAb aggregates. Trastuzumab (IgG1) biosimilar derived from human embryonic kidney 293 (293) cells was used as the primary model mAb in our study. The other mAbs investigated were Chinese hamster ovary (or CHO) cell line derived Alemtuzumab (Campath-1H) and a heavy chain chimeric mAb EG2-hFc. In each of these case-studies, aggregates were well-resolved from the respective monomer. The separated and collected monomer and aggregate fractions were analyzed using techniques such as hydrophobic interaction membrane chromatography (or HIMC), native polyacrylamide gel electrophoresis (or PAGE), and size-exclusion high-performance liquid chromatography (or SE-HPLC). The high efficiency of separation obtained in each case was due to a combination of the small membrane pore size (3-5 microns), and the use of LFMC technology, which has been shown to be suitable for high-resolution, multi-component protein separations. Also, the LFMC based separation processes reported in this study were more than an order of magnitude faster than equivalent resin-based, cation exchange chromatography.

**Keywords:** Monoclonal antibody; aggregates; laterally-fed membrane chromatography; device; protein purification; bioseparation

## 6.2. Introduction

Monoclonal antibodies (or mAbs) comprise the most widely used class of therapeutic proteins which have found a wide range of applications [1, 2]. Currently available mAbs are manufactured at large-scale using recombinant DNA technology, through which the formulation at high concentrations makes these molecules more prone to aggregation than serum antibodies. Monoclonal antibody aggregation could occur during all the different stages of the manufacturing process, and this results in problems such as reduced solubility, loss of biological activity, and increased immunogenicity [3]. Certain specific processing conditions such as use of low pH for mAb elution from protein-A columns further exacerbates aggregation.

Techniques such as size exclusion chromatography (or SEC) aka size-exclusion high-performance liquid chromatography (SE-HPLC) [4,5], hydrophobic interaction membrane chromatography (HIMC) [6], and asymmetric flow field fractionation (AFFF) [7] are generally used for both qualitative and quantitative analysis of mAb aggregates. However, SEC is very slow and poorly scalable, and is therefore rarely used for preparative separation of aggregates and it gives relatively poor monomer/dimer resolution. While HIMC is both scalable and fast, it has not found much use for large-scale mAb aggregate removal, presumably due to the requirement of large quantities of ammonium sulfate in the feed solution. AFFF, while promising in analytical applications is clearly not a preparative separation technique. In the “three column process”, commonly used for mAb purification, aggregates are separated along with high levels of other product-related impurities such as antibody fragments during the intermediate cation exchange (CEX) chromatography step [2, 8-12]. Such separation is carried out in the bind-and-elute mode as the antibody aggregates bind slightly more strongly than the monomeric form, to chromatographic media. However, monomer/aggregates resolution tends to be poor and the shallow salt gradients typically used for elution from the CEX column results in low mAb recovery. Solvent modulators such as

polyethyleneglycol (or PEG) have shown to improve mAb monomer aggregate resolution [13,14] based on hydration of the protein and the stationary phase by the neutral hydrophilic molecule, leading to increase in retention time in the ion exchange column. While this approach enhances mAb recovery in the CEX step, it introduces new challenges such as the possibility of protein precipitation at higher PEG concentrations and the need for PEG/mAb separation further down the line. While the first of these challenges could be addressed through the use of solubility enhancers [14], the latter continues to be a limiting factor. Aggregates removal using a two-column (anion and cation exchange in tandem) downstream process has been proposed [15] as an alternative. However, this method is not suitable for antibodies with higher pI values ( $\geq 9$ ) and also when high levels of aggregates are present.

Membrane chromatography has been proposed as a cost-effective alternative to column chromatography [16-19]. It is significantly faster due to the predominance of convective mass transport. The separation of mAb aggregates using hydrophobic interaction membrane chromatography (or HIMC) using environment-responsive hydrophilized polyvinylidene fluoride (or PVDF) membranes has been reported in several earlier papers from our group [6, 20, 21]. Monomeric mAb was separated from aggregates based on the hydrophobicity difference, and it was found that the hydrophobicity increased with degree of aggregation [6]. It has also been shown that immunoglobulin G (or IgG) class of antibodies bind to hydrophobic surfaces through the segment containing the hinge and C<sub>H2</sub> domain of Fc which also explained why aggregates have greater hydrophobicity [22]. HIMC gives excellent monomer/aggregates resolution in analytical-scale separation and is much faster and cheaper than SEC. However, it would be difficult to use HIMC for preparative separations, primarily due to the need for high salt concentration in the binding buffer, which would limit the mAb concentration in the feed solution. Generally, the application of membrane chromatography in the process scale mAb manufacture has been limited to the late stage polishing steps [23, 24]. The

primary reason is that currently used membrane adsorbers perform poorly (i.e. have poor resolution) when employed in the bind-and-elute mode [25]. In some recent papers we have discussed a new separation technique called laterally-fed membrane chromatography (or LFMC) which not only gives high productivity but is highly suitable for carrying out high-resolution multi-component separations in the bind-and-elute mode [26-28]. Some of the attributes of the LFMC device responsible for its superior performance include ease of pressure balancing, uniformity in solute residence time, low dead volume and low back-mixing, all of which contribute towards sharp and better resolved peaks [29].

In this paper we examine if cation-exchange LFMC could be used for separation of mAb aggregates. Three different devices housing strong cation-exchange S membrane stacks having bed volumes ranging from 1 to nearly 10 mL were used in the current study. Trastuzumab (IgG1) biosimilar, derived from human embryonic kidney 293 (or 293) cells, was used as the primary model mAb. The effect of salt gradient on the resolution of mAb monomer and aggregate peaks was studied. Next, the separation of Campath-1H (or Alemtuzumab) aggregates was examined using two different samples, i.e. with low and high aggregates. Campath-1H is a humanized IgG1 type mAb against human leukocyte antigen CD52 [30]. Separation of aggregates from chimeric heavy chain mAb EG2-hFc samples was also examined. EG2-hFc is a recombinant camelid antibody in which the camelid Fc is replaced with human [31-33]. Heavy chain antibodies have shown enhanced tissue penetration and more efficient antigen binding compared to whole IgG mAbs and are therefore being examined for certain niche therapeutic applications [34]. The purified samples obtained in the above studies were analyzed using analytical techniques such as analytical HPMC, size-exclusion high-performance liquid chromatography (or SE-HPLC) and native polyacrylamide gel electrophoresis (PAGE). The results obtained are discussed.

### **6.3. Materials and Methods**

#### **6.2.1. Materials**

Human embryonic kidney 293 (293) cell derived IgG1 (Trastuzumab biosimilar) was produced by large-scale transient gene expression [35] and purified by protein-A chromatography [36]. Humanized monoclonal antibody Campath-1H and its aggregate-rich sample (or “dimers”) were kindly donated by the Therapeutic Antibody Centre, University of Oxford, UK. EG2-hFc (~80 kDa MW) was produced by cell culture as described in the literature [33]. Sodium phosphate monobasic (S0751), sodium phosphate dibasic (S0876), ammonium sulfate (A4418), sodium citrate (S4641), citric acid (C0759), sodium chloride (S7653), hydrochloric acid (258148), glycine (G8898), 30% acrylamide solution (A3699), ammonium persulfate (A3678), glycerol (G2025), bromophenol blue (B0126), Brilliant blue R concentrate (B8647), sodium dodecyl sulfate (L3771), Trizma-hydrochloride (T3253), Trizma base (T1503), N,N,N',N'-tetramethyl ethylenediamine (T9281), and DL-dithiothreitol (43817) were purchased from Sigma-Aldrich, St. Louis, MO. Methanol (6700-1) and acetic acid (1000-1) were purchased from Caledon laboratories LTD. (Georgetown, ON, Canada). Sartobind S cation-exchange membrane sheets (94IEXS42-001) were purchased from Sartorius-Stedium Biotech (Gottingen, Germany). Hydrophilized polyvinylidene fluoride (PVDF) membranes (GVWP 14250; 0.22  $\mu\text{m}$  pore size) and Amicon centrifugal filters (30 kDa MWCO) were purchased from EMD Millipore Co. (Billerica, MA, USA). HiTrap protein-A HP column (1 mL) was purchased from GE Healthcare (Baie-d'Urfe, QC, Canada). Lepage epoxy glue was purchased from Hankel (Dusseldorf, Germany). Weld-on 16 glue was purchased from IPS Corporation (Compton, CA, USA). All buffers and solutions were prepared using deionized water obtained from a SIMPLICITY 185 water purification unit Millipore (Molsheim, France).

#### **6.2.2 Device fabrication**

The general design of the LFMC devices used for this study has been previously reported [37]. Three devices were fabricated to house rectangular stacks of

Sartobind S membranes with 1, 4.6 and 9.2 mL bed volume. Each device consisted of two acrylic plates with lateral pillared channels and a middle frame within which the membrane stack was glued in-place. The channel depth was 0.5 mm and the diameter of the pillars was 1.5 mm. The design specifications for the three devices are summarized in Table. 6.1.

**Table 6.1:** Design details of the LFMC devices

Membrane bed volume (mL)	Bed height (mm)	Number of membrane layers	Membrane dimensions (mm × mm)	Pillar array	Outer dimension of plate (mm × mm)	Dead volume (mL)
9.2	6.6	24	70 × 20	28 × 7	150 × 40	8.87
4.6	3.3	12	70 × 20	28 × 7	150 × 40	5.19
1.0	2.7	10	38 × 10	15 × 3	120 × 30	1.21

### 6.2.3. EG2-hFc Preparation

Heavy chain EG2-hFc mAb was prepared by cell culture as describe elsewhere [32, 33]. Day 7 culture samples were centrifuged (1500 rpm, 5 min) and the supernatant was clarified by sterile filtration using 25 mm syringe filters (hydrophilic polyethersulfone, 0.2 µm pore size, Acrodisc®, Pall Corporation, Port Washington, NY). The filtrate was then concentrated 10-folds and buffer exchanged using centrifugal ultrafilters (30 kDa MWCO, Pall Corporation, Port Washington, NY). EG2-hFc was then purified using a HiTrap protein-A HP column using PBS (pH 7.4) as running buffer and 0.1 M sodium citrate buffer (pH 3.6) as eluting buffer. The eluted monoclonal antibody was neutralized to pH 7.0 with 0.5M Tris-HCl buffer (pH 9.0).

#### **6.2.4. Cation-exchange laterally-fed membrane chromatography (LFMC)**

The LFMC devices were integrated with AKTA Prime liquid chromatography systems (GE Healthcare Biosciences, QC, Canada) using luer fittings and appropriate PEEK tubing. Purification of mAb aggregates using cation-exchange chromatography is based on their stronger interaction with the chromatographic. All cation-exchange LFMC experiments carried out in this study were done using 20 mM sodium phosphate buffer (of appropriate pH) as the binding buffer 0.5 M sodium chloride was used as eluent.

The purity values were calculated based on the ratio of the peak areas obtained with the CEX-LFMC chromatograms and the feed samples. The former was found using the Primeview Evaluation software (GE Healthcare Biosciences) with zero-baseline integration whereas the latter was measured based on size-exclusion chromatography which was previously carried out for the feed samples (not shown).

#### **6.2.5. Hydrophobic interaction membrane chromatography (HIMC)**

The peaks collected from the cation-exchange LFMC experiments for Trastuzumab (IgG1) aggregates separation were analyzed by hydrophobic interaction membrane chromatography (HIMC) using a stack of hydrophilized PVDF membranes which have previously been shown to have stimuli-responsive surfaces, i.e. the hydrophobicity of the surface can be manipulated by environmental conditions such as salt concentrations [6, 20]. The mAbs along with their aggregated forms bound on these membranes in the presence of high anti-chaotropic salt concentration conditions and were released by lowering the salt concentration in the order of increasing hydrophobicity. Feed solutions for the HIMC experiments were prepared by mixing the cation-exchange LFMC samples with concentrated ammonium sulfate solution so that the effective final salt concentration was 1.5 M. The presence of salt decreases mAb solubility and so the mAb concentration was adjusted to about 0.2 mg/mL [33, 38]. The HIMC module which housed ten layers of PVDF membrane disks (20 mm diameter) was

fabricated in-house based on an earlier-reported design reported [39]. The module was connected to an AKTA Prime liquid chromatography system (GE Healthcare Biosciences, QC, Canada) using appropriate PEEK tubing. The binding buffer consisted of 20 mM sodium phosphate buffer (pH 7.0) containing 1.5 M ammonium sulfate. The eluting buffer was the same except for the presence of ammonium sulfate. The HMC experiments were run at 4.0 mL/min flow rate and samples were injected using a 500  $\mu$ L loop. A 40 mL linear gradient was used to elute the bound mAb and aggregates.

#### **6.2.6. Native polyacrylamide gel electrophoresis**

Samples collected from the Trastuzumab (IgG1) separation experiments were also analyzed by native PAGE [40]. Using this technique the proteins were separated based on their intrinsic size and charge. The mAb aggregates, due to their bigger size and similar charge density moved slower than the monomer, and could be visualized as distinct bands. The samples were first desalted and concentrated using 30 kDa MWCO centrifugal ultrafilters and then loaded on 7% polyacrylamide gels. Sample buffer, containing acetic acid, Tris-base, glycerol, and pyronin imparted positive charge to the mAbs. Electrophoresis was carried out using reversed polarity at 200 V for 2 hrs. in a Hoefer miniVE system (GE healthcare biosciences, Baie-d'Urfe, QC, Canada). Tris-HCl buffer was used to prepare the separating (pH 4.8) and the stacking (pH 6.0) gels. The gels were then stained using Coomassie Brilliant Blue dye for 20 min and destained using a mixture of methanol (10%), acidic acid (15%), and water. The gels were then photographed using a digital camera.

#### **6.2.7. Size-exclusion high-performance liquid chromatography (SE-HPLC)**

Peaks from the EG2-hFc aggregates separation experiments were analyzed using size-exclusion high-performance liquid chromatography (SE-HPLC). The samples were initially concentrated using 10 kDa MWCO centrifugal ultrafilters at 4000 rpm for 30 minutes. During the process, the buffer was exchanged to 20 mM sodium phosphate buffer (pH 7.0) also containing 250 mM NaCl. The samples (10  $\mu$ L)

were then run on a TSK-GEL G3000SWXL column (7.8 mm× 300 mm, Tosoh Bioscience, Montgomeryville, PA) integrated with Alliance HPLC system (Waters Corp., Milford, MA, USA). The same buffer was used as the mobile phase at a flow rate of 0.3 mL/min and the peaks were monitored by UV absorbance at 280 nm.

### 6.2.8. Theoretical plate number determination

Number of theoretical plates for the 9.2 mL LFMC devices was determined using sodium chloride as tracer (Figure. 6.S1). The experiments were carried out at a flow rate of 15 mL/min. The mobile phase was 0.4 M sodium chloride solution while 0.8 M NaCl was injected to generate the conductivity peak. The injection volume was 0.1 mL which was roughly 1% of the membrane bed volume. The number of theoretical plates were calculated based on the conductivity peaks as described by in the literature [41].

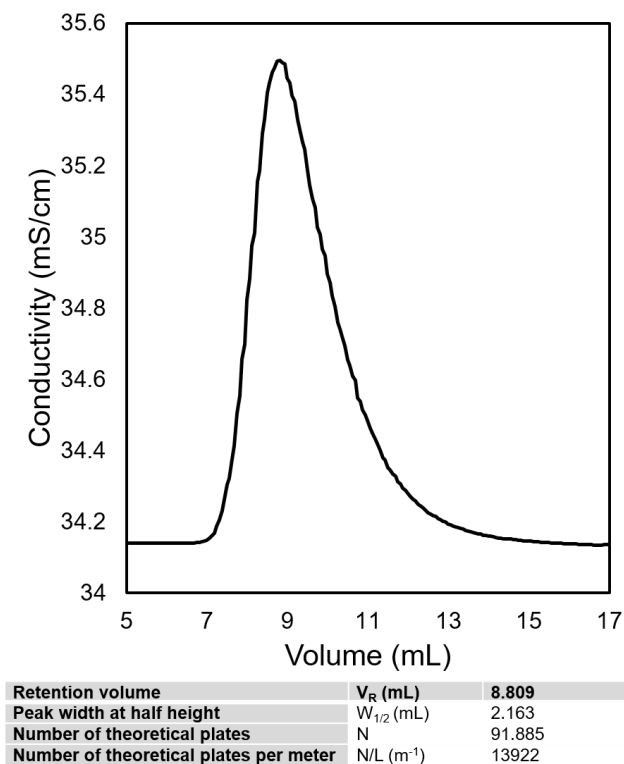


**Fig 6.S1:** Salt tracer using NaCl for determination of number of theoretical plates (membrane: Sartorius S, membrane bed volume: 9.2 mL, feed concentration: 0.8 M, sample volume: 100  $\mu$ L, running buffer: 0.4 M NaCl, flow rate: 15 mL/min)

### 6.3. Results and Discussion

The performance of a chromatography column is typically measured in terms of the number of theoretical plates. This parameter is also used to ensure robustness and reproducibility [41]. For Capto S resin, which is widely used in the biopharmaceutical industry for monoclonal antibody purification, the numbers of theoretical plates were reported to be 5000 and 3704 plates per meter respectively for 1 and 40 mL columns [42]. When high-performance resin particles of significantly smaller diameter were incorporated in the same columns, the values increased to 11111 and 7142 plates per meter [42]. For the 9.2 mL LFMC device used in this study, the number was found to be 13922 plates per meter, which was even higher than high-performance resins. Accordingly, it was expected that sharp and well resolved peaks would be obtained with the LFMC devices. Aggregates were separated from 293 derived IgG1 Trastuzumab using the 4.6 mL LFMC device. Initial experiments were performed to determine the effect of the length of linear gradient on the resolution of the mAb monomer from aggregates. These experiments were carried out at 20 mL/min flow rate (4.34 membrane bed volumes per min or MBV/min) by injecting 2 mL of 0.5 mg/mL mAb feed solution prepared in binding buffer (i.e. 20 mM sodium phosphate, pH 6.0). Figure.6.1 shows the chromatograms obtained using 100, 200, 250, and 300 mL linear gradients from binding to eluting buffer (0.5 M sodium chloride). With 100 mL linear gradient, the aggregates eluted as the tail following the mAb monomer peak. Well-resolved monomer and aggregates peak could be obtained using 250 and 300 mL gradients. A further increase in gradient length led to unnecessary peak broadening without a significant increase in resolution (data not shown). Therefore, preparative separation of the 293 derived Trastuzumab was carried out using 300 mL linear gradient at 20 mL/min.

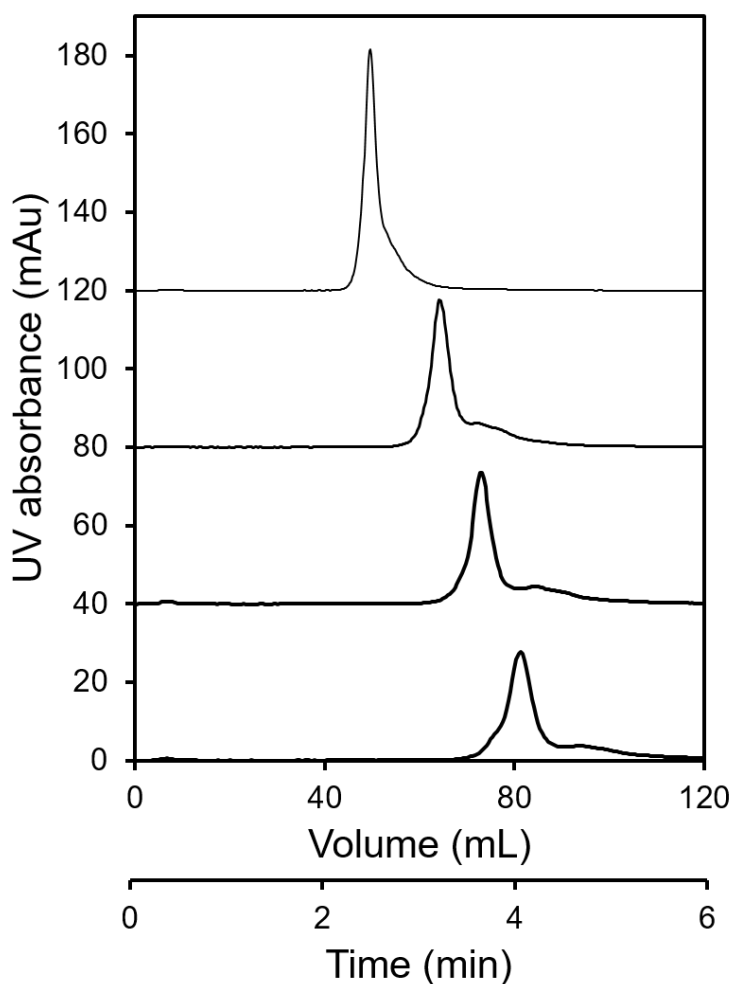


**Fig 6.1:** Optimization of gradient elution for separation of 293 derived IgG1 Trastuzumab aggregates (top to bottom: 100 mL, 200 mL, 250 mL, 300 mL gradient, membrane: Sartorius S, membrane bed volume: 4.6 mL, feed concentration: 0.5 mg/mL, sample volume: 2 mL, binding buffer: 20 mM sodium phosphate pH 6.0, eluting buffer: binding buffer + 0.5 M NaCl, flow rate: 20 mL/min)

The concentration of the mAb in the feed solution was increased to 5 mg/mL, while the sample volume was increased to 5 mL. The chromatogram obtained during the preparative separation experiment is shown in Figure. 6.2. The linear gradient was started 20 mL (or 1 min), i.e. after the tiny flow-through peak. The monomer which appeared around 4 minute retention time was sharp and symmetrical peak. The dimer was then eluted as a distinct peak, followed by a tail consisting of higher

aggregates. Thus, separation of aggregates could be carried out at high speed with resolution comparable to that reported in the literature [14], without the use of resolution enhancing additives. The separation time was less than 8 minutes, which was considerably faster than 150 minutes, reported for a similar separation using a 5 mL column [14]. It is also worth pointing out that in our experiments, the device was loaded with high-concentration mAb sample of volume comparable to the membrane bed volume, i.e. the separation was challenging. Orthogonal analytical methods were used to confirm the outcome of the above separation.

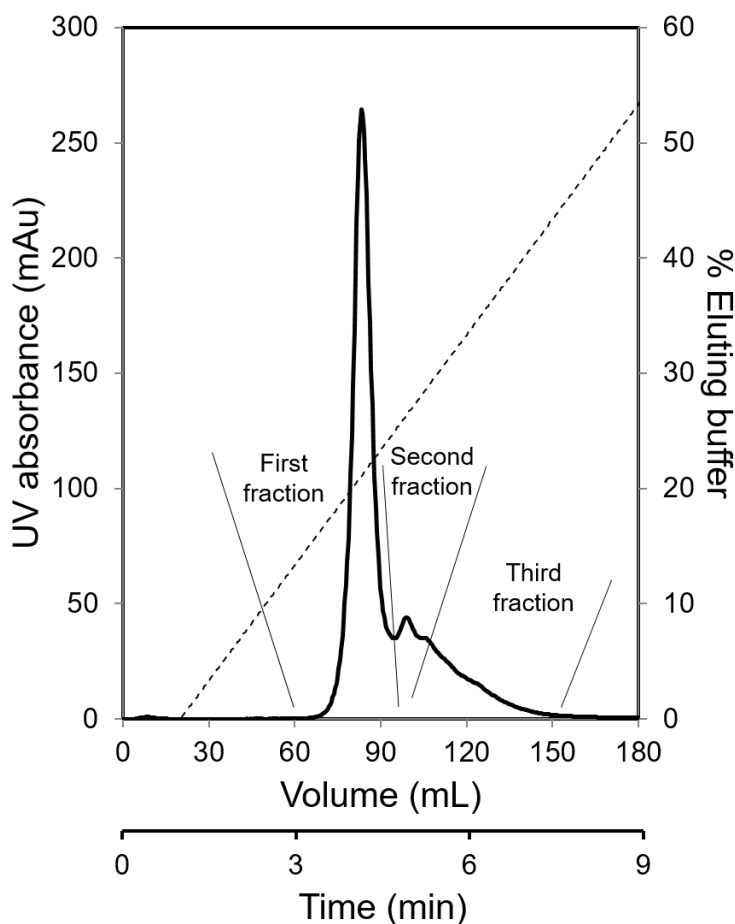


**Fig 6.2:** Preparative LFMC separation of Trastuzumab aggregates (membrane: Sartorius S, membrane bed volume: 4.6 mL, feed concentration: 2.5 mg/mL, sample volume: 5 mL, binding buffer: 20 mM sodium phosphate pH 6.0, eluting buffer: binding buffer + 0.5 M NaCl, linear gradient length: 300 mL, flow rate: 20 mL/min, solid line: UV absorbance, dashed line: percent eluting buffer)

Samples from the flow through, the separated monomer, and aggregate peaks from the above-mentioned experiments were collected and analyzed by HIMC. Monoclonal antibody aggregates have previously shown to be more hydrophobic than the monomer, and therefore eluted later [20]. Figure 6.3 shows the different chromatograms obtained by the above HIMC analysis, carried out using 500  $\mu\text{L}$  samples. A broad composite peak consisting of the monomer peak followed by a tail consisting of the aggregates was obtained from the feed sample. This was consistent with the profile obtained in the cation-exchange LFMC experiments. The first fraction which was expected to contain mainly monomer gave a sharper peak than the feed sample. The shoulder observed with the feed sample around 5-6 min was absent in this chromatogram, clearly indicating that this fraction consisted mainly of monomer with trace amounts of aggregates. The chromatogram obtained with the second fraction indicated a very small monomer content and a significantly greater aggregates content. Figure 6.4 shows the native PAGE gel obtained with the above samples. Consistent with the HIMC results, the feed sample contained both monomer and aggregates, the first fraction contained mainly monomer, while the second fraction contained mainly aggregates. Notably, the flow-through was free from any form of mAb. The above HIMC and native-PAGE results clearly indicate that mAb aggregates could be very efficiently and rapidly removed using cation-exchange LFMC.

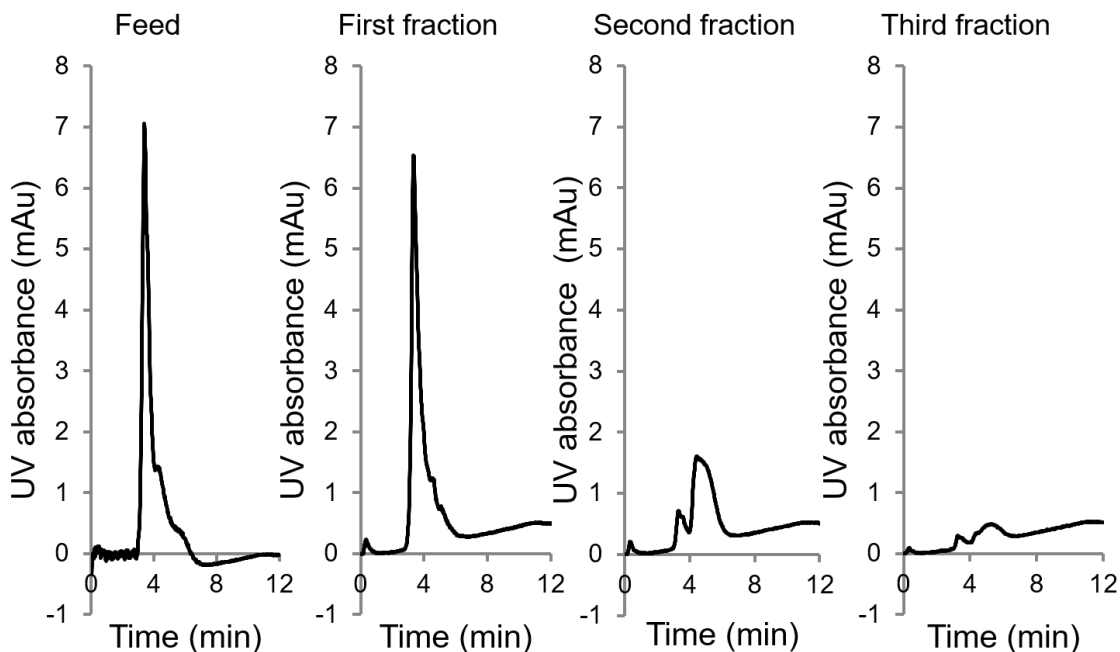


**Fig 6.3:** Analytical HPMC chromatograms obtained using samples collected from the preparative Trastuzumab aggregates separation experiment shown in Figure 6.2 (membrane: hydrophilized PVDF (0.22  $\mu\text{m}$  pore size), membrane bed volume: 0.4 mL, feed concentration: 0.2 mg/mL, sample volume: 500  $\mu\text{L}$ , binding buffer: 1.5 M ammonium sulfate in 20 mM sodium phosphate pH 7.0, eluting buffer: 20 mM sodium phosphate pH 7.0, linear gradient length: 40 mL, flow rate: 4 mL/min)

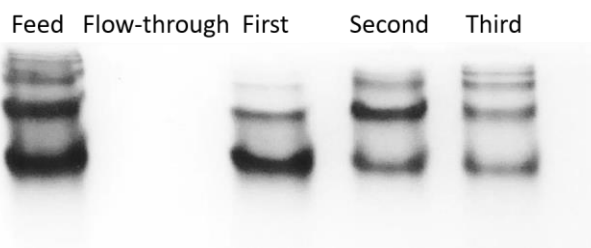


**Fig 6.4:** Native PAGE analysis of the samples collected from the preparative Trastuzumab aggregates separation experiment shown in Fig 6.2.

The removal of Campath-1H aggregates was attempted using the 1 mL LFMC device. Preliminary experiments were carried out using different linear gradient lengths (results not shown) and 150 mL linear gradient was found to be optimum

for aggregates separation. Experiments were carried out using both a monomer-rich and an aggregates-rich (or “dimers”) sample, by injecting 500  $\mu\text{L}$  of the 0.75 mg/mL feed solutions and the chromatograms thus obtained are shown in Figure. 6.5. The monomer-rich sample showed one major peak followed by a small shoulder, indicating that it contained mainly monomer and trace amounts of aggregates. The “dimers” sample contained mostly dimer and some higher aggregates and very small amount of monomer. The above results show that even at a very high flow rate of 10 mL/min (i.e. 10 MBV/min), the cation-exchange based LFMC technique was suitable for resolving and thereby removing aggregates from Campath-1H samples. While the resolution of dimer and higher aggregates was not as high as that attainable with preparative HIMC technique reported in the literature [6]; the cation-exchange based LFMC technique was much faster and free from difficulties caused by the high salt concentration binding buffer used for HIMC, namely, low protein solubility and thereby low processing capacity. The purity of the monomer was calculated for the chromatograms obtained with campath-1H. The values were 93.42% and 33.95% for the campath-1H and the dimers sample respectively.

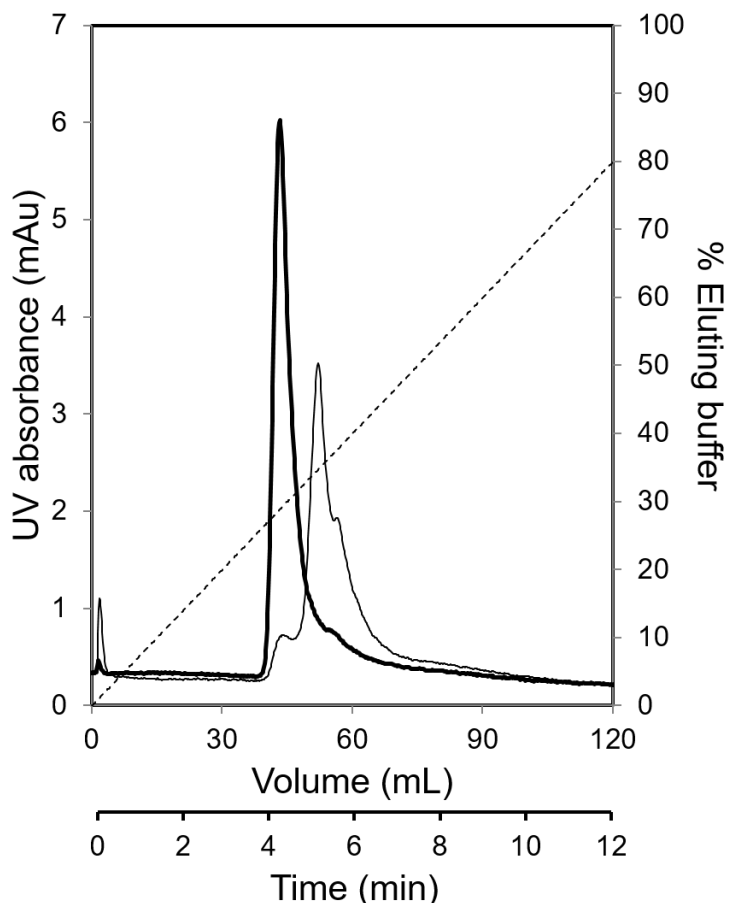


**Fig 6.5:** Preparative cation-exchange LFMC for separation of Campath-1H samples (thick solid line: UV absorbance for monomer-rich sample, thin solid line: UV absorbance for aggregates-rich sample or “dimers”, membrane: Sartorius S, membrane bed volume: 1.0 mL, feed concentration: 0.75 mg/mL, sample volume: 500  $\mu$ L, binding buffer: 20 mM sodium phosphate pH 6.0, eluting buffer: binding buffer + 0.5 M NaCl, linear gradient length: 150 mL, flow rate: 10 mL/min, dashed line: percent eluting buffer)

The above results demonstrate that the cation-exchange LFMC technique was suitable for aggregate removal from whole IgG mAbs. As the next step, we explored the potential for using this technique for removing aggregates from chimeric heavy chain mAb samples. In the initial experiments, the LFMC device with 4.6 mL bed volume was used. As the first step, the optimum pH for separating aggregates from protein-A purified EG2-hFc was determined. Chromatograms obtained at pH values 5.0, 5.5, and 6.0 respectively, using 5 mL of the 0.05 mg/mL

feed samples (see Figure 6.6). These pH optimization experiments were carried out at 20 mL/min flow rate (i.e. 4.34 MBV/min), using 30 mL linear gradient for elution. The best monomer/dimer separation was obtained at pH 6.0 and this pH value was used in all subsequent EG2-hFc aggregates removal experiments. As the next step, the effect of length of linear gradient elution on EG2-hFc monomer/dimer was examined. Figure 6.7 shows the chromatograms obtained using 30 and 60 mL linear gradients. Clearly, better peak resolution was obtained using 60 mL linear gradient. Therefore, preparative aggregate removal from EG2-hFc samples was carried out at pH 6.0 using 60 mL linear gradient elution (see Figure 6.8). This experiment was carried out at a flow rate of 20 mL/min (i.e. 2.17 MBV/min) using the 9.2 mL LFMC device by injecting 45 mL of 0.05 mg/mL EG2-hFc sample using a superloop. The linear gradient was applied immediately after the sample injection to reduce the separation time. In this experiment, the aggregates were excellently resolved from the monomer in less than 7 minutes. The flow through peak seen in Figures 6.6 and 6.7 consisted of unbound impurities which had remained in the protein-A affinity purified EG2-hFc sample. The peaks collected during the above preparative EG2-hFc aggregates separation experiment were analyzed by SEC (see Figure 6.9). The LFMC separated presumed monomer fraction gave a single SEC peak (~26 minute retention time), indicating that it contained only EG2-hFc monomer. The LFMC separated aggregates fraction also gave a single SEC peak (~16 minute retention time), indicating that it contained EG2-hFc aggregates. The SEC peak obtained with the aggregate sample was negatively skewed, which indicated that the proportion of higher aggregates was low, i.e. it consisted mainly of dimer. The above results demonstrate that the cation-exchange LFMC technique was indeed suitable for removing aggregates from EG2-hFc samples.

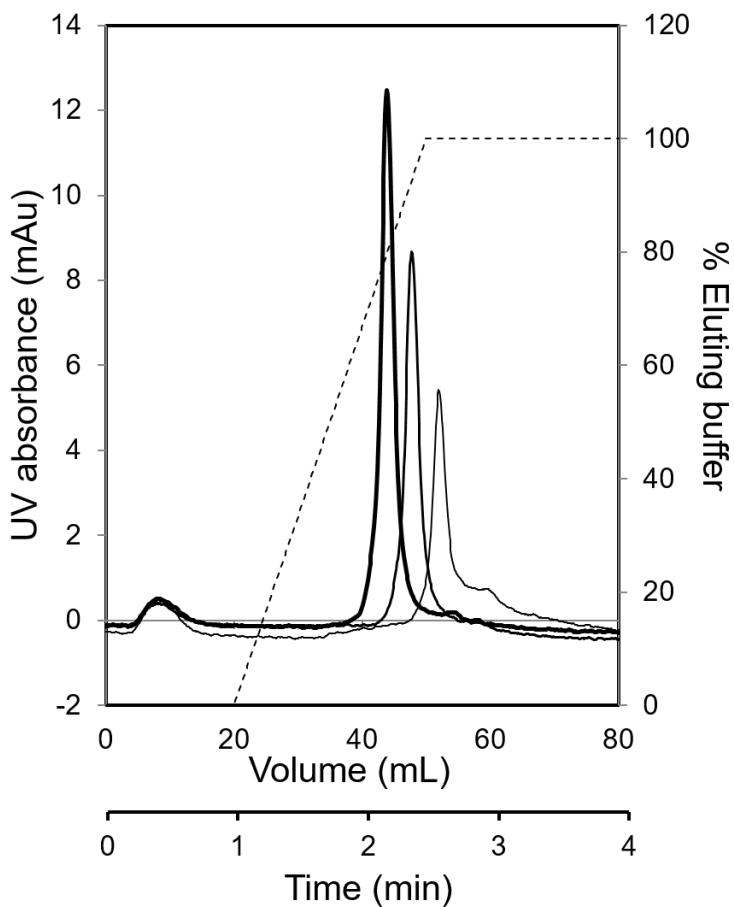


**Fig 6.6:** Optimization of operating pH for separation of EG2-hFc aggregates (thick solid line: pH 5.0, medium solid line: pH 5.5, thin solid line: pH 6.0, membrane: Sartorius S, membrane bed volume: 4.6 mL, feed concentration: 0.05 mg/mL, sample volume: 5 mL, binding buffer: 20 mM sodium phosphate, eluting buffer: binding buffer + 0.5 M NaCl, linear gradient length: 30 mL, flow rate: 20 mL/min, dashed line: percent eluting buffer)

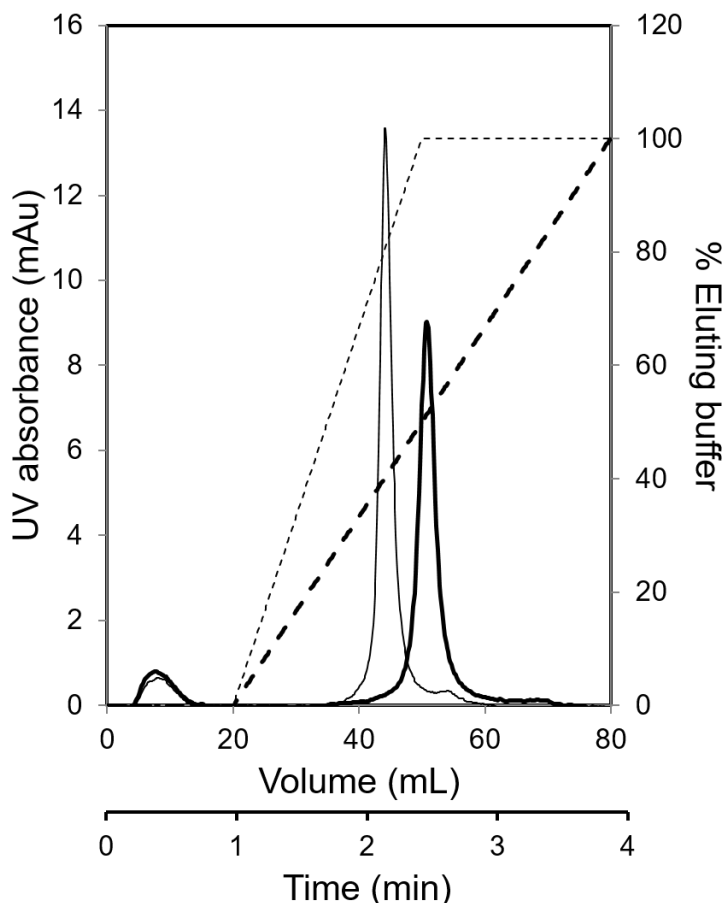


**Fig 6.7:** Optimization of gradient length for separation of EG2-hFc aggregates (thin line: 30mL linear gradient, thick line: 60 mL linear gradient, membrane: Sartorius S, membrane bed volume: 4.6 mL, feed concentration: 0.05 mg/mL, sample volume: 5 mL, binding buffer: 20 mM sodium phosphate pH 6.0, eluting buffer: binding buffer + 0.5 M NaCl, flow rate: 20 mL/min, dashed line: percent eluting buffer)

The results discussed in this paper clearly demonstrate the suitability of cation-exchange LFMC for separation of mAb aggregates. The bind-and-elute separation processes performed with the LFMC devices gave excellent monomer/aggregates resolutions. This can be explained based on the high theoretical plate numbers obtained with these devices. The LFMC devices were also able to sustain stable conductivity gradients, even when very shallow gradients were applied. The high-resolution combined with high-productivity makes LFMC device very attractive for

use in different stages in downstream processing of biopharmaceuticals, thereby extending the application range of membrane chromatography. The LFMC devices used in the current study could be manufactured quite inexpensively, allowing these to be disposable, thereby making these consistent with the bigger mandate of membrane chromatography, i.e. single-use bioprocessing.

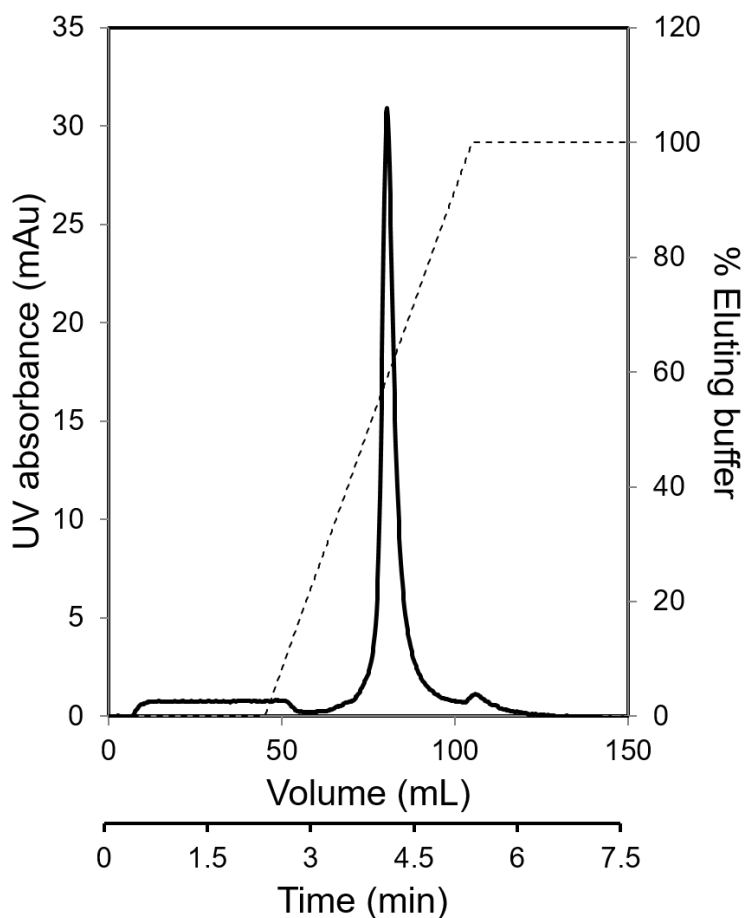


**Fig 6.8:** Preparative cation-exchange LFMC for separation of EG2-hFc aggregates (membrane: Sartorius S, membrane bed volume: 9.2 mL, feed concentration: 0.05 mg/mL, sample volume: 45 mL, binding buffer: 20 mM sodium phosphate pH 6.0, eluting buffer: binding buffer + 0.5 M NaCl, linear gradient length: 60 mL, flow rate: 20 mL/min, dashed line: percent eluting buffer)

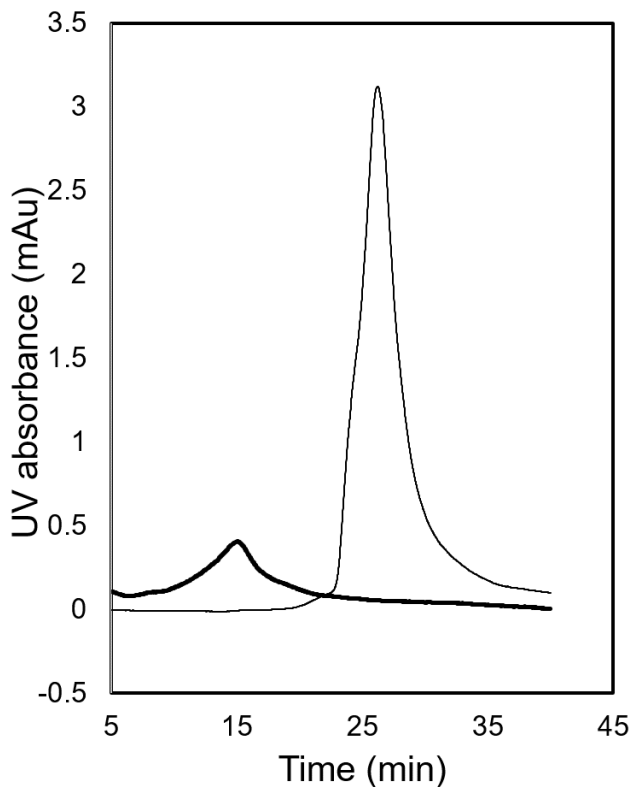


**Fig 6.9:** Size exclusion chromatography (SEC) of the samples collected during preparative separation of EG2-hFc aggregates (thin line: monomer peak, thick line: aggregate peak, column: TSK-GEL G3000SWXL 7.8 mm× 300 mm, sample volumes: 10  $\mu$ L, running buffer: 20 mM sodium phosphate buffer + 250 mM NaCl, flow rate: 0.3 mL/min)

#### 6.4. Conclusions

This study demonstrated the suitability of cation-exchange laterally-fed membrane chromatography (or LFMC) for rapid and high-resolution separation of monoclonal antibody (or mAb) aggregates. Aggregates were removed from three different mAbs: two whole IgG mAbs Trastuzumab and Campath-1H, and one heavy chain mAb EG2-hFc. Separation of aggregates was demonstrated using orthogonal analytical techniques such as hydrophobic interaction membrane chromatography (or HIMC), native polyacrylamide gel electrophoresis (or native PAGE) and size exclusion chromatography (or SEC). Three different devices containing cation-

exchange S membranes having bed volumes of 1, 4.6, and 9.2 mL were employed in this study. All these devices showed excellent performance in the aggregate removal experiments. All three preparative aggregative separations (i.e. for Trastuzumab, Campath-1H and EG2-hFc) could be carried out in 8 minutes. Different flow rates ranging from 2 - 10 membrane volumes per minute were used in the LFMC experiments. Consistently high resolution separations were obtained at all these flow rates. Higher monomer/aggregates resolution was obtained with EG2-hFc than with the whole IgG mAbs. Based on the results reported in this paper, it could be confidently stated that LFMC combines high-resolution with high-productivity and would be very effective in a wide range of bio-manufacturing applications, including mAb production.

### **6.5. Acknowledgements**

We thank the National Science and Engineering Research Council (NSERC) of Canada, and the Ontario Research Fund – Research Excellence (ORF-RE) for funding this project. We thank Dr. Geoff Hale and other members of the Therapeutic Antibody Center, Oxford University, UK for donating the Campath-1H monomer and “dimer” samples. We thank Elna Luckham and the Biointerfaces institute at McMaster for providing us with the HPLC system. We thank Paul Gatt for fabricating the devices based on design provided by RG and PM. We thank Denis L’Abbé (NRC) for the production of the Trastuzumab antibody. This is NRC publication #HHT\_53323.

### **6.6 References**

- [1] A.A. Shukla, J. Thommes, Recent advances in large-scale production of monoclonal antibodies and related proteins. *Trends Biotechnol.* 28 (2010) 253–261.
- [2] N. Singh, A. Arunkumar, S. Chollangi, Z.G. Tan, M. Borys, Z.J. Li, Clarification technologies for monoclonal antibody manufacturing processes: Current state and future perspectives. *Biotechnol. Bioeng.* 113 (2015) 698–716.

- [3] M. Vázquez-Rey, D.A. Lang, Aggregates in monoclonal antibody manufacturing processes. *Biotechnol. Bioeng.* 108 (2011) 1494–1508.
- [4] S. Fekete, A. Beck, J. Veuthey, D. Guilleme, Theory and practice of size exclusion chromatography for the analysis of protein aggregates. *J. Pharm. Biomed. Anal.* 101 (2014) 161–173.
- [5] K. Ahrer, A. Buchacher, G. Iberer, D. Josic, A. Jungbauer, Analysis of aggregates of human immunoglobulin G using size-exclusion chromatography, static and dynamic light scattering. *J. Chromatogr. A.* 1009 (2003) 89–96.
- [6] L. Wang, R. Ghosh, Fractionation of monoclonal antibody aggregates using membrane chromatography. *J. Memb. Sci.* 318 (2008) 311–316.
- [7] W. Fraunhofer, G. Winter, The use of asymmetrical flow field-flow fractionation in pharmaceuticals and biopharmaceuticals. *Eur. J. Pharm. Biopharm.* 58 (2004) 369–383.
- [8] S. Chen, H. Lau, Y. Brodsky, G.R. Kleemann, R.F. Latypov, The use of native cation-exchange chromatography to study aggregation and phase separation of monoclonal antibodies. *Protein Sci.* 19 (2010) 1191–1204.
- [9] S. Kluters, F. Wittkopp, M. Jöhnck, C. Frech, Application of linear pH gradients for the modeling of ion exchange chromatography: Separation of monoclonal antibody monomer from aggregates. *J. Sep. Sci.* 39 (2016) 663–675.
- [10] S. Kluters, S. Neumann, T. Von Hirschheydt, A. Grossmann, A. Schaubmar, C. Frech, Mechanism of improved antibody aggregate separation in polyethylene glycol-modulated cation exchange chromatography. *J. Sep. Sci.* 35 (2012) 3130–3138.
- [11] E.J. Suda, K.E. Thomas, T.M. Pabst, P. Mensah, N. Ramasubramanian, M.E. Gustafson, A.K. Hunter, Comparison of agarose and dextran-grafted agarose

strong ion exchangers for the separation of protein aggregates. *J. Chromatogr. A.* 1216 (2009) 5256–5264.

[12] Z. Xu, J. Li, J.X. Zhou, Process development for robust removal of aggregates using cation exchange chromatography in monoclonal antibody purification with implementation of quality by design. *Prep. Biochem. Biotechnol.* 42 (2012) 183–202.

[13] P. Gagnon, Improved antibody aggregate removal by hydroxyapatite chromatography in the presence of polyethylene glycol. *J. Immunol. Methods.* 336 (2008) 222–228.

[14] S. Kluters, C. Frech, T. von Hirschheydt, A. Schaubmar, S. Neumann, Solvent modulation strategy for superior antibody monomer/aggregate separation in cation exchange chromatography. *J. Chromatogr. B.* 1006 (2015) 37–46.

[15] H.F. Liu, B. McCooey, T. Duarte, D.E. Myers, T. Hudson, A. Amanullah, R. van Reis, B.D. Kelley, Exploration of overloaded cation exchange chromatography for monoclonal antibody purification. *J. Chromatogr. A.* 1218 (2011) 6943–6952.

[16] C. Charcosset, Review Purification of Proteins by Membrane Chromatography. *J. Chem. Technol. Biotechnol.* 71 (1998) 95-110.

[17] R. Ghosh, Protein separation using membrane chromatography: opportunities and challenges. *J. Chromatogr. A.* 952 (2002) 13–27.

[18] D.K. Roper, E.N. Lightfoot, Separation of biomolecules using adsorptive membranes. *J. Chromatogr. A.* 702 (1995) 3–26.

[19] T.B. Tennikova, F. Svec, B.G. Belenkii, High-Performance Membrane Chromatography. A Novel Method of Protein Separation. *J. Liq. Chromatogr.* 13 (1990) 63–70.

- [20] L. Wang, G. Hale, R. Ghosh, Non-size-based membrane chromatographic separation and analysis of monoclonal antibody aggregates. *Anal. Chem.* 78 (2006) 6863–6867.
- [21] S.M. Yoo, R. Ghosh, Simultaneous removal of leached protein-A and aggregates from monoclonal antibody using hydrophobic interaction membrane chromatography. *J. Memb. Sci.* 390–391 (2012) 263–269.
- [22] D. Yu, R. Ghosh, Method for studying immunoglobulin G binding on hydrophobic surfaces. *Langmuir.* 26 (2010) 924–929.
- [23] A.R. Lajmi, S. Nochumson, A. Berges, Impact of antibody aggregation on a flowthrough anion-exchange membrane process. *Biotechnol. Prog.* 26 (2010) 1654–1661.
- [24] V. Orr, L. Zhong, M. Moo-Young, C.P. Chou, Recent advances in bioprocessing application of membrane chromatography. *Biotechnol. Adv.* 31 (2013) 450–65.
- [25] H.L. Knudsen, R.L. Fahrner, Y. Xu, L.A. Norling, G.S. Blank, Membrane ion-exchange chromatography for process-scale antibody purification. *J. Chromatogr. A.* 907 (2001) 145–54.
- [26] P. Madadkar, R. Ghosh, High-resolution protein separation using a laterally-fed membrane chromatography device. *J. Memb. Sci.* 499 (2016) 126–133.
- [27] R. Ghosh, P. Madadkar, Laterally-fed membrane chromatography device. (2016) US 62304379.
- [28] P. Madadkar, Q. Wu, R. Ghosh, A laterally-fed membrane chromatography module. *J. Memb. Sci.* 487 (2015) 173–179.
- [29] R. Ghosh, P. Madadkar, Q. Wu, On the workings of laterally-fed membrane chromatography. *J. Memb. Sci.* 516 (2016) 26–32.

- [30] J. Phillips, A. Drumm, P. Harrison, P. Bird, K. Bhamra, E. Berrie, G. Hale, Manufacture and quality control of CAMPATH-1 antibodies for clinical trials. *Cytotherapy*. 3 (2001) 233–42.
- [31] U. Wernery, Camelid immunoglobulins and their importance for the newborn - A review. *J. Vet. Med. Ser. B*. 48 (2011) 561–568.
- [32] J. Zhang, X. Liu, A. Bell, R. To, T.N. Baral, A. Azizi, J. Li, B. Cass, Y. Durocher, Transient expression and purification of chimeric heavy chain antibodies. *Protein Expr. Purif.* 65 (2009) 77–82.
- [33] R. Sadavarte, M. Spearman, N. Okun, M. Butler, R. Ghosh, Purification of chimeric heavy chain monoclonal antibody EG2-hFc using hydrophobic interaction membrane chromatography: An alternative to protein-A affinity chromatography. *Biotechnol. Bioeng.* 111 (2014) 1139–1149.
- [34] A.P. Chapman, P. Antoniw, M. Spitali, S. West, S. Stephens, D.J. King, Therapeutic antibody fragments with prolonged in vivo half-lives. *Nat. Biotechnol.* 17 (1999) 780–783.
- [35] L. Delafosse, P. Xu, Y. Durocher, Comparative study of polyethylenimines for transient gene expression in mammalian HEK293 and CHO cells. *J. Biotechnol.* 227 (2016) 103-111.
- [36] J. Zhang, R. MacKenzie, Y. Durocher, Production of chimeric heavy chain antibodies, in: A.S. Dimitrov (Eds.), *Therapeutic antibodies: methods and protocols*, Humana Press, New York, 2009, pp. 323–336
- [37] P. Madadkar, S. Luna Nino, R. Ghosh, High-resolution, preparative purification of PEGylated protein using a laterally-fed membrane chromatography device. *J. Memb. Sci.* 1035 (2016) 1–7.

- [38] D. Yu, M.D. McLean, J.C. Hall, R. Ghosh, Purification of a human immunoglobulin G1 monoclonal antibody from transgenic tobacco using membrane chromatographic processes. *J. Chromatogr. A.* 1187 (2008) 128–137.
- [39] R. Ghosh, T. Wong, Effect of module design on the efficiency of membrane chromatographic separation processes. *J. Memb. Sci.* 281 (2006) 532–540.
- [40] U.K. Laemmli, Cleavage of structural proteins during the assembly of the head of bacteriophage T4. *Nature* 227 (1970) 680–685.
- [41] A.S. Rathore, R.M. Kennedy, J.K. O'Donnell, I. Bemberis, O. Kaltenbrunner, Qualification of a chromatographic column: Why and how to do it. *BioPharm Int.* 16 (2003) 30–40.
- [42] S. Gerontas, M. Asplund, R. Hjorth, D.G. Bracewell, Integration of scale-down experimentation and general rate modelling to predict manufacturing scale chromatographic separations. *J. Chromatogr. A* 1217 (2010) 6917–6926.

## **Chapter 7**

### **Ultra-Fast Separation of Monoclonal Antibody Aggregates Using Analytical Laterally-Fed Membrane Chromatography (LFMC)**

### 7.1. Abstract

We discuss the rapid analysis of monoclonal antibody (mAb) aggregates using a greatly cost-effective technique based on hydrophobic interaction membrane chromatography (HIMC). HIMC which was previously shown to be highly suitable for analytical separation of mAb aggregates was carried out in the format of the recently developed laterally-fed membrane chromatography (LFMC) technology. A stack of rectangular PVDF membranes (pore size of 0.22  $\mu\text{m}$ ) were integrated with a modified version of LFMC devices adapted to analytical scale operations. Chinese hamster ovary (or CHO) cell line derived Alemtuzumab (campath-1H) was used as the model mAb. High-resolution separations were achieved at 40 membrane bed volume (MBV)/min, offering analysis times below 1.5 min. The assay time challenges the currently developed size exclusion ultra-performance liquid chromatography (SE-UPLC) techniques; this is while the operating pressure was below 200 kPa, eliminating the need for high pressure pumps and chromatography systems. The analysis time was further improved by decreasing the dead volume within the LFMC device through increasing the pillar sizes embedded within the device. The validity of the technique was approved for other mAb samples.

**Keywords:** Analytical separation; hydrophobic interaction membrane chromatography; HIMC; Laterally-fed; UPLC; monoclonal antibodies

## 7.2. Introduction

Over the course of monoclonal antibodies (mAbs) manufacturing, the presence of soluble aggregates is monitored at different stages. Due to their potential immunogenicity, aggregate level should be kept below an acceptable grade in the final clinically used products [1]. Size exclusion chromatography (SEC) using HPLC systems (SE-HPLC) has been the standard technique in monitoring the aggregate levels [2]. Despite the simplicity which is owing to the isocratic nature of operation, conventional SEC is very slow, giving average throughput of roughly two samples per hour [3,4]. The productivity of SEC has been improved without sacrificing the resolution by using small resin particles within shorter columns via ultra-performance liquid chromatography (UPLC) systems. The so called SE-UPLC columns contain packing resins with sizes in the range of couple of microns with diverse pore sizes, the use of which brings down the solute diffusion path lengths. This is also reflected in the values of height equivalent to the theoretical plates (HETP), i.e. the measure of peak variance normalized for separation length [5], which is considerably lower for UPLC columns. Accordingly, the typical assay times for UPLC-based SEC is below 10 minutes which contributes to a dramatic increase in the analysis throughput [3,6,7]. UPLC systems benefit from having very low dead volumes and consequently an order of magnitude lower dispersion. This underestimated feature of UPLC is achieved by using zero dead-volume fittings, auto-sampling minute volumes, and smaller UV cells [8]. The current state-of-the-art in fast analysis of aggregates by UPLC makes use of sub-2  $\mu\text{m}$  packing material which are capable of characterizing recombinant mAbs in 3-4 minutes [9-11]. Furthermore, parallelization and interlacing the sample injections on such columns have reduced the processing time down to two minutes [3].

Nevertheless, the improved productivity and resolution is at the cost of pressure, the primary shortcoming of SE-UPLC [12]. While the pressure limit for conventional HPLC (Tosoh Biosciences, TSKgel) is below 100 bars, the number is often as high as 1000 bars for commonly used UPLC columns (Waters, AQUITY UPLC) [8]. The

result is the need for costly pumps and seals as well as intricate packing techniques [13]. Furthermore, the following friction heating might affect the temperature-sensitive proteins to the point of denaturation or further on-column aggregation [14]. The application of recently developed sub 3  $\mu\text{m}$  core-shell packing material has offered lower operating pressures. The particles are superficially porous material with a central core due to which they have higher mass transfer rates, higher packing density, and consequently smaller plate heights (HETPs). This is while the new generation of core-shell particles with sizes in the range of 1.3-1.7  $\mu\text{m}$  still deliver very high operating pressures [15]. Although it is expected that the particle sizes for chromatography goes down to 500 nm in the approaching decade, the concerns involve the analytes to heat-up under such high pressures and cause skewed results [16]. This remains controversial based on nano-fluidic studies which suggest that the needed pressure at such particle sizes would be lower than the theoretical limits due to the “slip-flow” conditions which can give flow enhancements [5,17].

Although UPLC is the most versatile approach in analysis of closely related species such as mAb aggregates, it is not the only one. Moving towards incorporation of lesser sample volumes and enhancing the sensitivity of the analysis, capillary SEC, capillary electrophoresis (CE), and light scattering (LS) are also capable of determining the aggregate levels in a mAb. However, the expansion of the application requires major changes in the liquid chromatography systems and neither of the techniques complement both the required speed and prevailing sample variability in the industry [2,18,19]. Hydrophobic interaction membrane chromatography (HIMC) has been used as a non-size-based method for analytical separation of mAb aggregates [20,21]. The technique is based on the reversible binding of the mAb and the aggregates on microporous poly(vinylidene fluoride) (PVDF) membranes. The binding occurs under high concentrations of antichaotropic salts followed by elution of the bound solutes using negative salt gradients. The aggregates are fractionated from the native form of the mAb due to

their higher hydrophobicity. In addition to the satisfactory resolution of separation, advantages include the inherent higher productivity associated with membrane chromatography and the insensitivity of resolution to the sample size as opposed to size-based assays [20,22]. This is while the currently used stacked-disk membrane adsorbers are fabricated in small diameter and operated at relatively low flow rates accordingly. The fabrication of these devices in bigger diameters would be at the sacrifice of resolution of separation [20,21,23,24].

In this work, we discuss the application of the hydrophobic interaction membrane chromatography in the format of the newly developed laterally-fed membrane chromatography devices (HI-LFMC) devices making use of PVDF membranes for mAb aggregate analysis. The LFMC technology offers high resolution membrane chromatography [24-26]. This is provided by balanced pressure over the stack of rectangular membranes, the evenness of flow-path lengths within the devices, and the uniformity of solute residence time as a result of these two factors. Therefore, it is possible to construct LFMC devices with higher membrane surface area and operate at significantly greater flow rates without disturbing the resolution. The device used in this work was fabricated based on a new layout which was designed to serve the analytical scale operations. Three layers of rectangular PVDF membranes were stacked within the device (0.4 mL membrane bed volume). Monoclonal antibody samples containing low and high aggregate levels of Chinese hamster ovary (or CHO) cell line derived Alemtuzumab (campath-1H), were used as the primary model mAbs. The campath-1H sample containing low level of aggregate is referred to as “monomer-rich” and the one containing high level of aggregates is referred to as “dimer-rich” for the rest of the paper. The optimized condition for achieving highest efficiency of aggregate fractionation was determined. Moreover, the system was further modified to give faster analysis through adapting the device to smaller dead volumes. Finally, the validity of the analytical LFMC system was tested for other mAb samples.

## **7.2. Experimental**

### **7.2.1. Materials**

Campath-1H (humanized monoclonal antibody monomer-rich and dimer-rich) and HIgG1-CD4 (campath-9 [27]) were kindly donated by the Therapeutic Antibody Centre, University of Oxford, UK. Human embryonic kidney 293 (HEK) cell derived IgG1 (Trastuzumab biosimilar) was kindly donated by the National Research Council of Canada. Ammonium sulfate (A4418), sodium phosphate monobasic (S0751), sodium phosphate dibasic (S0876), sodium chloride (S7653), hydrochloric acid (258148), 30% acrylamide solution (A3699), sodium dodecyl sulfate (L3771), glycine (G8898), glycerol (G2025), ammonium persulfate (A3678), N,N,N',N'-tetramethyl ethylenediamine (T9281), bromophenol blue (B0126), Brilliant blue R concentrate (B8647), Trizma-hydrochloride (T3253), Trizma base (T1503), and DL-dithiothreitol (43817) were purchased from Sigma-Aldrich, St. Louis, MO. Acetic acid (1000-1) and methanol (6700-1) were purchased from Caledon laboratories LTD. (Georgetown, ON, Canada). Hydrophilized poly(vinylidene fluoride) (PVDF) membranes (GVWP14250; 0.22  $\mu\text{m}$  pore size) and Amicon centrifugal filters (30 kDa MWCO) were purchased from EMD Millipore Co. (Billerica, MA, USA). The buffers and solutions used for this work were all prepared using deionized water obtained with a SIMPLICITY 185 water purification unit Millipore (Molsheim, France).

### **7.2.2. Size exclusion chromatography (SEC)**

Campath-1H monomer-rich and dimer-rich samples which were used as the model mAbs for this work were initially analyzed using SE-HPLC. Stock solutions were diluted to 0.25 mg/mL using 20 mM sodium phosphate buffer (pH 7) containing 250 mM NaCl. The SEC column, TSK-Gel G3000SWXL (7.8 mm $\times$ 300 mm Tosoh Bioscience, Montgomeryville, PA) was integrated with Alliance HPLC system (Waters Corporations, Milford, MA, USA). The column was initially equilibrated with the same buffer until stable baseline was achieved. The experiments were run at

0.3 mL/min with 10  $\mu$ L sample volumes. UV absorbance at 280 nm wavelength were monitored for 30 minutes.

### **7.2.3. Native polyacrylamide gel electrophoresis**

Further analysis of feed samples were carried out using acidic native PAGE by which the protein molecules are separated based on their intrinsic size and charge. The mAb samples were first desalted and concentrated using 30 kDa MWCO ultracentrifugal filters (3750 rpm, 30 min). They were then mixed with the sample buffer containing acetic acid, glycerol, Tris-base, and pyronin imparting positive net charge to the molecules and were loaded on 7% polyacrylamide gel. Accordingly, reverse polarity electrophoresis was carried out at 200 V for 2 hr using a Hoefer miniVE system (GE healthcare biosciences, Baie-d'Urfe, QC, Canada). Coomassie Brilliant Blue dye solution diluted to 1 liter was used to stain the gel for 20 min. The gels were then destained using a solution containing methanol (15%), acetic acid (10%), and water (75%) and were documented using a Bio-imaging MiniBis pro system (24-25-PR) (DNR-Imaging Systems, Jerusalem, Israel).

### **7.2.4. Device fabrication**

The analytical LFMC device consisted of three layers: the top and bottom acrylic plates and the middle spacer which was made of plastic shims (figure. 7.1). The outer dimension of all the three rectangular components was 150 mm  $\times$  40 mm. The plates had identical design and each contained a rectangular channel (100 mm  $\times$  10 mm) curved at the endings with the radius of 5 mm. The channels contained 140 cylindrical pillars with hexagonal arrays of 3 and 4 over the width of the channel. The height of the pillars were similar to the depth of the channel being 0.2 mm. Two ports were embedded on each side of the channel (109 mm center-to-center distance) which were compatible to luer fittings and were tapered down to 1 mm over the thickness of the plates. The middle spacer contained a rectangular slot which was 2.5 mm wider than the rectangular channels from each side (115 mm  $\times$  15 mm). Three layers of the PVDF membrane having the same dimension with the rectangular slot were cut, placed within the spacer, and

sandwiched between the plates. It is notable that the spacer thickness (317.5  $\mu\text{m}$ ) was slightly lower than the thickness of the membrane stack (375  $\mu\text{m}$ ) for the purpose of sealing. Nine screws on each side of the device over its length, 15 mm far from one another, were used to hold the three layers together.

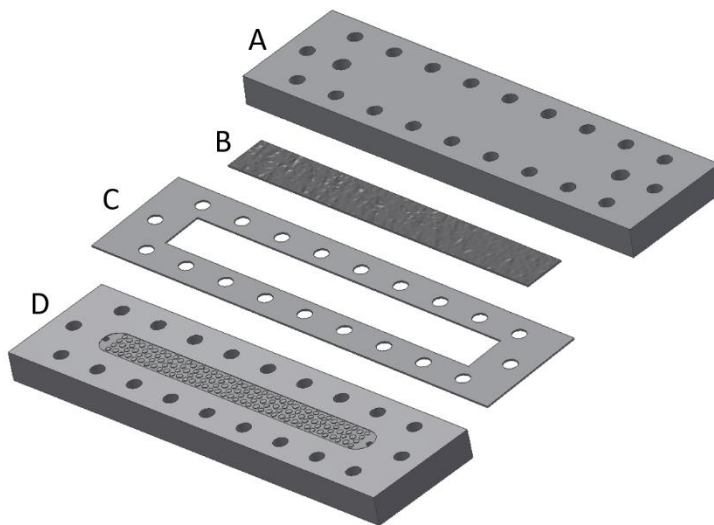


**Fig 7.1:** Blowout diagram of the analytical laterally-fed membrane chromatography device (LFMC), A: acrylic top plate; B: membrane stack (three layers of hydrophilized PVDF membranes; 0.22  $\mu\text{m}$  pore size; GVWP14250); C: plastic shim spacer; D: acrylic bottom plate.

The resulting device had the membrane bed volume (MBV) of 0.4 mL. The inlet and outlet ports were on the opposite ends of each plate. The other two ports were used for removing the bubbles and priming the device prior to the experiments and were kept closed via blocked fittings during the chromatographic operations.

#### 7.2.5. HETP determination

The HETP of the LFMC device was determined using sodium chloride as the tracer agent. The device was integrated with the AKTA prime liquid chromatography system (GE Healthcare Biosciences, QC, Canada) via the luer fittings and appropriate PEEK tubing. The running buffer was 0.4 M NaCl and 5  $\mu\text{L}$  of 0.8 M NaCl was injected as the sample. The sample volume was set to be almost 1% of

the device bed volume and the experiment was carried out at 16 mL/min (40 MBV/min). The conductivity peaks were attained and the HETP values were calculated based on the equations explained by Rathore *et al.*[28].

#### **7.2.6. Hydrophobic interaction LFMC**

The samples were injected using a 250  $\mu$ L sample loop. The eluting buffer was 20 mM sodium phosphate buffer (pH 7.0). The binding buffer was the same buffer containing 1.5 M ammonium sulfate as the antichaotropic salt. Linear gradient elution volume was 40 mL which was commenced at the same time with sample injection. All the experiments were run at feed concentration of 0.2 mg/mL and flow rate of 16 mL/min (40 MBV/min).

### **7.3. Results and Discussion**

#### **7.3.1. Feed analysis**

CHO cell line derived Alemtuzumab (campath-1H) monomer-rich and dimer-rich samples were analyzed by SE-HPLC and native PAGE (Figure. 7.2). Based on the chromatogram obtained with the dimer-rich campath-1H, the sample contained considerable amount of higher aggregates whereas that was not the case for the monomer-rich sample (figure 7.2, A). The peak was followed by mainly dimers and some monomers, retention time of which were consistent with the monomer-rich mAb sample. The results well-matched with the Native PAGE analysis (figure. 7.2, B).

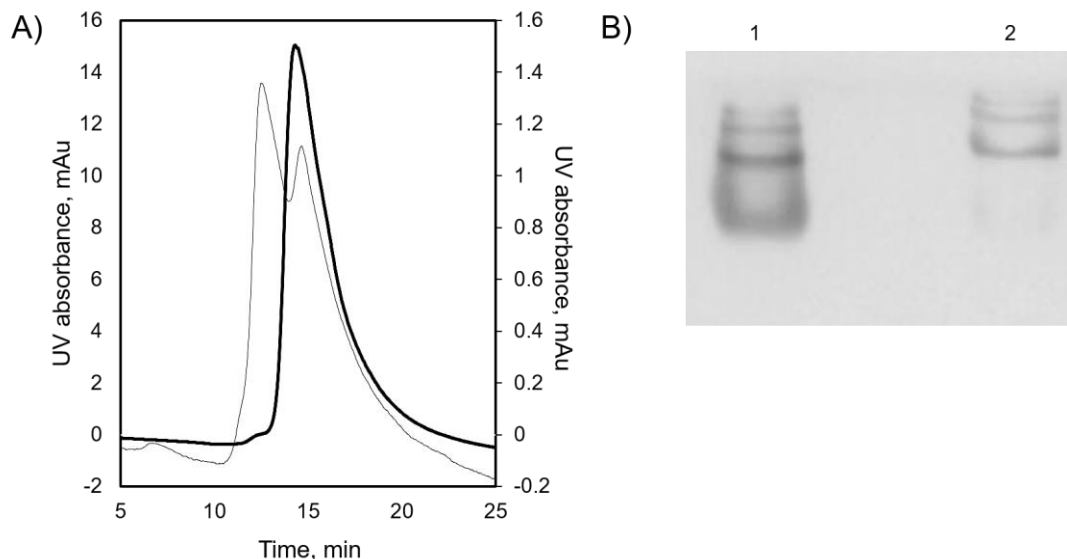


**Fig 7.2:** Feed analysis of the CHO cell line derived Alemtuzumab (campath-1H), A: SE-HPLC (thick line: monomer-rich sample; thin line: dimer rich sample; column: TSK-Gel G3000SWXL 7.8 mm× 300 mm; feed concentration: 0.25 mg/mL; sample volume: 10  $\mu$ L; running buffer: 20 mM sodium phosphate pH 7.0 + 250 mM NaCl; flow rate: 0.3 mL/min); B: native PAGE, 7% (1: monomer-rich sample; 2: dimer-rich sample)

### 7.3.2. Analytical HI-LFMC separation

Figure. 7.3 shows the HI-LFMC results of the samples discussed above. In case of the monomer-rich sample (figure. 7.3, B), the separation was achieved in less than 1.5 min with very high monomer/dimer resolution. The assay time is comparable with the fastest SE-UPLC techniques available [3,29]. The analytical LFMC device was also capable of separating the higher aggregates depicted as the peak shoulder for the mAb dimers in the dimer-rich sample (figure. 7.3, A). The results acquired matched very well with the SE-HPLC shown in figure. 7.1, A. The higher aggregates were further resolved from the dimers using shallower gradients for dimer-rich campath-1H mAbs. As it is shown in figure. 7.4, baseline resolution of monomer/dimer as well as excellent separation of higher aggregates was achieved within 3 minutes.

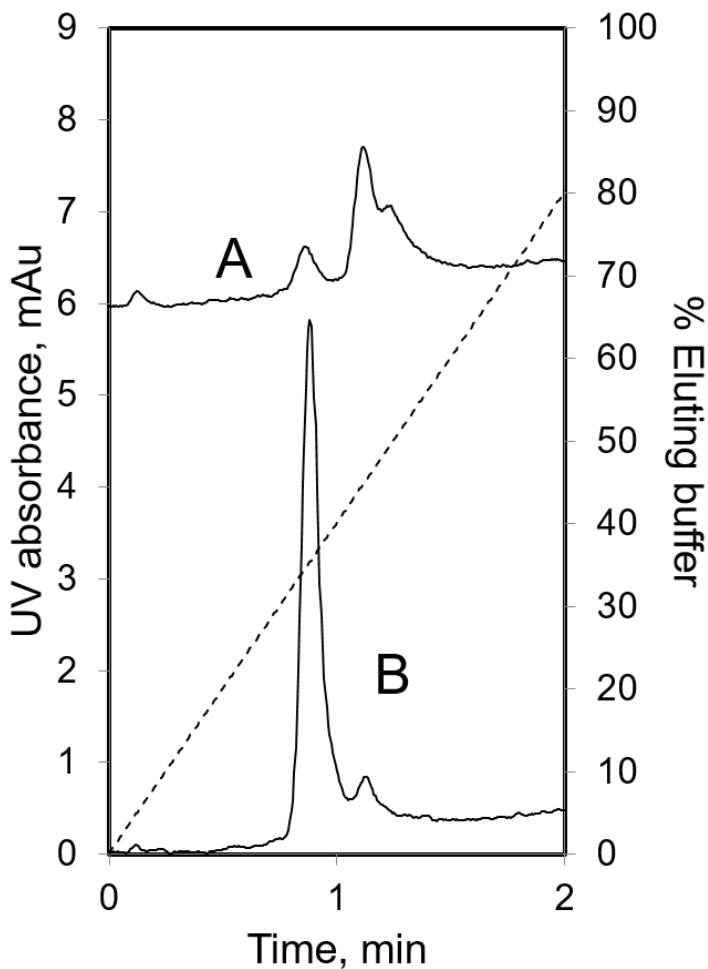


**Fig 7.3:** Analysis of CHO cell line derived Alemtuzumab (campath-1H) aggregates using HI-LFMC (A: dimer-rich sample; B: monomer-rich sample; membrane: hydrophilized PVDF, 0.22  $\mu\text{m}$  pore size, GVWP14250; membrane bed volume: 0.4 mL; feed concentration: 0.2 mg/mL; sample volume: 250  $\mu\text{L}$ ; eluting buffer: 20 mM sodium phosphate buffer pH 7.0; binding buffer: eluting buffer + 1.5 M ammonium; linear gradient: 40 mL; flow rate: 16 mL/min; dashed line: % eluting buffer)

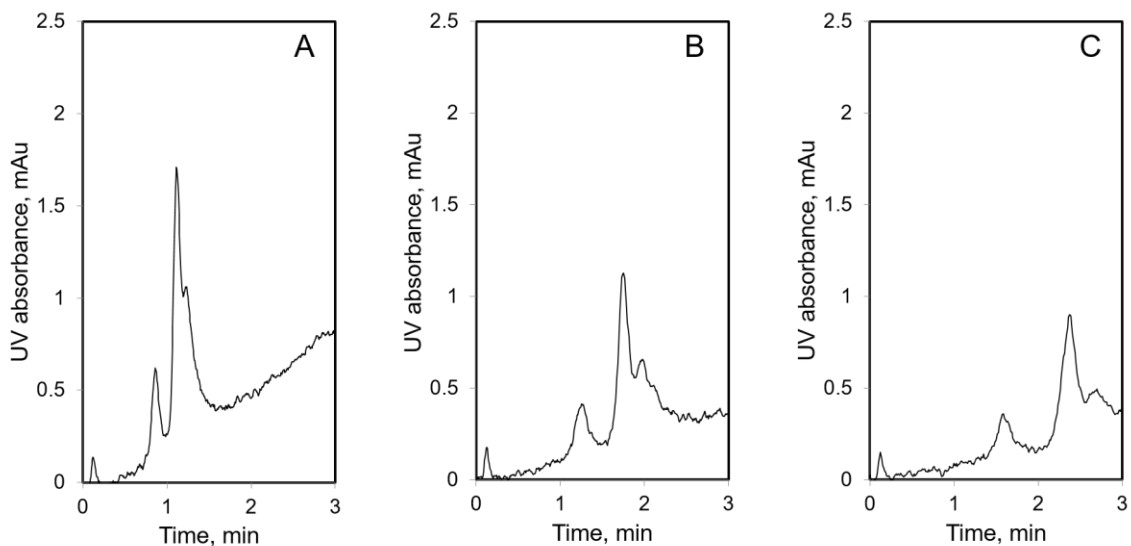


**Fig 7.4:** Analysis of dimer-rich CHO cell line derived Alemtuzumab (campath-1H) aggregates using HI-LFMC (A: 40 mL gradient; B: 80 mL gradient; C: 120 mL gradient; membrane: hydrophilized PVDF, 0.22  $\mu\text{m}$  pore size, GVWP14250; membrane bed volume: 0.4 mL; feed concentration: 0.2 mg/mL; sample volume: 250  $\mu\text{L}$ ; eluting buffer: 20 mM sodium phosphate buffer pH 7.0; binding buffer: eluting buffer + 1.5 M ammonium; flow rate: 16 mL/min)

As evident by the results, the utmost highlight of this technique is the rapidness while operating at very low pressure drops ( $\sim 165$  kPa). Having low bed heights and large membrane area made possible operating at flow rates as high as 40 min. At the same time, adequate resolution is provided even though the bed height was 375  $\mu\text{m}$  which is due to two major factors: using PVDF membranes with submicron pore sizes which offers low diffusion paths as well as having enhanced flow distribution which avoids peak broadening. This is evident from the very small HETP for the device used in this study which was found to be 8.19  $\mu\text{m}$  (equivalent to 122,109.33 theoretical plates/m). This is while with the currently available stacked-disk devices the flow rate is limited due to the use of small devices. Increasing the membrane area to work with higher flow rates would disturb the resolution which is due to the flow path variability over the central and peripheral regions and the resulting flow maldistribution within such devices. Assuming

having similar bed volume for the stacked-disk and LFMC, the LFMC device can be fabricated with much higher membrane area and utilized at much higher flow rates without sacrificing the resolution.

### **7.3.3. Further improvement at lower dead volume**

The LFMC device used to attain the results up to this point had pillars with diameter of 1 mm in both the top and bottom channels. New plates were fabricated with larger pillars having the same pattern as it is shown in figure. 7.1. The hexagonal pattern of the pillars in rows of 3 and 4 were kept unchanged, only that the diameters of the pillars were increased to 2 mm and 1.75 mm respectively, leading to decreasing the dead volume in each channel from 194  $\mu\text{L}$  to 139  $\mu\text{L}$ . The design criteria for the LFMC devices necessitates that the resistance in the top and bottom channels should be identical and smaller than the resistance of membrane stack. Otherwise, the balance in the pressure over the sides of the membrane stack would be disturbed [24]. Although increasing the pillar diameter even further would be in favor of having lower dead volumes, higher lateral resistance in the channels versus the membrane stack would contradict the design criteria. This would result in variety of permeate flux over the length of the membrane stack with the two ends [24]. The result would be the disruption of resolution which is highly unwanted.

Figure. 7.5, B demonstrates the results obtained with the identical experimental conditions when the low dead volume device was used. The monomer and dimer peaks acquired were much sharper and the resolution was improved. In order to benefit from this enhancement, the elution was further pushed to steeper gradient of 30 mL to facilitate even faster analysis. The analysis times achieved was 1.1 minute accordingly (figure. 7.5, A).

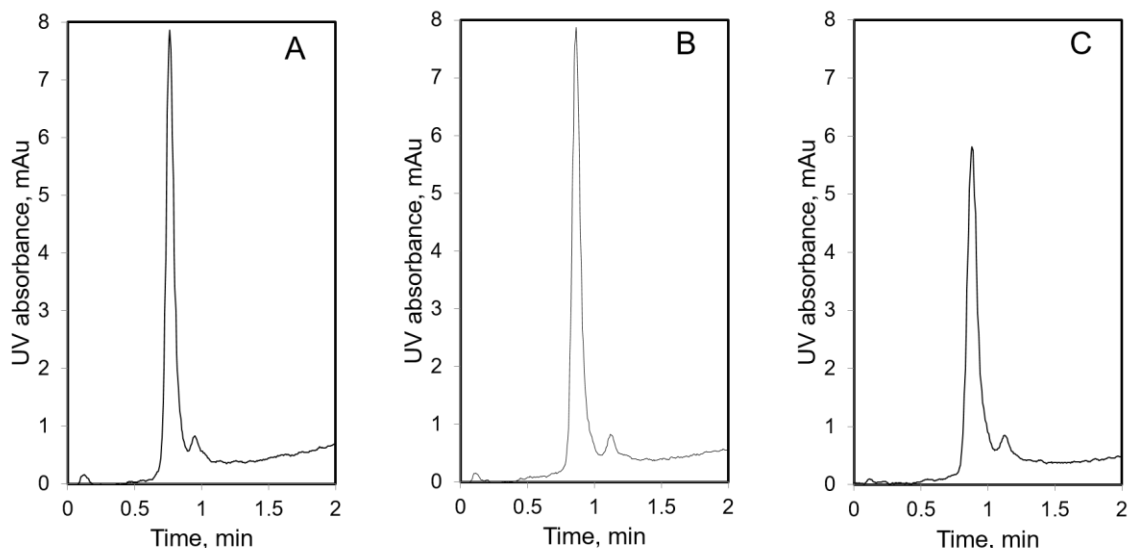


**Fig 7.5:** Analysis of monomer-rich CHO cell line derived Alemtuzumab (campath-1H) aggregates using HI-LFMC (A: 30 mL gradient, lower dead volume; B: 40 mL gradient, lower dead volume; C: 40 mL gradient, higher dead volume; membrane: hydrophilized PVDF, 0.22  $\mu\text{m}$  pore size, GVWP14250; membrane bed volume: 0.4 mL; feed concentration: 0.2 mg/mL; sample volume: 250  $\mu\text{L}$ ; eluting buffer: 20 mM sodium phosphate buffer pH 7.0; binding buffer: eluting buffer + 1.5 M ammonium; flow rate: 16 mL/min)

#### 7.3.4. Validation

Finally, the validity of the technique was approved for two other monoclonal antibody samples: Human IgG1-CD4 as well as HEK derived IgG1 (Trastuzumab biosimilar) (figure. 7.6). The HIgG1-CD4 mAbs contain very low amounts of aggregates which was previously studied using SE-HPLC (not shown). The results were obtained with the device with lower dead volume.

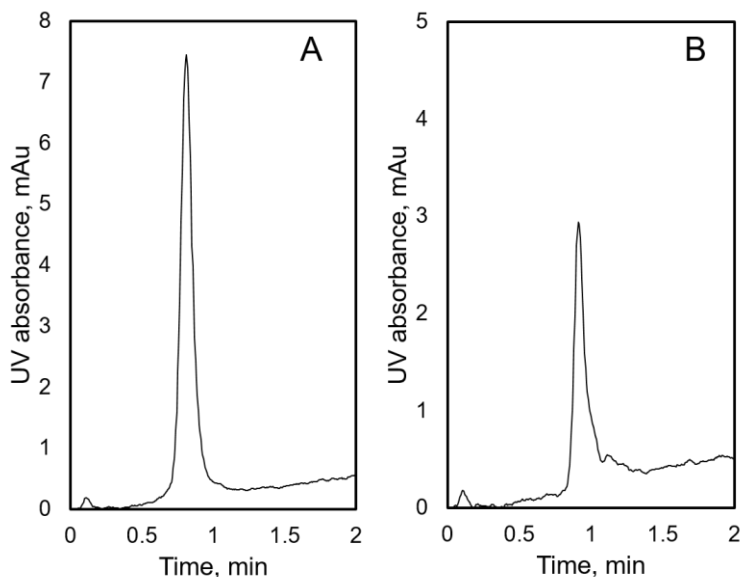


**Fig. 7.6:** Analysis of monoclonal antibody (mAb) aggregates using HI-LFMC (A: HlgG1-CD4; B: HEK cell line derived IgG1; membrane: hydrophilized PVDF, 0.22  $\mu\text{m}$  pore size, GVWP14250; membrane bed volume: 0.4 mL; feed concentration: 0.2 mg/mL; sample volume: 250  $\mu\text{L}$ ; eluting buffer: 20 mM sodium phosphate buffer pH 7.0; binding buffer: eluting buffer + 1.5 M ammonium; linear gradient: 40 mL; flow rate: 16 mL/min)

#### 7.4. Conclusions

Ultra-fast separation of monoclonal antibody aggregates was achieved using a new method benefitting from laterally-fed membrane chromatography (LFMC) technology. Previous studies proved that HIMC is greatly suitable for separation of mAb aggregates. In this work, hydrophilized PVDF membranes were integrated with a modified version of LFMC device appropriate for analytical hydrophobic interaction membrane chromatography (HIMC). The HI-LFMC technique was capable of completing mAb aggregate analysis in less than 1.5 minutes with operating pressures lower than 200 kPa. The assay time outclassed many of the currently available UPLC based techniques which deal with high pressure and high cost operations. This was feasible making use of relatively low membrane bed heights and high membrane area offered by the LFMC design due to which the separations were carried out at 40 MBV/min. Although having such low bed

heights, owing to the flow distribution within the device and the low diffusion paths brought by the submicron porosity of the PVDF membranes, the monomer/aggregate resolution was outstanding which is also evident from the very low HETP values measured. The assay time were even further enhanced decreasing the dead of the device. The separation technique discussed is highly rapid and cost-effective and has great potential for the analysis of aggregate content both in different stages of the process development as well as the quality control in mAb manufacturing and related biopharmaceutical processes.

### **7.5. Acknowledgements**

We thank Ontario Research Fund-Research Excellence (ORF-RE) and National Science and Engineering Research Council of Canada (NSERC) for funding this project. We thank Dr. Yves Durocher and other members of the National Research Council of Canada in Montreal, QC for donating the HEK derived IgG1 (Trastuzumab biosimilar). We thank Elna Luckham and the Biointerfaces institute at McMaster University for providing us with the HPLC system. We thank Paul Gatt for fabricating the devices based on the design provided by RG and PM.

### **7.6. References**

- [1] S. Fekete, A.L. Gassner, S. Rudaz, J. Schappler, D. Guillarme, Analytical strategies for the characterization of therapeutic monoclonal antibodies, *TrAC - Trends Anal. Chem.* 42 (2013) 74–83.
- [2] S. Fekete, A. Beck, J. Veuthey, D. Guillarme, Theory and practice of size exclusion chromatography for the analysis of protein aggregates., *J. Pharm. Biomed. Anal.* 101 (2014) 161–73.
- [3] P. Diederich, S.K. Hansen, S.A. Oelmeier, B. Stolzenberger, J. Hubbuch, A sub-two minutes method for monoclonal antibody-aggregate quantification using parallel interlaced size exclusion high performance liquid chromatography, *J. Chromatogr. A.* 1218 (2011) 9010–9018.

- [4] S. Fekete, K. Ganzler, D. Guillarme, Critical evaluation of fast size exclusion chromatographic separations of protein aggregates, applying sub-200 nm particles, *J. Pharm. Biomed. Anal.* 78–79 (2013) 141–149.
- [5] B.A. Rogers, Z. Wu, B. Wei, X. Zhang, X. Cao, O. Alabi, M.J. Wirth, Submicrometer particles and slip flow in liquid chromatography, *Anal. Chem.* 87 (2015) 2520–2526.
- [6] C. Wong, C. Strachan-Mills, S. Burman, Facile method of quantification for oxidized tryptophan degradants of monoclonal antibody by mixed mode ultra performance liquid chromatography, *J. Chromatogr. A.* 1270 (2012) 153–161.
- [7] S. Grotefend, L. Kaminski, S. Wroblewitz, S. El Deeb, N. Kühn, S. Reichl, M. Limberger, S. Watt, H. Wätzig, Protein quantitation using various modes of high performance liquid chromatography, *J. Pharm. Biomed. Anal.* 71 (2012) 127–138.
- [8] S. Fekete, J. Schappler, J.-L. Veuthey, D. Guillarme, Current and future trends in UHPLC, *Trends Anal. Chem.* 63 (2014) 2–13.
- [9] S. Fekete, D. Guillarme, Ultra-high-performance liquid chromatography for the characterization of therapeutic proteins, *TrAC - Trends Anal. Chem.* 63 (2014) 76–84.
- [10] P. Hong, K.J. Fountain, Method Development for Size-Exclusion Chromatography of Monoclonal Antibodies and Higher Order Aggregates, Waters Corporation, (2011) 1–8.
- [11] S. Koza, M. Lauber, K.J. Fountain, The Analysis of Multimeric Monoclonal Antibody Aggregates by Size-Exclusion UPLC, Waters Corporation, (2013) 1–8.
- [12] S. Fekete, J.L. Veuthey, D. V. McCalley, D. Guillarme, The effect of pressure and mobile phase velocity on the retention properties of small analytes and large biomolecules in ultra-high pressure liquid chromatography, *J. Chromatogr. A.* 1270 (2012) 127–138.

- [13] S. Fekete, I. Kohler, S. Rudaz, D. Guillarme, Importance of instrumentation for fast liquid chromatography in pharmaceutical analysis, *J. Pharm. Biomed. Anal.* 87 (2014) 105–119.
- [14] L. Nováková, J.L. Veuthey, D. Guillarme, Practical method transfer from high performance liquid chromatography to ultra-high performance liquid chromatography: The importance of frictional heating, *J. Chromatogr. A.* 1218 (2011) 7971–7981.
- [15] B. Bobály, D. Guillarme, S. Fekete, Systematic comparison of a new generation of columns packed with sub-2  $\mu\text{m}$  superficially porous particles, *J. Sep. Sci.* 37 (2014) 189–197.
- [16] C.H. Arnauld, C. Washington, 50 years of HPLC, *Am. Ethnol.* (2016) 29–33.
- [17] B. Wei, B.J. Rogers, M.J. Wirth, Slip flow in colloidal crystals for ultraefficient chromatography, *J. Am. Chem. Soc.* 134 (2012) 10780–10782.
- [18] J.C. Rea, G.T. Moreno, L. Vampola, Y. Lou, B. Van Haan, G. Tremintin, L. Simmons, A. Nava, Y.J. Wang, D. Farnan, Capillary size exclusion chromatography with picogram sensitivity for analysis of monoclonal antibodies purified from harvested cell culture fluid, *J. Chromatogr. A.* 1219 (2012) 140–146.
- [19] C. Gourmel, A. Grand-Guillaume Perrenoud, L. Waller, E. Reginato, J. Verne, B. Dulery, J.L. Veuthey, S. Rudaz, J. Schappler, D. Guillarme, Evaluation and comparison of various separation techniques for the analysis of closely-related compounds of pharmaceutical interest, *J. Chromatogr. A.* 1282 (2013) 172–177.
- [20] L. Wang, G. Hale, R. Ghosh, Non-size-based membrane chromatographic separation and analysis of monoclonal antibody aggregates., *Anal. Chem.* 78 (2006) 6863–7.

- [21] L. Wang, R. Ghosh, Fractionation of monoclonal antibody aggregates using membrane chromatography, *J. Memb. Sci.* 318 (2008) 311–316.
- [22] D. Yu, R. Ghosh, Method for studying immunoglobulin G binding on hydrophobic surfaces, *Langmuir*. 26 (2010) 924–929.
- [23] R. Ghosh, T. Wong, Effect of module design on the efficiency of membrane chromatographic separation processes, *J. Memb. Sci.* 281 (2006) 532–540.
- [24] R. Ghosh, P. Madadkar, Q. Wu, On the workings of laterally-fed membrane chromatography, *J. Memb. Sci.* 516 (2016) 26–32.
- [25] R. Ghosh, P. Madadkar, Laterally-fed membrane chromatography device, 62304379, 2016.
- [26] P. Madadkar, Q. Wu, R. Ghosh, A laterally-fed membrane chromatography module, *J. Memb. Sci.* 487 (2015) 173–179.
- [27] S.D. Gorman, M.R. Clark, E.G. Routledge, S.P. Cobbold, H. Waldmann, Reshaping a therapeutic CD4 antibody., *Proc. Natl. Acad. Sci. U. S. A.* 88 (1991) 4181–4185.
- [28] A.S. Rathore, R.M. Kennedy, J.K. O'Donnell, I. Bemberis, O. Kaltenbrunner, Qualification of a chromatographic column: Why and how to do it, *BioPharm Int.* 16 (2003) 30–40.
- [29] S. Fekete, D. Guillarme, Kinetic evaluation of new generation of column packed with 1.3 $\mu$ m core-shell particles, *J. Chromatogr. A.* 1308 (2013) 104–113.

## **Chapter 8**

### **Contributions and Recommendations**

### 8.1. Contributions

The overall body of the work presented in this thesis discusses the design, development, and applications of laterally-fed membrane chromatography devices. Owing to the unique and novel design features which provide uniform solute flow path lengths and balanced pressure over the sides of the housed membrane stack, the superficial velocity over the membrane area is unvarying, all contributing to highly uniform solute residence time within the devices. As opposed to the currently available membrane chromatography devices, these features make the LFMC technology highly suitable for high-resolution separations in the bind and elute mode. Together with the intrinsic advantages of adsorptive membranes, the devices address an ongoing deficiency in downstream processing of biopharmaceuticals which is the combination of high-throughput and high-resolution. Remarkably, this progression has been brought about by simple design and easy fabrication which make the LFMC devices very cost-effective. In addition, owing to their rectangular and flat shape, the devices are stackable with low footprints and greatly suitable for multiplexing.

The comparison of novel laterally-fed modules with the conventional stacked-disk modules which are the most widely used in lab-scale studies demonstrated how uniform solute flow path lengths can revolutionize the chromatographic efficiency (chapter 1). The differences in flow distribution were clearly shown by investigating dye pulses in non-binding conditions. It was demonstrated that the enhanced flow distribution leads to significantly higher breakthrough binding capacities. The results reported almost five times higher incipient (1%) breakthrough binding capacity as well as two times higher 10% breakthrough binding capacity for membrane bed volume as small as 0.34 mL with only one membrane layer. The early breakthrough in stacked-disk adsorbers is caused by the uneven flow path lengths and variety of superficial velocity between the central and peripheral regions; the same reason behind tailed eluted peaks obtained and the unsuitability for scale-up. This issue is completely resolved in LFMC devices, giving sharp and

symmetrical flow through and eluting peaks, efficient binding capacity utilization, and great scalability.

The results discussed in chapter 3 clearly stated that LFMC devices are highly suitable for separation of multi-component proteins in bind and elute mode of operation. This feature makes the LFMC devices the only membrane adsorbers capable of performing high-resolution separations. Owing to the enhanced flow distribution, both the binding and elution stages are carried out in a uniform manner, giving sharp eluted peaks which can be resolved in significantly low volumes, contributing to excessively lower sterile buffer usage. The resolutions obtained with LFMC devices are highly comparable with resin columns (chapter 4) which is the direct contribution of the device design. The pressure drops obtained were also noticeably lower. Moreover, performance of LFMC devices are highly consistent over a wide range of flow rates as opposed to the resin columns which is outstanding from the manufacturing point of view. This is clearly regarded to the nature of solute transport within the adsorptive membranes and resins. The consistency was approved even at flow rates as high as twice the maximum operating limit for the equivalent columns, this is while resin columns still give better resolutions at very low flow rates. The results from these two chapters evidently concluded that using the LFMC technology, membrane chromatography can be employed in wide range of applications beyond the flow through polishing.

Different case study applications with major focus on purification of monoclonal antibodies discussed in this thesis confirmed the findings in the earlier chapters. This was also approved by the measured number of theoretical plates prior to the experiments. Separation of mAb charge variants using CEX chromatography is a very challenging separation with regards to the close physicochemical properties of the acidic and basic variants of the mAbs. The separation demands for very shallow gradients. LFMC devices undoubtedly provided the required resolution of separation as well as stable shallow conductivity gradients (chapter 4). Single-step

purification of mono-PEGylated lysozyme in significantly short times also approved the combined high resolution and high productivity of CEX-LFMC (chapter 5).

Industrial application of the currently available membrane adsorbers in production of mAbs is only limited to polishing steps through flow-through anion-exchange separations. The results manifested in chapter 6 clearly stated that the LFMC devices can be used in earlier stages of mAb downstream purification based on offering high-resolution for separation of mAb aggregates. The results reported preparative separation of aggregates in less than 10 minutes when a 5 mL (MBV) LFMC device was used with relatively high amounts of the target molecule. The technology would then be highly advantageous in improving the processing times in downstream purification of mAbs considering for the simple and cost-efficient scale-up of these devices.

Although the development of LFMC devices targets the large-scale downstream purifications in biotechnology, the devices were shown to be highly beneficial in analytical separations. The HI-LFMC device discussed in chapter 7 showed that fabrication of devices based on the concept of LFMC, at the same time with being very simple and cost effective, can deliver improved assay times of when compared with UPLC columns. It is notable that such devices can be used in a single-use manner while UPLC columns are very costly. Therefore, analytical applications is definitely another avenue in which the LFMC devices should be explored.

## **8.2. Recommendations for Future Work**

This work notifies the importance of device design in chromatographic processes and stimulates research on the area of device development. Concerning the LFMC devices, modeling and simulation is of high importance. Despite the simplicity of the design, there are many parameters which would affect the efficiency of separation with regards to the targeted unit operation. The optimization of these parameters should be studied in advance by CFD modeling and simulation tools

such as COMSOL. Aspect ratio of the channels and membrane stack, channel heights, arrangement and diameter of pillars (void percentage within the lateral channels), as well as inlet and outlet flow distribution are among the suggested parameters for future studies. It is notable that comprehensive understanding of these design features is necessary for scale-up studies.

The application of LFMC devices for affinity membrane chromatography, with considerations on protein-A membrane chromatography is another area which was not studied in this thesis. This would expand the application of LFMC devices specifically in downstream processing of mAbs.

With biotechnology companies constantly looking for lower costs of manufacturing, future trends in downstream purification will target higher productivity, low manufacturing costs, single-use operations, and faster speed of development [1]. Based on the findings presented in this thesis, the LFMC technology would be a great fit.

The outcomes of this thesis have already opened a new pathway in resin chromatography. The application of rectangular boxes compared to columns with high radiuses was shown to highly impact the efficiency even when resins are employed as the chromatographic media [2]. The enhancement in the flow distribution giving more uniform solute residence times is highly advantageous for large-scale separations. The initial studies showed much less peak broadening for flow through and eluted peaks and higher resolution for binary and tertiary protein separation.

Conventional packed-bed chromatography involves loading (binding), washing, and elution in sequence which makes it inherently a batch process. This is while continuous manufacturing is beneficial both in terms of productivity and reducing the footprint. Moreover, in case of labile molecules, variations in the final product would be avoided [3]. In order to operate chromatographic separation in the continuous mode normally several columns are integrated in a way through which

loading, washing, and elution steps are occurring at the same time followed by switching the columns to other steps [4]. This is while membrane chromatography and LFMC devices would be highly advantageous in the sense that they offer much higher cycling speeds and would be highly suitable for continuous operations [5]. Utilization of the devices in series or in parallel would be something to consider in advance [6]

Finally, with increasing the number of the biopharmaceutical products and their biosimilars, improved characterization and fast quality control are required. High-throughput and high precision analytical methods are developing to evaluate the micro-heterogeneity among the biological products [7,8]. LFMC devices would greatly serve this section.

### **8.3. References**

- [1] R. Bhambure, K. Kumar, A.S. Rathore, High-throughput process development for biopharmaceutical drug substances., *Trends Biotechnol.* 29 (2011) 127–35.
- [2] R. Ghosh, Using a box instead of a column for process chromatography, *J. Chromatogr. A.* 1468 (2016) 164–172.
- [3] A. Jungbauer, Continuous downstream processing of biopharmaceuticals, *Trends Biotechnol.* 31 (2013) 479–492.
- [4] A.L. Zydney, Continuous downstream processing for high value biological products: A Review, *Biotechnol. Bioeng.* 113 (2016) 465–475.
- [5] J.H. Vogel, H. Nguyen, R. Giovannini, J. Ignowski, S. Garger, A. Salgotra, J. Tom, A new large-scale manufacturing platform for complex biopharmaceuticals, *Biotechnol. Bioeng.* 109 (2012) 3049–3058.

- [6] Z. Yu, T. Karkaria, M. Espina, M. Hunjun, A. Surendran, T. Luu, J. Telychko, Y.P. Yang, Comparing multi-module connections in membrane chromatography scale-up, *J. Biotechnol.* 206 (2015) 38–41.
- [7] S. Fekete, A. Beck, J.L. Veuthey, D. Guillarme, Ion-exchange chromatography for the characterization of biopharmaceuticals, *J. Pharm. Biomed. Anal.* 113 (2015) 43–55. doi:10.1016/j.jpba.2015.02.037.
- [8] A.T. Hanke, M. Ottens, Purifying biopharmaceuticals: Knowledge-based chromatographic process development, *Trends Biotechnol.* 32 (2014) 210–220. doi:10.1016/j.tibtech.2014.02.001.

**Appendices**

**Copyrights**

1/7/2017

RightsLink - Your Account



RightsLink®

[My Orders](#)[My Library](#)[My Profile](#)Welcome p.madadkar@gmail.com [Log out](#) | [Help](#)[My Orders](#) > [Orders](#) > [All Orders](#)

## License Details

This Agreement between Pedram Madadkar ("You") and Elsevier ("Elsevier") consists of your license details and the terms and conditions provided by Elsevier and Copyright Clearance Center.

[printable details](#)

<a href="#">License Number</a>	4018830342832
<a href="#">License date</a>	Dec 30, 2016
<a href="#">Licensed Content Publisher</a>	Elsevier
<a href="#">Licensed Content Publication</a>	Journal of Membrane Science
<a href="#">Licensed Content Title</a>	A laterally-fed membrane chromatography module
<a href="#">Licensed Content Author</a>	Pedram Madadkar,Qijiyu Wu,Raja Ghosh
<a href="#">Licensed Content Date</a>	1 August 2015
<a href="#">Licensed Content Volume</a>	487
<a href="#">Licensed Content Issue</a>	n/a
<a href="#">Licensed Content Pages</a>	7
<a href="#">Type of Use</a>	reuse in a thesis/dissertation
<a href="#">Portion</a>	full article
<a href="#">Format</a>	both print and electronic
<a href="#">Are you the author of this Elsevier article?</a>	Yes
<a href="#">Will you be translating?</a>	No
<a href="#">Order reference number</a>	
<a href="#">Title of your thesis/dissertation</a>	High-Efficiency Membrane Chromatography Devices for Downstream Purification of Biopharmaceuticals: Design, Development, and Applications
<a href="#">Expected completion date</a>	Jan 2017
<a href="#">Estimated size (number of pages)</a>	220
<a href="#">Elsevier VAT number</a>	GB 494 6272 12
<a href="#">Requestor Location</a>	Pedram Madadkar 121 Hunter St W unit 802  Hamilton, ON L8P1R2 Canada Attn: Pedram Madadkar
<a href="#">Total</a>	<b>0.00 CAD</b>

Copyright © 2017 Copyright Clearance Center, Inc. All Rights Reserved. [Privacy statement](#) . [Terms and Conditions](#) . Comments? We would like to hear from you. E-mail us at [customercare@copyright.com](mailto:customercare@copyright.com)

1/7/2017

RightsLink - Your Account



RightsLink®

[My Orders](#)[My Library](#)[My Profile](#)Welcome p.madadkar@gmail.com [Log out](#) | [Help](#)[My Orders > Orders > All Orders](#)

## License Details

This Agreement between Pedram Madadkar ("You") and Elsevier ("Elsevier") consists of your license details and the terms and conditions provided by Elsevier and Copyright Clearance Center.

[printable details](#)

<a href="#">License Number</a>	4018830240352
<a href="#">License date</a>	Dec 30, 2016
<a href="#">Licensed Content Publisher</a>	Elsevier
<a href="#">Licensed Content Publication</a>	Journal of Membrane Science
<a href="#">Licensed Content Title</a>	High-resolution protein separation using a laterally-fed membrane chromatography device
<a href="#">Licensed Content Author</a>	Pedram Madadkar,Raja Ghosh
<a href="#">Licensed Content Date</a>	1 February 2016
<a href="#">Licensed Content Volume</a>	499
<a href="#">Licensed Content Issue</a>	n/a
<a href="#">Licensed Content Pages</a>	8
<a href="#">Type of Use</a>	reuse in a thesis/dissertation
<a href="#">Portion</a>	full article
<a href="#">Format</a>	both print and electronic
<a href="#">Are you the author of this Elsevier article?</a>	Yes
<a href="#">Will you be translating?</a>	No
<a href="#">Order reference number</a>	
<a href="#">Title of your thesis/dissertation</a>	High-Efficiency Membrane Chromatography Devices for Downstream Purification of Biopharmaceuticals: Design, Development, and Applications
<a href="#">Expected completion date</a>	Jan 2017
<a href="#">Estimated size (number of pages)</a>	220
<a href="#">Elsevier VAT number</a>	GB 494 6272 12
<a href="#">Requestor Location</a>	Pedram Madadkar 121 Hunter St W unit 802  Hamilton, ON L8P1R2 Canada Attn: Pedram Madadkar
<a href="#">Total</a>	<b>0.00 CAD</b>

Copyright © 2017 Copyright Clearance Center, Inc. All Rights Reserved. [Privacy statement](#) . [Terms and Conditions](#) . Comments? We would like to hear from you. E-mail us at [customercare@copyright.com](mailto:customercare@copyright.com)

1/7/2017

RightsLink - Your Account



RightsLink®

[My Orders](#)[My Library](#)[My Profile](#)Welcome p.madadkar@gmail.com [Log out](#) | [Help](#)[My Orders > Orders > All Orders](#)

## License Details

This Agreement between Pedram Madadkar ("You") and Elsevier ("Elsevier") consists of your license details and the terms and conditions provided by Elsevier and Copyright Clearance Center.

[printable details](#)

<a href="#">License Number</a>	4018830707389
<a href="#">License date</a>	Dec 30, 2016
<a href="#">Licensed Content Publisher</a>	Elsevier
<a href="#">Licensed Content Publication</a>	Journal of Chromatography B
<a href="#">Licensed Content Title</a>	High-resolution, preparative purification of PEGylated protein using a laterally-fed membrane chromatography device
<a href="#">Licensed Content Author</a>	Pedram Madadkar,Sergio Luna Nino,Raja Ghosh
<a href="#">Licensed Content Date</a>	1 November 2016
<a href="#">Licensed Content Volume</a>	1035
<a href="#">Licensed Content Issue</a>	n/a
<a href="#">Licensed Content Pages</a>	7
<a href="#">Type of Use</a>	reuse in a thesis/dissertation
<a href="#">Portion</a>	full article
<a href="#">Format</a>	both print and electronic
<a href="#">Are you the author of this Elsevier article?</a>	Yes
<a href="#">Will you be translating?</a>	No
<a href="#">Order reference number</a>	
<a href="#">Title of your thesis/dissertation</a>	High-Efficiency Membrane Chromatography Devices for Downstream Purification of Biopharmaceuticals: Design, Development, and Applications
<a href="#">Expected completion date</a>	Jan 2017
<a href="#">Estimated size (number of pages)</a>	220
<a href="#">Elsevier VAT number</a>	GB 494 6272 12
<a href="#">Requestor Location</a>	Pedram Madadkar 121 Hunter St W unit 802  Hamilton, ON L8P1R2 Canada Attn: Pedram Madadkar
<a href="#">Total</a>	<b>0.00 CAD</b>

Copyright © 2017 Copyright Clearance Center, Inc. All Rights Reserved. [Privacy statement](#) . [Terms and Conditions](#) . Comments? We would like to hear from you. E-mail us at [customercare@copyright.com](mailto:customercare@copyright.com)